THE UNIVERSITY OF CHICAGO

NEURAL MECHANISMS OF CONTEXT-DEPENDENT SENSORY CODING IN THE MAMMALIAN RETINA

A DISSERTATION SUBMITTED TO
THE FACULTY OF THE DIVISION OF THE BIOLOGICAL SCIENCES
AND THE PRITZKER SCHOOL OF MEDICINE
IN CANDIDACY FOR THE DEGREE OF
DOCTOR OF PHILOSOPHY

COMMITTEE ON NEUROBIOLOGY

BY
XIAOLIN HUANG

CHICAGO, ILLINOIS
DECEMBER 2021

TABLE OF CONTENTS

LIST OF FIGURES

ABBREVIATIONS

AC	Amacrine Cell
BC	Bipolar Cell
CBC	Cone Bipolar Cell
CMI	Contextual Modulation Index
cKO	Conditional knock-out
DSGC	Direction Selective Ganglion Cell
DSI	Direction Selectivity Index
EPSC	Excitatory postsynaptic current
IPL	Inner Plexiform Layer
IPSC	Inhibitory postsynaptic current
pDSGC	posterior-preferred Direction Selective Ganglion Cell
RF	Receptive Field
PSP	Postsynaptic potential
RGC	Retinal Ganglion Cell
SAC	Starburst Amacrine Cell
SI	Suppression Index
WAC	Wide-field Amacrine Cell

ACKNOWLEDGMENTS

We ride a stream of naked neurons, stripped of their sheaths, to the most blissful moments and deepest intimacies of life.

— *Steven M Phelps*

My obsession with the mystery of the brain started early since I was a kid, probably owing to my insistent inquiry of infinity. At that time, I considered what is buried deepest inside the brain as infinite as what is hidden furthest in the universe. And I still firmly believe so at present. The spiking neurons in the brain are like the blinking stars in the space, privily communicating in their unique language and "quietly" creating miracles in every second. I want to pick up their language and peer at what is happening down there. With reckless zeal and a naïve understanding of neuroscience, 12 years ago the teenager me determined a path of pursuing neuroscience, without truly realizing how challenging it will be. And that curiosity and enthusiasm for neuroscience drove me from my hometown Quanzhou in the south of China, to the capital city Beijing in the north, and eventually here in front of a desk at the University of Chicago. During the journey, there are up and down times, and there are encouraging and discouraging voices. I appreciate the me from the last 12 years for her determination and persistence all the way here. And I sincerely hope she can keep her curiosity and passion for neuroscience into the future, no matter if she eventually becomes a neuroscientist or not.

In my journey of pursuing neuroscience, I have met quite some incredible women scientists who are my role models and from whom I have learned a lot. Being a woman in science is not easy, especially in terms of reconciling a science career with family life, balancing the responsibility of being a scientist, a mentor, and a mother. But they demonstrate the possibility of being a successful woman in science, and show me the happiness, satisfaction and fulfillment when staying in the academic area and persisting in their beloved scientific research. From Yan Zhang, my undergraduate research advisor at Peking University, I learned the importance of seizing opportunities, which are only open to the hard-working and the prepared. From Bryndis Birnir, my bachelor thesis advisor at Uppsala University, I learned humbleness, focus and rigor. From Ruth Anne Eatock, my Ph.D. thesis committee member, I learned her remarkable kindness to young students and her sense of responsibility to the neuroscience community. And particularly, I want to express my exceptional gratitude to my Ph.D. thesis advisor Wei Wei, who has always been extremely dedicated, approachable, patient and supportive during my graduate training. She can always provide

insightful instructions and point out the key point of the projects. And I am so fortunate to have her alongside me when I learned every step in conducting research, from setting up a rig from scratch, performing dissection and patch-clamp, troubleshooting and data analysis, eventually to writing a manuscript together. And when I got stuck outside the states for 8 months due to the pandemic and the travel restriction (including about 2 months in an unfamiliar country Cambodia), she always considered my health and safety in the first place, and gave me lots of comforts. Without her generous support and encouragement, I could not get through those stressful days and be back to finish the thesis. She is the best mentor, and she is more than a PI to me, giving me the warmest supports like an elder sister.

The members in Wei lab are another big reason why I joined the lab. They enriched the lab with a fabulously comfortable and creative vibe. Our diverse cultural and academic backgrounds always create sparks of ideas and fun. I would like to thank Chris Chen, a graduate student from the Computational Neuroscience program, for his hands-on and generous training to me. It was a pleasant and inspiring experience to sit next to him on the rig, watching him conducting experiments or trouble-shooting; Hector Acaron Ledesma, a graduate student from the Biophysics program, for all the delightful afternoon conversations. We should have written down all our brainstorms that include countless potential projects - no matter they are promising or funny; David Koren, a graduate student from the Medical Scientist Training Program, for his critical feedback on my project; Chen Zhang, our respected lab manager and lab technician, for taking care of lab supplies, animal colony and genotyping. And it is also warm and sweet to learn the planting tricks from her; Alan Jaehyun Kim, a smart undergrad student, for his great help in recording alpha ganglion cells and tracing On-Off DSGC dendrites; Jennifer Ding, a graduate student from the Committee on Neurobiology program, for being a good company in the experimental days; other lab members, including Swen Oosterboer, Benno Giammarinaro and Janet Chung, for the numerous terrific moments that we spent together.

I am truly grateful to the members of my thesis committee, including John Maunsell, Ruth Anne Eatock and 'JC' Jianhua Cang. They all provided invaluable feedbacks to my projects, as well as insightful advice and generous supports when I sought help with career development. Especially I would like to thank JC for being supportive and generous with his time to join my committee as a faculty outside of UChicago. I also appreciate the help from the administration of the neuroscience cluster, especially Stephanie Thomas, Sharon Montgomery and Elena Rizzo. They are so kind and helpful to make sure every student is

on track. And I also want to thank a lot of other faculties at Uchicago. I also got great mentorship and learned a lot from them. When I was an undergraduate, I did a summer research internship at Dave's lab, which left me incredible impression of the research atmosphere at Uchicago. And I did rotation projects at Christian and Paschalis's lab. They are all great mentors. And also thank Dan, Xiaoxi, Wei-jen and other faculties at Uchicago who gave me invaluable advices of career development.

I would like to thank my cohort and friends for creating the terrific and unforgettable memory in my graduate school. And especially, I have made two best friends in neuroscience cluster, Can Dong and Qinpu He. Thank them for sharing the most exciting as well as the most tedious moments of our lives. We will for sure be lifelong friends.

And I am appreciative of the supports from my family. My parents are always supportive of my every decision and back me up to seek the career I want. I am so fortunate to have them stand by me with their unconditional and unwavering love. In the end, I want to convey my deepest thanks to my husband Siyu Chen. We have been together for nearly 10 years, and he has always been such a great listener with sympathy, and talented expertise in cheering me up. He is the one who understands me the best in the world, and he is always incredibly supportive of my career. It is hard for me to imagine how I can make this journey without his encouragement. Thank him for enriching our life with tremendous delight and fun.

ABSTRACT

Our sensory inputs from the natural environment always come in contexts of the surrounding environment. Visual perception of animals is profoundly influenced by these spatial and temporal contexts, which is called contextual modulation. Contextual modulation is a ubiquitous phenomenon in visual perception and it underlies different phenomena such as visual saliency, illusions and adaptation aftereffects. These perceptual attributes have been linked to contextual modulation of visual neuronal responses: the activity of neurons to a target stimulus can be shaped by the spatial and temporal visual environments. Contextual modulation arises early in the visual pathway and is readily detectable in multiple types of retinal ganglion cells including the On-Off direction selective ganglion cells (DSGCs). On-Off DSGCs are the output neurons of the well-studied direction selective circuit, and the neural networks wired to these ganglion cells are one of the best known circuits in the retina. However, the neural mechanisms underlying the spatial and temporal contextual modulation of DSGCs are not fully understood. Delineating the pattern and mechanism of spatial and temporal contextual modulation in DSGC will give us a more comprehensive understanding of the retinal code that DSGC conveys to the brain. Therefore, the central goal of this thesis was to identify how DSGC responses are modulated by visual contexts in both spatial and temporal dimension, and to investigate how these contextual effects are accomplished at the synaptic and network levels.

First, from the spatial perspective, I determined how the responses of DSGCs are modulated by different patterns of surrounding visual stimuli. I found that DSGCs are sensitive to discontinuities of moving contours between the stimuli in the center and the background. Using a combination of synapse-specific genetic manipulations, patch clamp electrophysiology and connectomic analysis, we identified distinct circuit motifs that are required for the spatial contextual modulation of pDSGC activity for bright and dark contours. Further-

more, our results revealed a class of wide-field amacrine cells (WACs) with long, straight and unbranched dendrites that function as "continuity detectors" of moving contours.

Second, I examined the influence of previous visual stimuli on the response sensitivity of DSGCs in the form of temporal contextual modulation. I found that DSGC light responses can be acutely enhanced by previous visual stimulation. Moreover, DSGCs from the dorsal and the ventral retina, which receive visual inputs from the lower and upper visual fields respectively, show divergent patterns of sensitization. After a full set of whole-cell voltage clamp, current clamp and pharmacological experiments, our results revealed that glycinergic disinhibition of Off bipolar cell inputs to DSGC plays an essential role in the DSGC sensitization after induction stimulus. Furthermore, DSGCs from the dorsal retina gain a sustained membrane depolarization from the Off pathway that propagates into the On pathway and sensitizes the subsequent On spiking activity. We corroborated the functional measurements with anatomical reconstruction and simulation computational modeling, and found that a substantial percentage of "crossover dendrites" in DSGC provides physical subtracts for efficient electronic spread between DSGC Off and On layers.

Overall, these results link the existing circuit motifs mediating direction selectivity to the extensive inner retinal network, highlighting a multilayered circuit architecture that dynamically engages specific microcircuit motifs and synaptic plasticity to process motion information according to the composition of visual features in the spatial and temporal context of the stimulus. Results from my thesis therefore fill the important knowledge gaps in the mechanistic understanding of contextual modulation in the visual system, and also lead to a deeper understanding of motion computation in natural complex visual environment.

CHAPTER 1

INTRODUCTION

In this Chapter, **section 1.2** and **section 1.3** are partially reprinted from Huang et al., Chapter 9 of *Synapse Development and Maturation*, in which I am the primary author. The work is included with permission from all authors.

Relevant Publication

Huang, X., Acarón Ledesma, H.E., Wei, W. (2020). **Synapse formation in the developing vertebrate retina.** In *Synapse Development and Maturation: Comprehensive Developmental Neuroscience* (pp. 213-230). Academic Press, Elsevier Inc.

For full chapter, please refer to `https://doi.org/10.1016/B978-0-12-823672-7.00009-0`

1.1 Contextual modulation in the visual system

Visual stimulations in the natural world are embedded with diverse environments, including the spatial environment (the background of the target) and the temporal environment (the stimulus pattern in the recent past). These contexts of the target stimulus can profoundly influence visual responses, which has been detected from neuronal to perceptual level. The modulation of visual responses by visual contexts is termed contextual modulation. Psychological studies have identified how the level of brightness/blurriness or the pattern of motion/orientation/faces in the visual contexts can modulate visual perceptions (Kamkar et al., 2018; Schwartz et al., 2007; Theeuwes, 2013; Torralba et al., 2006). There are also extensive physiological evidences revealing the neural basis of contextual modulation from different levels of the visual system (Akyuz et al., 2020; Albright and Stoner, 2002; Barchini et al., 2018; Chiao and Masland, 2003; Clifford et al., 2000; Gilbert and Wiesel, 1990; Kohn, 2007; Schwartz et al., 2007). It is worth noting that contextual modulation of neural responses was not only reported in the visual system, but also detected in sensory circuits of

other modalities including auditory (Oxenham, 2001) and somatosensory systems (Wallace et al., 2004). The prevalence of contextual modulation in divergent sensory circuits connotes the commonality and importance of context-dependent coding in the sensory neural circuits.

Neurons in the early stage of the visual system, the retina, are known to be subject to contextual modulation. The light responses of retinal neurons can be powerfully modulated by ambient illumination (Farrow et al., 2013; Pearson and Kerschensteiner, 2015; Tikidji-Hamburyan et al., 2014), background pattern (Chiao and Masland, 2003; Kuhn and Gollisch, 2016; Ölveczky et al., 2003) or previous visual stimulations (Appleby and Manookin, 2019; Demb, 2008; Kastner and Baccus, 2011, 2013; Kastner et al., 2019; Khani and Gollisch, 2017; Kim and Rieke, 2001; Manookin and Demb, 2006; Matulis et al., 2020; Nikolaev et al., 2013; Rieke and Rudd, 2009; Wark et al., 2009). Despite its peripheral location, retina is part of the central nervous system. However, in contrast to the other parts of the brain, retina is relatively isolated and easier for experimental access, which makes it an outstanding and convenient platform to study the fundamental principles and mechanisms of contextual modulation in the visual system.

1.2 Retinal neural circuit as a model system

The vertebrate retina consists of around 100 cell types that are assembled into intricate circuitry for visual processing. As one of the most approachable parts of the central nervous system (CNS), the retina is an excellent model system to study the principles of neural encodings by microcircuits owing to its highly ordered architecture, well-defined cell types, and experimental accessibility. Retina contains five neuronal cell classes: photoreceptors (PR), horizontal cells (HC), bipolar cells (BC), amacrine cells (AC), and retinal ganglion cells (RGCs). Their cell bodies and neuronal processes are segregated into three cellular or

nuclear layers and two intercalating synaptic or plexiform layers (Figures 1.1a and 1.1b). Incoming photons are first detected by photoreceptors and converted to chemical signals in the form of glutamate release. Next, the visually-evoked signals are relayed and transformed by a myriad of synaptic connections and ultimately lead to distinct firing patterns of around 30 types of output neurons, RGCs (Baden et al., 2016; Sanes and Masland, 2015). The spiking activity of each RGC type encodes a specific feature of the visual scene, and is conveyed to one or more retinorecipient brain regions via the optic nerve for further processing.

While the spiking patterns of different RGC types are dictated by distinct wiring patterns of their underlying synaptic circuits, the cellular organization of the retina by the five broad retinal cell classes follows a general scheme (Figure 1.1c). Common to all ganglion cells is a serial glutamatergic pathway from photoreceptors to bipolar cells, and subsequently from bipolar cells to RGCs. This glutamatergic pathway provides the primary excitatory drive to RGCs and is profoundly modified by local interneurons in the two plexiform layers. In the outer plexiform layer (OPL), horizontal cells are activated by photoreceptor glutamate release, and mediate the inhibition of photoreceptor-bipolar cell signaling through their laterally extending neurites. In the inner plexiform layer (IPL), diverse types of amacrine cells receive bipolar cell inputs, and subsequently synapse onto bipolar cells and/or RGCs in a cell-type specific manner. Different types of amacrine cells stratify their neurites and form synapses with specific types of bipolar cells and/or RGCs in distinct IPL sublaminae, contributing to the diversity of RGC firing patterns. The two prominent features of the retina, the laminar organization of cell bodies and neurites, and diverse synaptic circuits assembled from canonical microcircuit motifs, are also prevalent throughout the brain and conserved across animal species. The neural mechanisms discovered in the retina have yielded important insights into fundamental principles of neural coding in the central neural circuit.

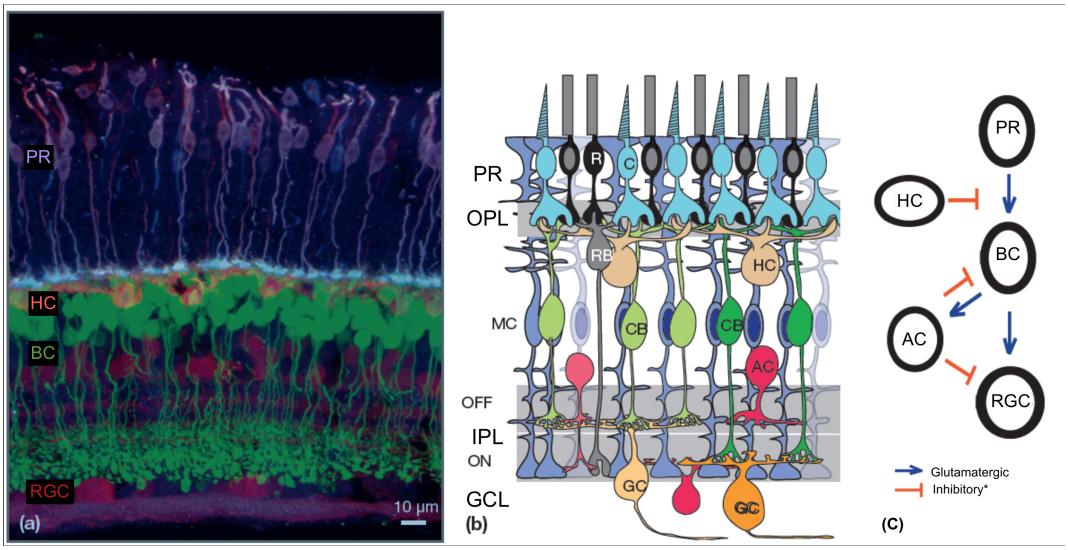

Figure 1.1: **Synaptic organization of the vertebrate retina.**
a, Cross section of an adult mouse retina in which a subclass of bipolar cells (BC) expresses green fluorescent protein. The section was immunostained for photoreceptors (PR) using anti-cone arrestin, horizontal cells (HC), amacrine cells (AC), and retinal ganglion cells (RGC) using anti-calbindin. Reproduced from Morgan JL, Dhingra A, Vardi N, Wong ROL, 2006. Neuroepithelial-like processes provide the substrate for axo- and dendrogenesis in retinal bipolar cells. Nature Neuroscience 9: 85-92.
b, Schematic of the laminar organization of retinal neurons. OPL, IPL: outer and inner plexiform layers; GCL: ganglion cell layer; PR, photoreceptor; MC: Muller glial cell; R, rod; C, cone; RB, rod bipolar cell; CB, cone bipolar cell; AC, amacrine cell; GC, ganglion cell. ON, ON sublamina; OFF, OFF sublamina.
a and **b** are adapted from Fig 36.1 of Yoshimatsu et al. Chapter 36 in Rubenstein, J. L. R., and Rakic, P. 2013. Cellular Migration and Formation of Neuronal Connections: Comprehensive developmental neuroscience. Volume 2 http://dx.doi.org/10.1016/B978-0-12-397266-8.00114-9 Amsterdam: Elsevier/AP. 2013).
c, Canonical circuit of the retina. Most amacrine cell types are inhibitory and release GABA or glycine, with exceptions that certain ACs are glutamtergic or co-release two neurotransmitter types (see text for details).

1.3 Shaping of RGC spiking activities by inputs from bipolar cells and amacrine cells

Inner retinal circuitry converges on RGC dendrites with spatially distributed excitatory and inhibitory inputs. Spiking activities of RGCs are profoundly shaped these inputs from bipolar cells and amacrine cells. Therefore, a thorough understanding of the inner retinal circuitry involving bipolar cells, amacrine cells and RGCs is critical for investigation of neural mechanisms of contextual modulation in RGCs.

In the inner retina, both amacrine cells and RGCs use ionotropic glutamatergic receptors (iGluRs) to transform glutamatergic inputs from bipolar cells into membrane depolarization (excitation). Amacrine cells, once activated by bipolar cells, provide conventional feedforward synapses to RGCs and/or feedback synapses to bipolar cell axons. Therefore, amacrine cell signaling profoundly shapes the retinal outputs both by directly synapsing onto RGCs and by shaping the excitatory inputs to RGCs. Most amacrine cells are either GABAergic (Pourcho and Goebel, 1983; Wassle and Boycott, 1991) or glycinergic (Hendrickson et al., 1988; Okada et al., 1994; Pourcho and Goebel, 1985, 1987), with the exceptions of an amacrine cell type that is non-GABAergic and non-glycinergic (nGnG AC) (Kay et al., 2011) and a glutamatergic monopolar interneuron (GluMI) (Della Santina et al., 2016). Additionally, there are dual-neurotransmitter releasing amacrine cells, including starburst amacrine cells (SACs) (co-releasing GABA and acetylcholine) (Brecha et al., 1988; Famiglietti, 1991; Kosaka et al., 1988; O'Malley and Masland, 1989; Vaney and Young, 1988), VGluT3 amacrine cells (co-releasing glycine and glutamate) (Haverkamp and Wässle, 2004; Lee et al., 2014) and TH-expressing amacrine cell (co-releasing GABA and dopamine) (Hirasawa et al., 2009). Subsets of GABAergic amacrine cells have also been shown to contain neuromodulators such as serotonin, catecholamines or neuropeptides (Karten and Brecha, 1983). In addition, gap junctions are present in multiple types of bipolar cells, amacrine cells

and RGCs and mediate specific aspects of visual processing in the IPL (Völgyi et al., 2013). Together, diverse and specialized synaptic connections between amacrine cells, bipolar cells and RGCs build up the elaborate IPL circuitry that essentially shape the spiking activities of RGCs.

1.4 Encoding of motion direction by the direction-selective circuit

1.4.1 Directional tuning in the On-Off DSGC

Within the RGC population, On-Off direction selective ganglion cell (On-Off DSGC) is one of the most representative cell types and well known for its robust encoding of motion direction. The firing rate of On-Off DSGC is strongest during motion in the preferred direction but weakest during motion in the opposite direction ("null direction") (Barlow et al., 1964). There are four subtypes of On-Off DSGCs, each preferring motion in one of the four cardinal directions (superior, inferior, anterior and posterior) (Oyster and Barlow, 1967; Sabbah et al., 2017). Among them, the posterior direction preferred On-Off DSGC (pDSGC) is the most numerous subtype and is selectively activated by motion direction from head to tail (Sabbah et al., 2017).

On-Off DSGC light responses can be triggered by both increment (On) or decrement (Off) of light luminance. These On and Off responses are processed by the On and Off layers of their bistratified dendritic arbors respectively. Within each layer, On-Off DSGC receives glutamatergic excitatory inputs from cone bipolar cells CBC2/CBC5 (Duan et al., 2014; Morrie and Feller, 2016), as well as cholinergic and GABAergic inputs from starburst amacrine cell (SAC) (Brecha et al., 1988; Famiglietti, 1991, 1992; Kosaka et al., 1988;

O'Malley and Masland, 1989; Vaney and Young, 1988). The directional preference of On-Off DSGC mainly depends on asymmetric GABAergic inhibition from starburst amacrine cell (SAC) (Figure 1.2a) (Chen and Wei, 2018; Wei, 2018), while the contribution of the excitatory inputs to the direction selectivity is still controversial (Park et al., 2014; Pei et al., 2015; Taylor and Vaney, 2002).

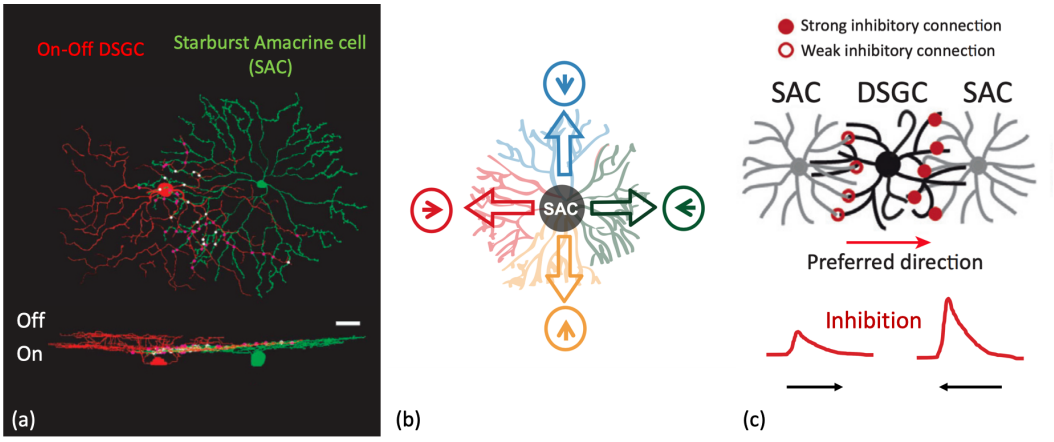

Figure 1.2: **Direction-selective inhibition from SAC onto On-Off DSGC.**
a, Morphology and co-stratification of On-Off DSGC and an On SAC. Reproduced from Wei, W., Hamby, A.M., Zhou, K., and Feller, M.B, 2011. Development of asymmetric inhibition underlying direction selectivity in the retina. Nature 469, 402–406.
b, Schematic of the centrifugal preference of SAC as well as the antiparallel wiring between SAC and DSGC. Reproduced from Chen, Q., and Wei, W. (2018). Stimulus-dependent engagement of neural mechanisms for reliable motion detection in the mouse retina. Journal of Neurophysiology 120, 1153–1161.
c, Schematic shows the directionally tuned inhibitory inputs from SAC onto DSGC. Top: the asymmetric SAC-DSGC wiring in the preferred side versus the null side of the DSGC. Bottom, the direction-selective inhibitory postsynaptic currents detected in DSGC during motion in the preferred versus null direction.

1.4.2 Physiological properties of SAC

SAC shows three properties that are crucial for providing the directionally tuned inhibition onto On-Off DSGC:

First, the activation of SAC is compartmentalized within dendritic sectors. Each dendritic sector can thus be considered as a relatively electronically isolated unit for encoding of motion direction (Figure 1.2b) (Euler et al., 2002; Koren et al., 2017; Miller and Bloomfield, 1983).

Second, SAC is preferentially activated by motion in the centrifugal direction rather than centripetal direction (Euler et al., 2002). That means, each dendritic sector of SAC is strongly activated by visual stimulus moving from their soma to dendritic distal tips, but not the opposite direction (Figure 1.2b).

Third, each dendritic sector of SAC is synaptically wired to DSGC preferring the antiparallel direction (Figure 1.2b) (Barlow and Levick, 1965; Briggman et al., 2011; Fried et al., 2002; Lee et al., 2010; Wei et al., 2011). Therefore, from the perspective of DSGC, there is little synaptic contact with SAC dendrites whose distal tips pointing to the preferred direction, but strong inhibitory connection with SAC dendrites oriented towards the DSGC null direction (Figure 1.2c).

Overall, asymmetric inhibition onto DSGC can thus be generated after taking these three physiological properties of SAC into consideration. When motion is along the preferred direction, the SAC dendritic sectors parallel to the preferred direction are strongly activated but only weakly connected to DSGC. Therefore, SAC provides mild inhibitory postsynaptic current (IPSC) that allows for high firing rate in DSGC. In contrast, when motion is along the null direction, it maximally activates the SAC dendrites antiparallel to the preferred direction, and thus triggers pronounced IPSC that suppresses the DSGC firing rate (Figure 1.2c).

1.5 Aim of this study

Although On-Off DSGC has been voluminously investigated about its robust encoding of motion direction, how its light responses can be dynamically modulated by surrounding or prior visual stimulus is not fully understood. Therefore, the goal of this study was to use electrophysiology, genetic manipulations, pharmacology, morphological reconstruction, and computational modeling to delineate the phenomenon of contextual modulation in the On-Off DSGC, and also to gain insight into the underlying mechanisms in the mouse retina. The investigation of contextual modulation in On-Off DSGC was conducted from spatial and temporal perspectives, which are described in Chapter 2 and Chapter 3 of this thesis respectively. Together, our results uncover the neural mechanisms of spatial and temporal contextual modulation in the mouse direction-selective circuit, and highlight a multiplexed and extended neural network that integrate divergent synaptic inputs under various environmental conditions. The findings from this thesis will therefore contribute to a more comprehensive understanding of the retinal encoding of motion direction in the ever-changing naturalistic environment.

1.6 References

Akyuz, S., Pavan, A., Kaya, U., and Kafaligonul, H. (2020). Short- and long-term forms of neural adaptation: An ERP investigation of dynamic motion aftereffects. Cortex 125, 122–134.

Albright, T.D., and Stoner, G.R. (2002). Contextual Influences on Visual Processing. Annual Review of Neuroscience 25, 339–379.

Appleby, T.R., and Manookin, M.B. (2019). Neural sensitization improves encoding fidelity in the primate retina. Nature Communications 2019 10:1 10, 1–15.

Baden, T., Berens, P., Franke, K., Román Rosón, M., Bethge, M., and Euler, T. (2016). The functional diversity of retinal ganglion cells in the mouse. Nature 529, 345–350.

Barchini, J., Shi, X., Chen, H., and Cang, J. (2018). Bidirectional encoding of motion contrast in the mouse superior colliculus. ELife 7.

Barlow, H.B., and Levick, W.R. (1965). The mechanism of directionally selective units in rabbit's retina. The Journal of Physiology 178, 477–504.

Barlow, H.B., Hill, R.M., and Levick, W.R. (1964). Retinal ganglion cells responding selectively to direction and speed of image motion in the rabbit. The Journal of Physiology 173, 407.

Brecha, N., Johnson, D., Peichl, L., and Wässle, H. (1988). Cholinergic amacrine cells of the rabbit retina contain glutamate decarboxylase and gamma-aminobutyrate immunoreactivity. Proceedings of the National Academy of Sciences of the United States of America 85, 6187–6191.

Briggman, K.L., Helmstaedter, M., and Denk, W. (2011). Wiring specificity in the direction-selectivity circuit of the retina. Nature 471, 183–188.

Chen, Q., and Wei, W. (2018). Stimulus-dependent engagement of neural mechanisms for reliable motion detection in the mouse retina. Journal of Neurophysiology 120, 1153–1161.

Chiao, C.-C., and Masland, R.H. (2003). Contextual tuning of direction-selective retinal

ganglion cells. Nature Neuroscience 6, 1251–1252.

Clifford, C.W.G., Wenderoth, P., and Spehar, B. (2000). A functional angle on some after-effects in cortical vision. Proceedings of the Royal Society of London. Series B: Biological Sciences 267, 1705–1710.

Demb, J.B. (2008). Functional circuitry of visual adaptation in the retina. The Journal of Physiology 586, 4377–4384.

Duan, X., Krishnaswamy, A., de la Huerta, I., and Sanes, J.R. (2014). Type II cadherins guide assembly of a direction-selective retinal circuit. Cell 158, 793–807.

Euler, T., Detwiler, P.B., and Denk, W. (2002). Directionally selective calcium signals in dendrites of starburst amacrine cells. Nature 418, 845–852.

Famiglietti, E. v (1991). Synaptic organization of starburst amacrine cells in rabbit retina: analysis of serial thin sections by electron microscopy and graphic reconstruction. The Journal of Comparative Neurology 309, 40–70.

Famiglietti, E. v. (1992). Dendritic Co-stratification of ON and ON-OFF directionally selective ganglion cells with starburst amacrine cells in rabbit retina. The Journal of Comparative Neurology 324, 322–335.

Farrow, K., Teixeira, M., Szikra, T., Viney, T.J.J., Balint, K., Yonehara, K., and Roska, B. (2013). Ambient illumination toggles a neuronal circuit switch in the retina and visual perception at cone threshold. Neuron 78, 325–338.

Fried, S.I., Münch, T.A., and Werblin, F.S. (2002). Mechanisms and circuitry underlying directional selectivity in the retina. Nature 420, 411–414.

Gilbert, C.D., and Wiesel, T.N. (1990). The influence of contextual stimuli on the orientation selectivity of cells in primary visual cortex of the cat. Vision Research 30, 1689–1701.

Haverkamp, S., and Wässle, H. (2004). Characterization of an amacrine cell type of the mammalian retina immunoreactive for vesicular glutamate transporter 3. Journal of Comparative Neurology 468, 251–263.

Hendrickson, A.E., Koontz, M.A., Pourcho, R.G., Sarthy, P.V., and Goebel, D.J. (1988). Localization of glycine-containing neurons in the Macaca monkey retina. Journal of Comparative Neurology.

Hirasawa, H., Puopolo, M., and Raviola, E. (2009). Extrasynaptic Release of GABA by Retinal Dopaminergic Neurons. Journal of Neurophysiology 102, 146–158.

Kamkar, S., Moghaddam, H.A., and Lashgari, R. (2018). Early Visual Processing of Feature Saliency Tasks: A Review of Psychophysical Experiments. Frontiers in Systems Neuroscience 12, 54.

Karten, H.J., and Brecha, N. (1983). Localization of neuroactive substances in the vertebrate retina: evidence for lamination in the inner plexiform layer. Vision Research 23, 1197–1205.

Kastner, D.B., and Baccus, S.A. (2011). Coordinated dynamic encoding in the retina using opposing forms of plasticity. Nature Neuroscience 2011 14:10 14, 1317–1322.

Kastner, D.B., and Baccus, S.A. (2013). Spatial Segregation of Adaptation and Predictive Sensitization in Retinal Ganglion Cells. Neuron 79, 541–554.

Kastner, D.B., Ozuysal, Y., Panagiotakos, G., and Baccus, S.A. (2019). Adaptation of Inhibition Mediates Retinal Sensitization. Current Biology 29, 2640-2651.e4.

Kay, J.N., Voinescu, P.E., Chu, M.W., and Sanes, J.R. (2011). Neurod6 expression defines new retinal amacrine cell subtypes and regulates their fate. Nature Neuroscience 14, 965–972.

Khani, M.H., and Gollisch, T. (2017). Diversity in spatial scope of contrast adaptation among mouse retinal ganglion cells. Journal of Neurophysiology 118, 3024–3043.

Kim, K.J., and Rieke, F. (2001). Temporal contrast adaptation in the input and output signals of salamander retinal ganglion cells. Journal of Neuroscience 21, 287–299.

Kohn, A. (2007). Visual adaptation: physiology, mechanisms, and functional benefits. Journal of Neurophysiology 97, 3155–3164.

Koren, D., Grove, J.C.R., and Wei, W. (2017). Cross-compartmental Modulation of Den-

dritic Signals for Retinal Direction Selectivity. Neuron 95, 914-927.e4.

Kosaka, T., Tauchi, M., and Dahl, J.L. (1988). Cholinergic neurons containing GABA-like and/or glutamic acid decarboxylase-like immunoreactivities in various brain regions of the rat. Experimental Brain Research 70, 605–617.

Kuhn, N.K., and Gollisch, T. (2016). Joint Encoding of Object Motion and Motion Direction in the Salamander Retina. Journal of Neuroscience 36, 12203–12216.

Lee, S., Kim, K., and Zhou, Z.J. (2010). Role of ACh-GABA cotransmission in detecting image motion and motion direction. Neuron 68, 1159–1172.

Lee, S., Chen, L., Chen, M., Ye, M., Seal, R.P., and Zhou, Z.J. (2014). An unconventional glutamatergic circuit in the retina formed by vGluT3 amacrine cells. Neuron 84, 708–715.

Manookin, M.B., and Demb, J.B. (2006). Presynaptic Mechanism for Slow Contrast Adaptation in Mammalian Retinal Ganglion Cells. Neuron.

Matulis, C.A., Chen, J., Gonzalez-Suarez, A.D., Behnia, R., and Clark, D.A. (2020). Heterogeneous Temporal Contrast Adaptation in Drosophila Direction-Selective Circuits. Current Biology 30, 222-236.e6.

Miller, R.F., and Bloomfield, S.A. (1983). Electroanatomy of a unique amacrine cell in the rabbit retina. Proceedings of the National Academy of Sciences of the United States of America 80, 3069–3073.

Morrie, R.D., and Feller, M.B. (2016). Development of synaptic connectivity in the retinal direction selective circuit. Current Opinion in Neurobiology 40, 52.

Nikolaev, A., Leung, K.-M., Odermatt, B., and Lagnado, L. (2013). Synaptic mechanisms of adaptation and sensitization in the retina. Nature Neuroscience 2013 16:7 16, 934–941.

Okada, M., Erickson, A., and Hendrickson, A. (1994). Light and electron microscopic analysis of synaptic development in Macaca monkey retina as detected by immunocytochemical labeling for the synaptic vesicle protein, SV2. Journal of Comparative Neurology 339, 535–558.

Ölveczky, B.P., Baccus, S.A., and Meister, M. (2003). Segregation of object and background motion in the retina. Nature 423, 401–408.

O'Malley, D.M., and Masland, R.H. (1989). Co-release of acetylcholine and gamma-aminobutyric acid by a retinal neuron. Proceedings of the National Academy of Sciences of the United States of America 86, 3414–3418.

Oyster, C.W., and Barlow, H.B. (1967). Direction-selective units in rabbit retina: Distribution of preferred directions. Science.

Park, S.J.H., Kim, I.-J., Looger, L.L., Demb, J.B., and Borghuis, B.G. (2014). Excitatory Synaptic Inputs to Mouse On-Off Direction-Selective Retinal Ganglion Cells Lack Direction Tuning. The Journal of Neuroscience 34, 3981.

Pearson, J.T., and Kerschensteiner, D. (2015). Ambient illumination switches contrast preference of specific retinal processing streams. Journal of Neurophysiology 114, jn.00360.2015.

Pei, Z., Chen, Q., Koren, D., Giammarinaro, B., Acaron Ledesma, H., and Wei, W. (2015). Conditional Knock-Out of Vesicular GABA Transporter Gene from Starburst Amacrine Cells Reveals the Contributions of Multiple Synaptic Mechanisms Underlying Direction Selectivity in the Retina. The Journal of Neuroscience 35, 13219–13232.

Pourcho, R.G., and Goebel, D.J. (1983). Neuronal subpopulations in cat retina which accumulate the GABA agonist, (3H)muscimol: A combined Golgi and autoradiographic study. Journal of Comparative Neurology.

Pourcho, R.G., and Goebel, D.J. (1985). Immunocytochemical demonstration of glycine in retina. Brain Research.

Pourcho, R.G., and Goebel, D.J. (1987). A combined Golgi and autoradiographic study of 3H-glycine-accumulating cone bipolar cells in the cat retina. J Neurosci.

Rieke, F., and Rudd, M.E. (2009). The Challenges Natural Images Pose for Visual Adaptation. Neuron 64, 605–616.

Sabbah, S., Gemmer, J.A., Bhatia-Lin, A., Manoff, G., Castro, G., Siegel, J.K., Jeffery, N.,

and Berson, D.M. (2017). A retinal code for motion along the gravitational and body axes. Nature 546.

Sanes, J.R., and Masland, R.H. (2015). The types of retinal ganglion cells: current status and implications for neuronal classification. Annual Review of Neuroscience 38, 221–246.

Della Santina, L., Kuo, S.P., Yoshimatsu, T., Okawa, H., Suzuki, S.C., Hoon, M., Tsubo-yama, K., Rieke, F., and Wong, R.O.L. (2016). Glutamatergic Monopolar Interneurons Provide a Novel Pathway of Excitation in the Mouse Retina. Current Biology: CB 26, 2070–2077.

Schwartz, O., Hsu, A., and Dayan, P. (2007). Space and time in visual context. Nature Reviews Neuroscience 8, 522–535.

Taylor, W.R., and Vaney, D.I. (2002). Diverse synaptic mechanisms generate direction selectivity in the rabbit retina. The Journal of Neuroscience 22, 7712–7720.

Theeuwes, J. (2013). Feature-based attention: it is all bottom-up priming. Philosophical Transactions of the Royal Society of London. Series B, Biological Sciences 368.

Tikidji-Hamburyan, A., Reinhard, K., Seitter, H., Hovhannisyan, A., Procyk, C.A., Allen, A.E., Schenk, M., Lucas, R.J., and Münch, T.A. (2014). Retinal output changes qualitatively with every change in ambient illuminance. Nature Neuroscience 18, 66–74.

Torralba, A., Oliva, A., Castelhano, M.S., and Henderson, J.M. (2006). Contextual guidance of eye movements and attention in real-world scenes: The role of global features in object search. Psychological Review.

Vaney, D.I., and Young, H.M. (1988). GABA-like immunoreactivity in cholinergic amacrine cells of the rabbit retina. Brain Research 438, 369–373.

Völgyi, B., Kovács-Öller, T., Atlasz, T., Wilhelm, M., and Gábriel, R. (2013). Gap junctional coupling in the vertebrate retina: Variations on one theme? Progress in Retinal and Eye Research 34, 1–18.

Wark, B., Fairhall, A., and Rieke, F. (2009). Timescales of Inference in Visual Adaptation.

Neuron 61, 750–761.

Wassle, H., and Boycott, B.B. (1991). Functional Architecture of the Mammalian Retina. Physiological Reviews.

Wei, W. (2018). Neural Mechanisms of Motion Processing in the Mammalian Retina. Annual Review of Vision Science 4, 165–192.

Wei, W., Hamby, A.M., Zhou, K., and Feller, M.B. (2011). Development of asymmetric inhibition underlying direction selectivity in the retina. Nature 469, 402–406.

CHAPTER 2

SPATIAL CONTEXTUAL MODULATION IN THE RETINAL DIRECTION SELECTIVE CIRCUIT

This chapter is a full reprint of Huang et al., *Nature Communications*, in which I am the primary author. The work is included with permission from all authors.

Relevant Publication

Huang, X., Rangel, M., Briggman, K.L., Wei, W., **Neural mechanisms of contextual modulation in the retinal direction selective circuit.** *Nat Commun* **10**, 2431 (2019).

For supplementary multimedia documents, please refer to

`https://doi.org/10.1038/s41467-019-10268-z`

2.1 Abstract

Contextual modulation of neuronal responses by surrounding environments is a fundamental attribute of sensory processing. In the mammalian retina, responses of On-Off direction selective ganglion cells (DSGCs) are modulated by motion contexts. However, the underlying mechanisms are unknown. Here, we show that posterior-preferring DSGCs (pDSGCs) are sensitive to discontinuities of moving contours owing to contextually modulated cholinergic excitation from starburst amacrine cells (SACs). Using a combination of synapse-specific genetic manipulations, patch clamp electrophysiology and connectomic analysis, we identified distinct circuit motifs upstream of On and Off SACs that are required for the contextual modulation of pDSGC activity for bright and dark contrasts. Furthermore, our results reveal a class of wide-field amacrine cells (WACs) with straight, unbranching dendrites that function as "continuity detectors" of moving contours. Therefore, divergent circuit motifs in the On and Off pathways extend the information encoding of On-Off DSGCs beyond their direction selectivity during complex stimuli.

2.2 Introduction

The visual information an animal obtains at a local region is profoundly shaped by the surrounding environment. This perceptual attribute has been linked to context-dependent modulation of visual neuronal responses: the activity of a neuron driven by a target stimulus in its classic receptive field (RF) (referred to as RF center) is differentially facilitated or suppressed based on the luminance, contrast and spatiotemporal properties of the stimuli in the surround (Albright and Stoner, 2002). Contextual modulation arises early in the visual pathway and is readily detectable in multiple retinal ganglion cell types in the vertebrate retina (Farrow et al., 2013; Kuhn and Gollisch, 2016; Ölveczky et al., 2003; Pearson and Kerschensteiner, 2015; Tikidji-Hamburyan et al., 2014).

On-Off DSGCs, which are well-studied for their encoding of motion direction, are subject to contextual modulation. Sensitivity to motion contexts has been reported in rabbit DSGCs using preferred-direction drifting gratings in the center and surround that differ in spatial phase, spatial frequency or temporal frequency (Chiao and Masland, 2003). However, whether On-Off DSGCs prefer discontinuities in spatial texture in the absence of motion is unclear. Furthermore, the contextual modulation of the On and Off responses of DSGCs has not been separately examined. And importantly, the synaptic mechanisms underlying the contextual modulation of On-Off DSGCs are unknown.

A mechanistic understanding of the contextual tuning of On-Off DSGCs requires investigation of the underlying synaptic circuitry. In accordance with the general rule of retinal circuit organization, the responses of DSGCs to bright and dark moving edges are separately processed by the On and Off pathways. The bistratified dendritic arbors of On-Off DSGCs are located in the On and Off sublaminae of the inner plexiform layer that are specialized for processing bright and dark contrasts. At each sublamina, the On or Off den-

dritic layer receives glutamatergic input from On or Off bipolar cells and lateral cholinergic and GABAergic inputs from On or Off starburst amacrine cells (SACs) (Figures. 2.1a and 2.1b) (Famiglietti, 1991, 1992). GABAergic inputs from On and Off SACs to DSGCs are strongest during motion in the null direction and weakest in the preferred direction (Figure. 2.1b) (Briggman et al., 2011; Euler et al., 2002; Fried et al., 2002; Lee et al., 2010; Taylor and Vaney, 2002). This directionally tuned inhibition, together with a rich set of other circuit and intrinsic mechanisms, form the neural basis of retinal direction selectivity (Chen and Wei, 2018). Despite an increasingly detailed wiring diagram for the direction selectivity of On-Off DSGCs, contextual modulation of On-Off DSGCs by motion stimuli in the RF surround eludes the current circuit model.

In this study, we determine how the On and Off spiking responses of mouse posterior-preferring On-Off DSGCs (pDSGCs) are differentially modulated by motion contexts and identified the underlying microcircuit motifs in the On and Off pathways. We found that SAC-mediate cholinergic outputs at On and Off sublamina are differentially modulated by a class of WACs with long, straight dendrites that are sensitive to continuity of moving contours. These WACs confer contextual sensitivity of pDSGC responses by shaping SAC-mediated cholinergic excitation. Our results link the existing circuit motifs mediating direction selectivity to the extensive inner retinal network, highlighting a multilayered circuit architecture that dynamically engages specific microcircuit motifs to process motion information according to the composition of visual features in the visual stimulus.

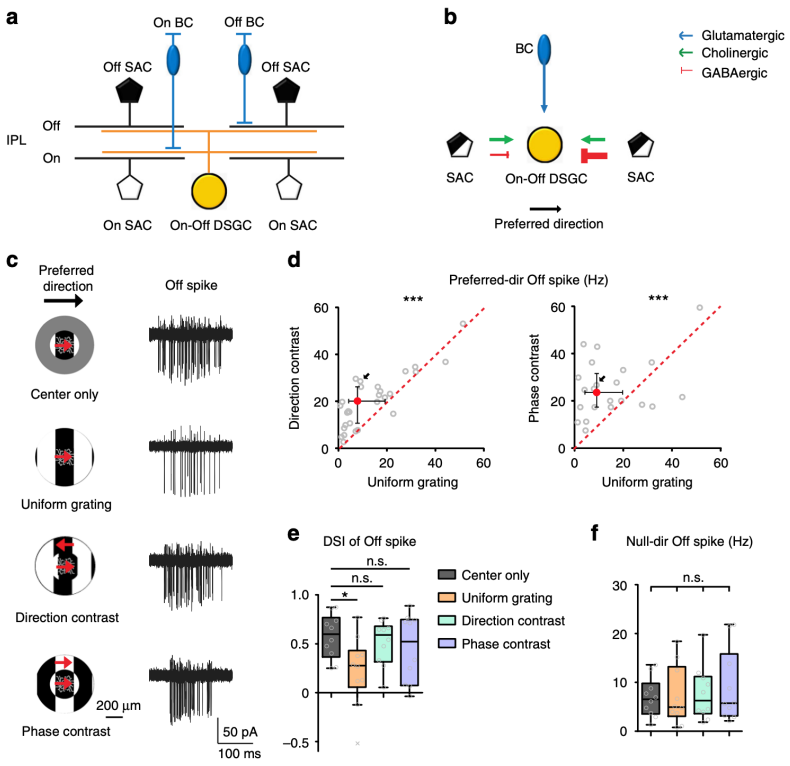

Figure 2.1: **pDSGC Off responses are contextually modulated.**
a, Schematic shows side view of the laminar organization of bipolar cells (BCs), SACs and On-Off DSGCs in the inner plexiform layer (IPL).
b, Simplified schematic shows major types of synaptic inputs onto On-Off DSGCs.
c, Left: Schematics show the visual stimulus conditions. A schematic of a pDSGC is shown in the center of each stimulus to indicate the relative sizes of DSGC dendritic arbors and visual stimuli. The red arrows indicate the moving directions of the drifting gratings, and the black arrow at the top indicates the preferred direction of the pDSGC. Right: Example Off spike traces of a pDSGC from a control mouse evoked by the stimuli on the left. Spike traces are overlays of 10 grating cycles (also see Methods) for this and subsequent figures.
d, Scatter plots compare Off firing rate during uniform versus compound gratings. Direction-contrast vs uniform grating: n = 29 cells from 13 mice; phase-contrast vs uniform grating: n = 22 cells from 9 mice. Wilcoxon signed-rank test, ***p $<$ 0.001. Grey dots represent individual cells, red dots with error bars indicate the median ± IQR, and diagonal red dashed lines are unity lines. The data point corresponding to the example traces was labelled by the black arrow.
e, Direction selectivity index (DSI) of pDSGC Off spiking in different stimulus contexts. Friedman test: n = 10 cells from 4 mice, *p = 0.025. Wilcoxon signed-rank test with Bonferroni correction: center only vs uniform grating: *p = 0.0039; center only vs direction-contrast: p = 0.23; center only vs phase-contrast: p = 0.70. Box plots represent minimum / first quartile / median / third quartile / maximum values, open grey dots represent individual cells, grey crosses are outliers defined by Tukey's fences.
f, pDSGC Off firing rate when center gratings drift in the null direction. Friedman test: n = 10 cells from 4 mice, p = 0.29.

2.3 Materials and Methods

2.3.1 Mice

The $Gabra2^{flox/flox}$ mouse line was a generous gift from Dr. Uwe Rudolph at Harvard Medical School. $Vgat^{flox/flox}$ mice ($Slc32a1 < tm1Lowl > /J$), $Chat-IRES-Cre$ mice ($129S6-Chat^{tm2(cre)Lowl}/J$) and floxed $tdTomato$ mice ($129S6-Gt(ROSA)26Sor^{tm9(CAG-tdTomato)Hze}/J$) were acquired from the Jackson Laboratory. $Drd4$–GFP mice were originally developed by MMRRC (`http://www.mmrrc.org/strains/231/0231.html`) in the Swiss Webster background, and were subsequently backcrossed to $C57BL/6$ background. All strains were backcrossed to the C57BL/6 background in our laboratory, and crossed to each other to create the lines used in this study. Mice of ages P22-P68 of either sex were used. All procedures to maintain and use mice were in accordance with the University of Chicago Institutional Animal Care and Use Committee (Protocol number ACUP 72247) and in conformance with the NIH Guide for the Care and Use of Laboratory Animals and the Public Health Service Policy.

Control mice with normal retinal circuitry contain the following transgenes: $Drd4-GFP$ for labeling of On-Off DSGCs, and $ChAT-Cre$ and $floxedtdTomato$ for labeling of SACs. Vgat conditional KO mice contain additional homozygous $Vgat^{flox/flox}$ alleles. Gabra2 conditional KO mice contain additional homozygous $Gabra2^{flox/flox}$ alleles.

2.3.2 Whole-mount retina preparation

After dark adaptation for > 30 min, mice were anesthetized with isoflurane and euthanized by decapitation. Retinas were isolated from the pigment epithelium under infrared illumination at room temperature in oxygenated Ames' medium (Sigma-Aldrich, St. Louis, MO).

The retinas were then cut into halves and mounted ganglion-cell-layer-up on top of a $\sim$1.5 mm^2 hole in a small piece of filter paper (Millipore, Billerica, MA). Cells in the center of the hole were used for experiments. The mounted retinas were kept in darkness at room temperature in Ames' medium bubbled with 95% O_2/5% CO_2 until use (0–8 hr).

2.3.3 Visual stimulation

A white organic light-emitting display (OLEDXL, eMagin, Bellevue, WA; 800 $\times$ 600 pixel resolution, 60 Hz refresh rate) was controlled by an Intel Core Duo computer with a Windows 7 operating system and was presented to the retina at a resolution of 1.1 μm/pixel. All stimuli were generated by MATLAB and the Psychophysics Toolbox (Brainard, 1997), projected through the condenser lens of the two-photon microscope focusing on the photoreceptor layer, and centered to the cell somas.

The diameter of center stimuli is 330 μm to ensure complete coverage of the receptive field center for all pDSGCs with diverse dendritic morphology (Huberman et al., 2009; Pei et al., 2015). This center size is also near the peak of spatial tuning curve of mouse On-Off DSGCs using bright spots of increasing size (Hoggarth et al., 2015; Jacoby and Schwartz, 2017; Trenholm et al., 2011). The surround diameter is 660 μm, which is the maximum diameter in our visual stimulus setup and evokes significant suppression of the center response (Hoggarth et al., 2015; Trenholm et al., 2011). The spatial (412 μm/cycle, corresponding to 12.5 degree/cycle, or 0.08 cycle/degree) and temporal frequencies (2 cycles/second) of the square gratings lie in the optimal range for mouse On-Off DSGCs to maximize the center response in the preferred direction (Hoggarth et al., 2015). These frequencies correspond to alternating bright and dark 206 μm-width bars moving at a speed of 824 μm/s over the retina. Contrast-reversing square gratings share the same size and spatial frequency as drift-

ing gratings, and the gratings were counterphased at 0.5Hz, or say, the duration of bright and dark bars is 1 s respectively.

All experiments used a mean light intensity of $\sim$ 1.6 x 10^5 isomerizations (R*)/rod/s in the photopic range. 100% square wave grating with a periodicity of 412 μm was used for both drifting grating and contrast-reversing grating stimuli. The light intensity for the white bar of the grating was $\sim$ 3.2 x 10^5 isomerizations (R*)/rod/s. The drifting grating moves at 2 Hz with duration of 3 s (6 grating cycles in total). In each set of stimuli, center gratings were always moving in the same direction while different stimulus contexts were presented in 3-6 trials of pseudorandomized sequence by Matlab. And the inter-trial-interval is 2s. When the direction of center drifting grating was altered in preferred or null directions, these two sets of stimuli were presented in random sequence as well. The light intensity of the gray area used in center-only and surround-only stimuli is the mean luminance of the square wave grating. A gray background with the same light intensity was used before stimuli for 10 s adaptation and also at inter-stimulus interval.

2.3.4 Cell targeting for electrophysiology

Cells were visualized with infrared light and an IR-sensitive video camera (Watec). GFP-labelled pDSGCs in $Drd4{-}GFP$ mice and floxed-tdTomato-labelled SACs in $Chat{-}IRES{-}Cre$ mice were targeted using a two-photon microscopy (Scientifica) and a Ti:sapphire laser (Spectra-Physics) tuned to 920 nm. DSGC identity was further confirmed physiologically by electrophysiological recordings of the responses to drifting grating and/or anatomically using internal solution containing 25 μM Alexa Fluo 594 (Life Technologies) to show the bistratified dendritic arbor and the cofasciculation with tdTomato-expressing SACs. For wild type mouse, the preferred direction of pDSGCs was determined physiologically. We also noted the

anatomical direction during the dissection, and physiologically measured preferred direction matched well with anatomical nasal direction, as reported by many other studies on this mouse line such as (Huberman et al., 2009; Kay et al., 2011; Pei et al., 2015; Sabbah et al., 2017). For Vgat cKO and Gabra2 cKO mouse where direction selectivity is impaired (Chen et al., 2016; Pei et al., 2015), the preferred direction of pDSGC was determined anatomically.

2.3.5 Electrophysiology recordings

Data were acquired using PCLAMP 10 recording software and a MultiClamp 700B amplifier (Molecular Devices, Sunnyvale, CA), low-pass filtered at 4 kHz and digitized at 10 kHz. Retina was kept in Ames' medium with a bath temperature of $32 - 34\,^{\circ}\mathrm{C}$. Recording electrodes of $3.5 - 5\ M\Omega$ were filled with Ames' medium for loose cell-attached recordings or a cesium-based internal solution for whole-cell recordings, which contains 110 mM $CsMeSO_4$, 2.8 mM NaCl, 4 mM EGTA, 5 mM TEA-Cl, 4 mM adenosine 5'-triphosphate (magnesium salt), 0.3 mM guanosine 5'-triphosphate (trisodium salt), 20 mM HEPES, 10 mM phosphocreatine (disodium salt), 5 mM N-Ethyllidocaine chloride (QX314) (Sigma), pH 7.25. Light-evoked EPSCs and IPSCs in pDSGCs and SACs were isolated by holding the cells at reversal potentials (0 mV for GABAergic and -60 mV for cholinergic). Liquid junction potential ($\sim$10 mV) was corrected. To investigate the contribution of different synaptic inputs, synaptic blockers 0.008 mM Dihydro-b-erythroidine hydrobromide (DHβE; from Tocris, Cat#2349; CAS: 29734-68-7) or 0.001 mM tetrodotoxin (TTX; from Tocris, Cat#1078; CAS: 4368-28-9) were used to selectively block the nicotinic acetylcholine receptors or voltage-gated Na^+ channels respectively.

2.3.6 Analysis of electrophysiological data

Data were averaged across 3-6 trials to obtain the mean response for each stimulus condition. Responses during the second to the sixth grating cycles were averaged and the responses during the first cycle were discarded to avoid the impact of wake-up responses to the onset of the stimulus. On and Off responses were separated based on the time window of the visual stimulus. For all the drifting grating stimuli, the center gratings always start at the same spatial location relative to the pDSGC, with the left dark edge moving from outside the outer rim of the pDSGC dendritic field (103 μm away from the soma) toward the center. During the five grating cycles in each trial (500 ms per cycle), we used alternating 250 ms windows for Off and On responses based on the periodic Off and On spiking and PSP waveforms. The same time window was used for both spiking and PSC recordings, and for all drifting grating stimuli in all mouse lines. The start of the Off window in each cycle corresponds to the center dark edge moving ~ 45 μm into the pDSGC dendritic field. For both spike and PSC recordings, responses were first averaged across trials, and then responses during second to sixth grating cycles were averaged.

For loose cell-attached recordings, data were analyzed using custom protocols in MATLAB to count the total number of spikes within each 250 ms On or Off window. Small spike-counts of center-only response are difficult to quantify further suppressive contextual modulation effects since the baseline response is too low to begin with. Therefore, for On or Off spiking datasets, cells with < 10 spike/trial during center-only stimulus were discarded. For whole-cell voltage clamp recordings, data were analyzed using PCLAMP 10 software to obtain the peak amplitude and total charge transfer of EPSCs and IPSCs. Membrane tests were performed to check the whole-cell recording quality, and recordings with series resistances > 25 $M\Omega$ were discarded. Correlation between EPSC waveform and the spiking activity was calculated based on PSTH with 100-ms bin size.

Suppression index (SI) was used to quantify the suppression strength, which is defined as: SI $= \frac{N_{center-only\,grating} - N_{full-field\,grating}}{N_{center-only\,grating} + N_{full-field\,grating}}$, where N is the firing rate. A higher positive SI value indicates stronger suppression, while a negative SI value indicates facilitation. Direction selective index (DSI) was used to quantify the direction selectivity, which is defined as DSI $= \frac{N_{preferred\,direction} - N_{null\,direction}}{N_{preferred\,direction} + N_{null\,direction}}$, where N is the firing rate. Contextual modulation index (CMI) was used to quantify the level of contextual modulation, which is defined as: CMI $= \frac{N_{compound\,grating} - N_{uniform\,grating}}{N_{compound\,grating} + N_{uniform\,grating}}$, where N is the firing rate. Compound grating here refers to direction-contrast or phase-contrast. For On SAC results, SI and CMI were calculated in the same way but with charge transfer instead of firing rate.

2.3.7 Connectomic reconstruction / Skeleton tracing and contact annotation

A previously published dataset acquired using scanning SBEM was analyzed (retina k0725; Ding et al., 2016). Voxel dimensions were 13.2 x 13.2 x 26 nanometer (nm) (x, y, and z, respectively). On sublamina WACs were first identified by exploratory tracing of dendrites postsynaptic to an On SAC. The dendrites of On WACs were readily distinguishable from postsynaptic On SACs due to the relatively straight trajectories of their dendrites. The presynaptic release sites along the dendrites of 3 On WACs (whose somata were also found within the EM volume) were then manually annotated. We sampled 59 of these release sites and classified the postsynaptic partners classified as either ganglion cell (n=6, 10%), amacrine cell (n=28, 47%) or bipolar cell (n=25, 42%).

We then examined the connections between the On WAC dendrites and previously reconstructed type 7 bipolar cells (Ding et al, 2016) and identified 23 synapses between the

On WACs and type 7 bipolar cells. Because we did not perform a complete sampling and only targeted the analysis to type 7 bipolar cell terminals, we cannot rule out whether the On WAC dendrites additionally synapse onto additional bipolar cell terminals.

All analyses were performed by tracing skeletons and annotating synapses using the Knossos software package (`https://knossostool.org/`, Helmstaedter et al., 2011).

2.3.8 Statistical analysis

Statistical comparisons were performed using Wilcoxon signed-rank test for single samples and paired samples or Wilcoxon rank-sum test for group samples. For multiple comparisons, Friedman test was used for repeated measurements while Kruskal-Wallis test was used for non-repeated measurements, and both were followed by post-hoc tests with Bonferroni correction. $p < 0.05$ was considered significant. *$p < 0.05$; **$p < 0.01$; ***$p < 0.001$.

Data Availability

All relevant data generated and analyzed in this study are available from the authors on reasonable request.

Acknowledgements

We thank Chen Zhang for managing mouse colony, Dr. Uwe Rudolph at Harvard Medical School for the generous gift of the $Gabra2^{flox/flox}$ mouse line. This work was supported by NIH R01 EY024016, McKnight Scholarship Award and Sloan Research Fellowship to WW.

Author contributions

X.H. conducted all the physiological experiments and data analysis. W.W. conducted ex-

periments in Figures 2.10c and 2.10d. M.R. and K.L.B. conducted connectomic analysis in Figure 2.15. X.H., K.L.B. and W.W. designed the experiments and wrote the paper.

Competing Interests

The authors declare no competing interests.

2.4 Results

2.4.1 pDSGC Off responses are sensitive to motion discontinuities

To determine how On and Off responses of On-Off DSGCs to motion stimuli in the RF center are modulated by motion patterns in the surround, we performed loose-patch recordings from a subtype of On-Off DSGCs that prefer motion in the posterior direction (pDSGCs), which are labeled by the Drd4-GFP transgenic mouse line (Huberman et al., 2009). Full-field motion stimuli were divided into center and surround areas where drifting square-wave gratings with the same spatial and temporal frequency were presented (see Methods). The center gratings always moved in the preferred direction of the pDSGCs, while the surround gratings differed in direction or spatial phase to create direction-contrast or phase-contrast between center and surround regions (Figure. 2.1c, schematics; Supplementary Movie). We refer to both direction-contrast and phase-contrast gratings as compound gratings. Off and On responses of pDSGCs to these drifting gratings showed comparable spike firing rates, and were well separated as dark and bright edges of the gratings traveled across the cell's RF (Figures. 2.2a and 2.2d). We examined the Off and On responses separately for their contextual modulation.

pDSGC Off responses in the preferred direction were maximal when the drifting grating was confined to the RF center, and decreased by the inclusion of stimuli in the surround during uniform and compound grating stimulation (Figure. 2.2b). Moreover, surround gratings alone did not evoke spiking of pDSGCs regardless of motion directions (Figures. 2.2d and 2.2e), consistent with the presence of a suppressive surround in these cells (Barlow and Levick, 1965). Although gratings in the surround suppressed the center response, this surround suppression was significantly stronger for uniform grating than compound gratings (Figures. 2.1c and 2.1d), suggesting that the Off response is sensitive to motion contexts.

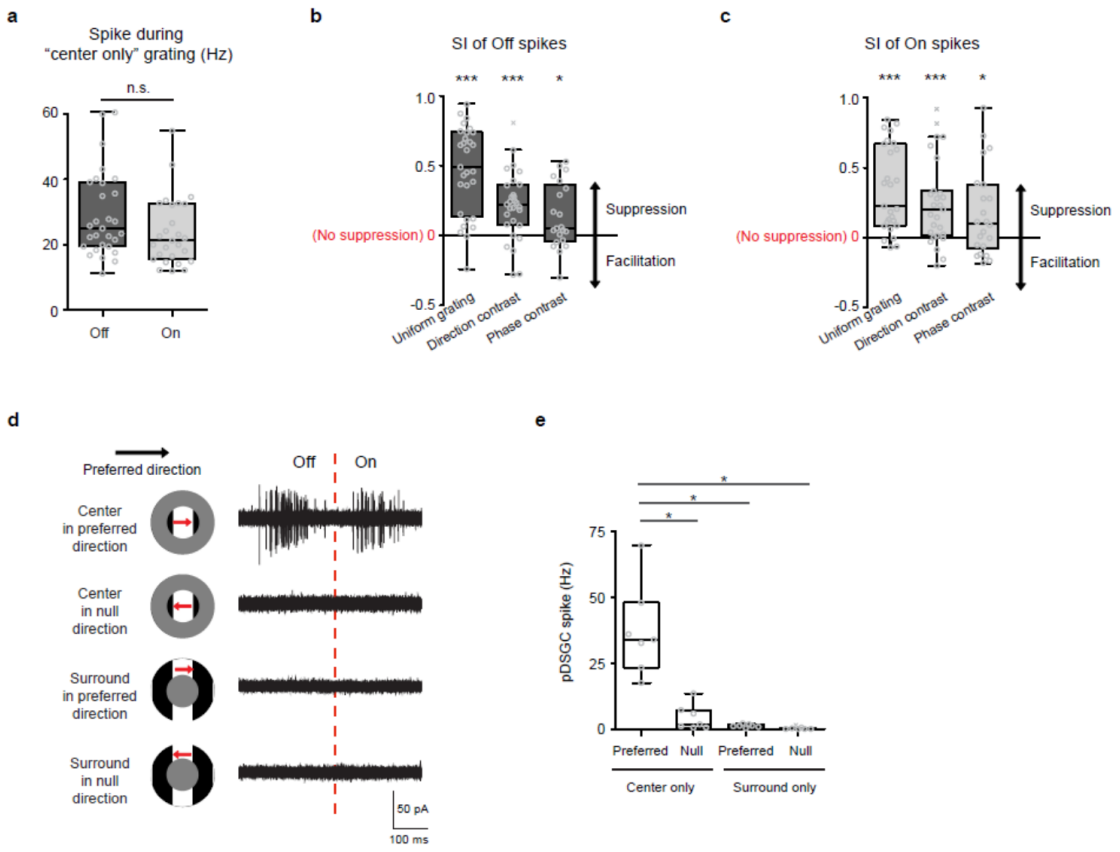

Figure 2.2: **pDSGCs have suppressive RF surrounds.**
a, Comparison of Off and On spike firing rate during "center only" stimulus. Wilcoxon signed-rank test, p = 0.079, the same sample groups as Figures 2.1d and 2.9b.
b and **c**, Surpression index (SI) of pDSGC Off and On spikes in different motion contexts. Suppression index (SI) of DSGC spiking was calculated as (N center only grating - N full-field grating) / (N center only grating + N full-field grating), where N is the spike firing rate. An SI of 0 indicates no suppression, an SI $>$ 0 indicates surround suppression, and an SI $<$ 0 indicates surround facilitation. Wilcoxon signed-rank test was used to test whether the SI value is significantly higher than 0.
b, Off SI, the same sample group as Figure 2.1d. Wilcoxon signed-rank test was used to test whether the SI of "surround in orthogonal" is significantly higher than 0: uniform grating: ***p $<$ 0.001; direction-contrast: ***p $<$ 0.001; phase-contrast: *p = 0.033.
c, On SI, the same sample group as Figure 2.9b: uniform grating: ***p $<$ 0.001; direction-contrast: ***p $<$ 0.001; phase-contrast: *p = 0.050.
d and **e**, Surround grating alone does not evoke pDSGC spiking regardless of motion directions.
d, Left: Schematic diagrams show the "center only" and the "surround only" stimuli. Right: Example spike traces of a pDSGC from a control mouse. Red dashed line shows the boundary of the Off and On spiking.
e, Summary of pDSGC spike firing rate under the visual stimuli conditions shown in c. n = 7 cells. "Center only" in preferred direction vs the other three stimuli, *p = 0.016.

We next tested the impact of stimulus contexts on the direction selectivity of pDSGCs by calculating direction selectivity index (DSI, see Methods) of their spiking activity evoked by uniform and compound grating stimuli. Compared to center-only condition, DSI was unaffected by the inclusion of surround gratings with direction-contrast or phase-contrast, but was significantly reduced during uniform grating (Figure. 2.1e; the DSI values represented as mean ± SEM: Center only = 0.58 ± 0.07; uniform grating = 0.23 ± 0.11; direction contrast: 0.51 ± 0.07; phase contrast: 0.45 ± 0.11; n = 10 cells. Wilcoxon signed rank test with Bonferroni correction: center only vs uniform grating: *p = 0.0039; center only vs direction or phase contrast, p ¿ 0.05). This reduction was due to the stronger surround suppression of preferred-direction response during uniform grating, since the null-direction spike counts remained low and were comparable under all conditions (Figure. 2.1f). Therefore, compared to continuous moving edges, discontinuities of contours between center and surround improve the direction selectivity of pDSGC Off response by enhancing the preferred-direction spiking.

2.4.2 Cholinergic excitation of pDSGCs is contextually sensitive

The stronger surround suppression of the Off spiking response by uniform grating may result from stronger suppression of excitatory inputs or stronger enhancement of inhibitory inputs onto pDSGCs. To understand the synaptic mechanism underlying this differential suppression effect, we measured the excitatory and inhibitory postsynaptic currents (EPSCs and IPSCs) of pDSGCs using whole-cell voltage clamp recording. We separated the postsynaptic currents into On and Off components based on the temporal windows during which the pDSGCs were activated by bright and dark phases of the square-wave gratings (see Methods). Consistent with the spiking response, the Off component of EPSCs showed stronger surround suppression by uniform grating (Figures. 2.3a and 2.3b). In addition to

EPSCs, the Off component of IPSCs of pDSGCs also showed stronger surround suppression by uniform grating (Figure. 2.3c), indicating that the suppressive mechanism affects both excitatory and inhibitory inputs of pDSGCs. However, stronger surround suppression of pDSGC spiking activity by uniform grating indicates that the effect of reduced inhibition is not sufficient to offset the effect of reduced excitation. We reason that excitation onto pDSGCs plays a dominant role in shaping the spiking response when motion is in the preferred direction. In contrast to the strong excitatory drive, the directionally tuned inhibition is the weakest and the most delayed in this direction (Taylor and Vaney, 2002), and therefore contribute little to pDSGC spiking generation. In support of this hypothesis, we found a strong correlation between EPSC waveform and spiking activity in the preferred direction ($r = 0.77 \pm 0.03$ for center-only stimulus, $n = 6$ cells). Therefore, contextually sensitive Off EPSCs are responsible for the stronger surround suppression of the pDSGC Off response by uniform grating.

Excitation onto pDSGCs consists of glutamatergic inputs from bipolar cells and cholinergic inputs from SACs. Previous studies using moving spots have shown that the relative contributions of these two types of excitation depend on stimulus conditions (Sethuramanujam et al., 2016, 2018). We thus examined the relative contributions of glutamatergic and cholinergic components to pDSGC EPSCs measured under our visual stimulus conditions. Since we observed concomitant contextual modulation of EPSCs and IPSCs of pDSGCs, this suggests that the modulatory mechanism may target SACs to simultaneously reduce their acetylcholine and GABA release onto pDSGCs. To test whether cholinergic input is the predominant mode of excitation during the drifting grating stimuli used in our study, we applied the nicotinic acetylcholine receptor antagonist DHβE to selectively block the cholinergic component of EPSCs (Pei et al., 2015; Wei et al., 2011). Both On and Off components of EPSCs during center-only gratings were dramatically reduced in the presence of DHβE

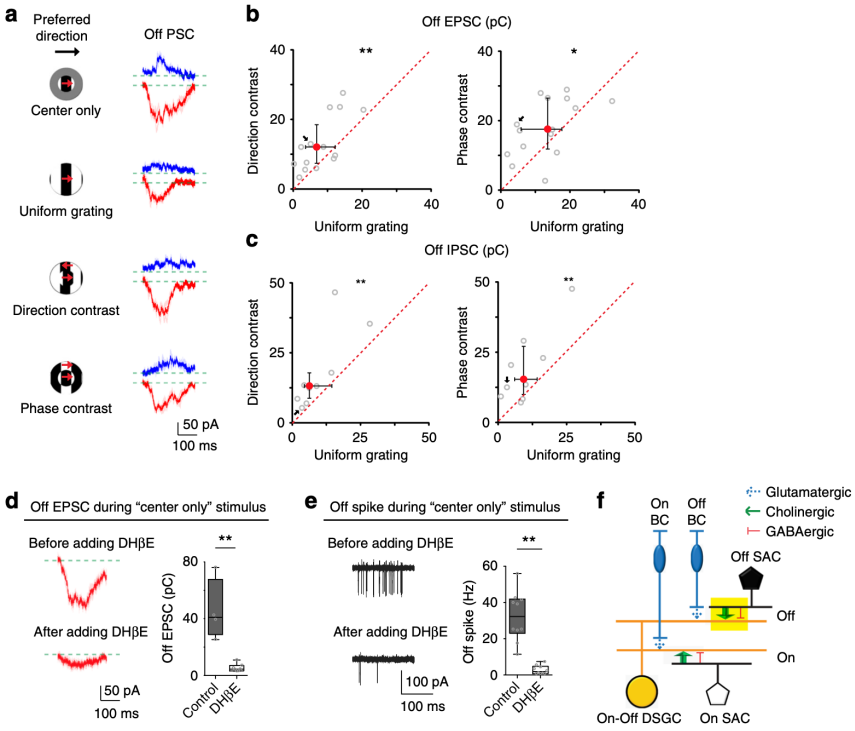

Figure 2.3: **Contextually sensitive cholinergic excitation underlying the differential modulation of pDSGC Off response.**

a, Whole-cell recording traces of Off IPSCs (blue) and Off EPSCs (red) from a pDSGC in a control mouse. PSC traces represent trial average (darker traces) and SEM (lighter traces) for this and subsequent figures.

b, Scatter plots compare Off EPSC charge transfer between uniform grating and compound gratings. Direction-contrast vs uniform grating: n = 15 cells from 11 mice, **p = 0.0043; Phase-contrast vs uniform grating: n = 15 cells from 9 mice, *p = 0.035 (Wilcoxon signed-rank test).

c, Same as **b**, but for Off IPSC charge transfer. Direction-contrast vs uniform grating: n = 9 cells from 5 mice, **p = 0.0039; Phase-contrast vs uniform grating: n = 10 cells from 6 mice, **p = 0.0098.

d, Left: Example Off EPSC traces of a pDSGC during center only grating before and after adding DHβE. Right: Summary graph of pDSGC Off excitatory charge transfer in control (Ames' solution, n = 4 cells from 2 mice) or in the presence of DHβE (n = 7 cells from 2 mice): ** p = 0.0061 (Wilcoxon rank-sum test). See Figure. 2.4a for Off IPSC as a negative control.

e, Left: Example Off spike traces of a pDSGC during center only grating before and after adding DHβE. Right: Summary graph of pDSGC Off spike firing rate before (in Ames' solution) or after adding DHβE: n = 10 cells from 6 mice, ** p = 0.0020 (Wilcoxon signed-rank test).

f, Schematic shows the synaptic connections modulated by motion context in the Off pathway (yellow filled rectangle). Glutamatergic BC inputs are shown in dotted arrows indicating their contribution is little under the experimental conditions in this study.

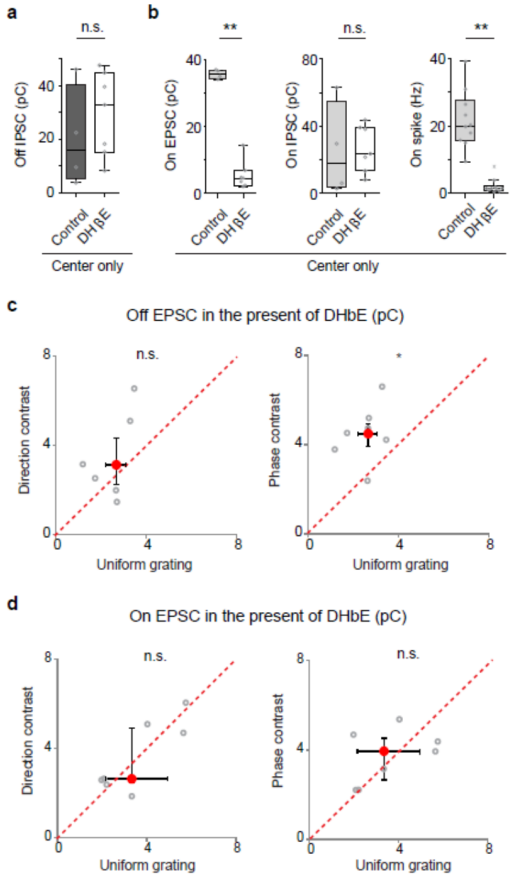

Figure 2.4: **Contextual modulation was not detected in the weak pDSGC responses in the presence of DHβE.**
a, Summary graph of pDSGC Off inhibitory charge transfer in control (Ames' solution) or in the presence of DHβE: Wilcoxon rank-sum test, p = 0.53, the same sample group as pDSGC Off excitatory charge transfer in Figure 2.3d.
b, Left: Summary graph of pDSGC On excitatory charge transfer in control (Ames' solution, n = 4 cells from 2 mice) or in the presence of DHβE (n = 7 cells from 2 mice): Wilcoxon rank-sum test, ** p = 0.0061. Middle: Summary graph of pDSGC On inhibitory charge transfer in control (Ames' solution) or in the presence of DHβE: Wilcoxon rank-sum test, p = 0.65; the same sample group as pDSGC On excitatory charge transfer on the left. Right: Summary graph of pDSGC On spike firing rate before (in Ames' solution) or after adding DHβE: n = 10 cells from 6 mice, Wilcoxon signed-rank test, ** p = 0.0020.
c, Scatter plots compare Off EPSC charge transfer between uniform grating and compound gratings in the presence of DHβE, n = 7 cells from 2 mice, the same sample group as Figure 2.3d. Left: Direction-contrast vs uniform grating: Wilcoxon signed-rank test, p = 0.2188. Right: Phase-contrast vs uniform grating: *p = 0.0313.
d, Scatter plots compare On EPSC charge transfer between uniform grating and compound gratings in the presence of DHβE, n = 7 cells from 2 mice, the same sample group as Figure 2.4b. Left: Direction-contrast vs uniform grating: Wilcoxon signed-rank test, p = 0.8125. Right: Phase-contrast vs uniform grating: p = 0.9375.

(Figure. 2.3d and Figure. 2.4b), indicating that the main component of pDSGC EPSCs was cholinergic. Consistent with the significantly reduced EPSCs, pDSGC spiking responses were largely eliminated after adding DHβE (Figure. 2.3e and Figure. 2.4b). We didn't detect a statistically significant contextual modulation in the residual weak EPSCs (Figures. 2.4c and 2.4d). The spiking data were not analyzed since there were barely any spikes for quantification during full-field gratings in the presence of DHβE. Therefore, the differential surround suppression of pDSGC Off spiking by continuous and discontinuous drifting gratings in this study is primarily due to the modulation of the cholinergic inputs from Off SACs to pDSGCs (Figure. 2.3f).

2.4.3 Direct GABAergic inhibition from WACs onto Off SACs

What mediates the contextually sensitive surround suppression of the cholinergic inputs from Off SACs to pDSGCs? One candidate is the GABAergic inhibition from neighboring SACs (Lee and Zhou, 2006), since reciprocal inhibitory inputs between neighboring SACs are the most numerous among the total GABAergic inputs onto SACs (Ding et al., 2016). In addition to the reciprocal SAC – SAC inhibition, Off SACs also receive GABAergic inhibition from non-starburst amacrine cells (Chen et al., 2016), which are identified to be WACs based on connectomic tracing (Ding et al., 2016) (Figure. 2.5a, Control). To determine the synaptic locus that mediates the differential surround suppression, we applied a loss-of-function approach using two types of SAC-targeted genetic manipulations. The first one perturbs GABA release from the SAC by conditionally knocking out the vesicular GABA transporter (Vgat) gene in SACs. In these Vgat cKO mice, both SAC – DSGC and SAC – SAC inhibition are disrupted with no detectable developmental compensation in the rest of the direction selective circuit (Figure. 2.5a, Vgat cKO) (Chen et al., 2016; Pei et al., 2015). As previously reported (Pei et al., 2015), IPSCs of pDSGCs are strongly reduced in Vgat cKO

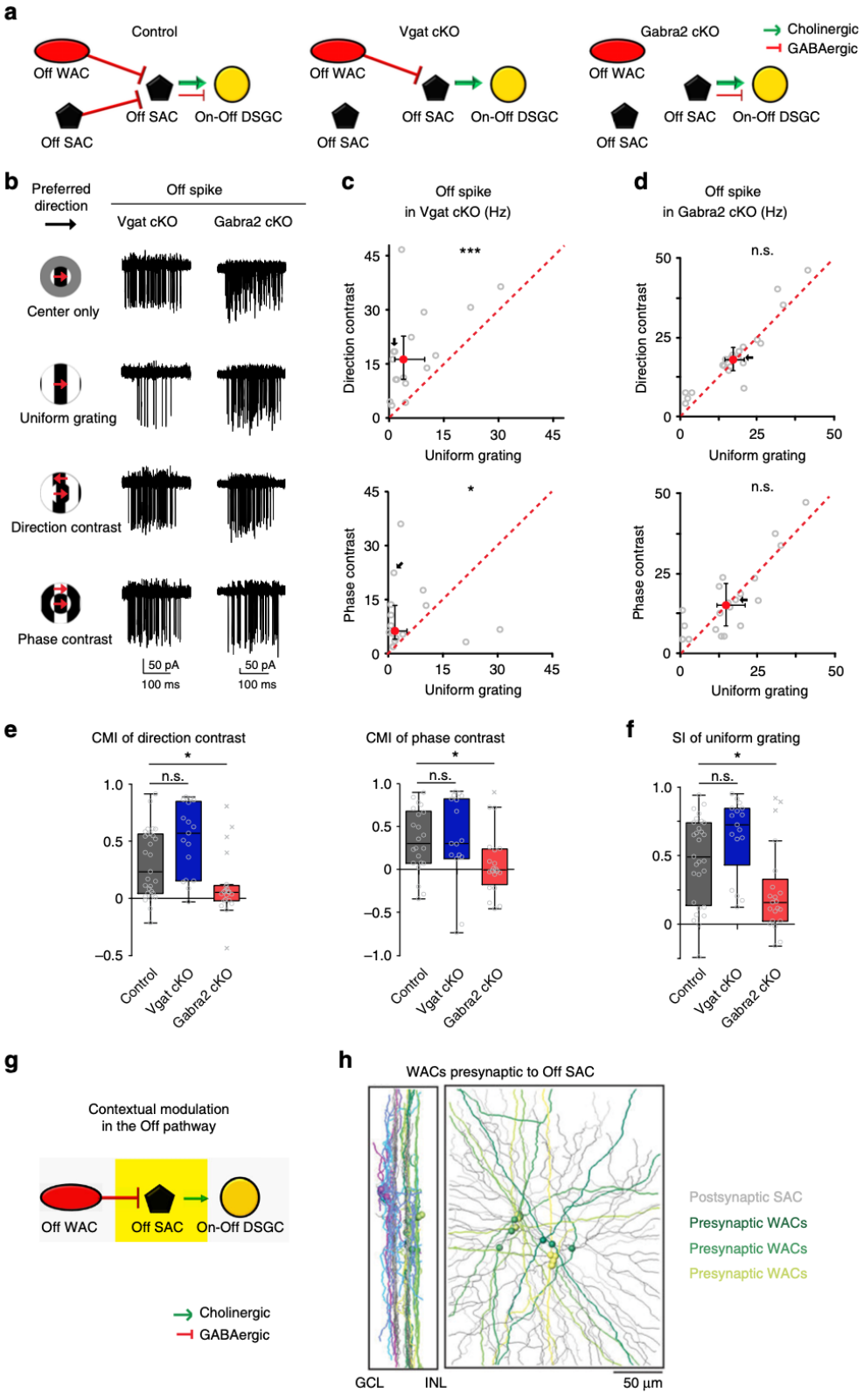

Figure 2.5: **Contextual modulation of pDSGC Off response is mediated by direct inhibition onto SACs.**

Figure 2.5, continued.
a, Schematic diagrams show the GABAergic synaptic connections in control, Vgat cKO and Gabra2 cKO mice.
b, Example pDSGC Off spike traces from a Vgat cKO mouse and a Gabra2 cKO mouse.
c, Scatter plots compare pDSGC Off firing rate in Vgat cKO mice during uniform grating and compound gratings. Direction-contrast vs uniform grating: n = 17 cells from 11 mice, ***p < 0.001; Phase-contrast vs uniform grating: n = 16 cells from 10 mice, *p = 0.039 (Wilcoxon signed-rank test).
d, Same as c, but for Gabra2 cKO mice. Direction-contrast vs uniform grating: n = 21 cells from 9 mice, p = 0.065; Phase-contrast vs uniform grating: n = 20 cells from 9 mice, p = 0.88.
e, Summary graphs compare CMI of pDSGC Off response in control, Vgat cKO and Gabra2 cKO mice. CMI of direction-contrast: Kruskal-Wallis test, ***p = 0.0004. Wilcoxon rank-sum test with Bonferroni correction: Control vs Vgat cKO: p = 0.028; Control vs Gabra2 cKO: *p = 0.019. CMI of phase-contrast, Kruskal-Wallis test: *p = 0.024. Wilcoxon rank-sum test with Bonferroni correction: Control vs Vgat cKO: p = 0.40; Control vs Gabra2 cKO: *p = 0.015.
f, Summary graph compares SI of pDSGC Off firing rate during uniform grating stimulus between control, Vgat cKO and Gabra2 cKO mice. Kruskal-Wallis test: **p = 0.0012. Wilcoxon rank-sum test with Bonferroni correction: Control vs Vgat cKO: p = 0.041; Control vs Gabra2 cKO: *p = 0.020.
g, Schematic shows the synaptic connections involved in contextual modulation in the Off pathway of the direction selective circuit (yellow filled rectangle).
h,Connectomic reconstruction of wide-field amacrine cells (WACs) presynaptic to Off SACs. Off SACs are colored in grey, while Off WACs presynaptic to Off SACs are colored in green, yellow-green and yellow. Balls represent somas. (Modified from Ding et al., 2016, Extended Figure 4D)

mice and the residual inhibition is non-directional (Figure. 2.6). In the other conditional knock-out mouse line, all direct GABAergic inhibition onto SACs, including SAC – SAC mutual inhibition and WAC – SAC inhibition, is abolished by selectively removing the $\alpha 2$ subunit of $GABA_A$ receptors (Gabra2) from SACs (Figure. 2.5a, Gabra2 cKO) (Auferkorte et al., 2012; Brandstätter et al., 2009; Chen et al., 2016).

In Vgat cKO mice where GABA release from SACs was disrupted, the contextual sensitivity of pDSGC Off response was not affected. We found both the Off spiking and Off EPSCs were still more strongly suppressed by uniform grating than by compound gratings

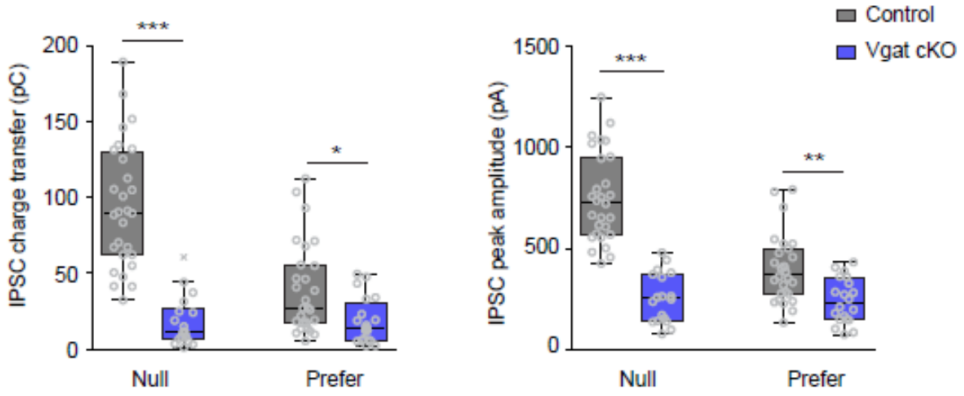

Figure 2.6: **pDSGC IPSCs are diminished and non-directional in Vgat cKO mice.**
Left: Summary of pDSGC IPSC charge transfer during center only gratings in control and Vgat cKO mice. Center gratings moving in null direction: control: n = 28 cells; Vgat cKO: n = 18 cells; Wilcoxon rank-sum test, ***p $<$ 0.001. Center gratings moving in preferred direction: control: n = 28 cells; Vgat cKO: n = 20 cells; Wilcoxon rank-sum test, *p = 0.0077.
Right: Summary of pDSGC IPSC peak amplitude during center only gratings in control and Vgat cKO mice. Center gratings moving in null direction: control: n = 28 cells; Vgat cKO: n = 18 cells; Wilcoxon rank-sum test, ***p $<$ 0.001. Center gratings moving in preferred direction: control: n = 28 cells; Vgat cKO: n = 20 cells; Wilcoxon rank-sum test, **p = 0.0013.

(Figures. 2.5b and 2.5c for spiking, Figures. 2.7a and 2.7b for EPSCs). To quantify the level of contextual modulation, a contextual modulation index (CMI) of pDSGC spiking is calculated as (Ncompound grating - Nuniform grating)/(Ncompound grating + Nuniform grating), where N is the spike count. For both direction-contrast and phase-contrast gratings, the CMI of pDSGC Off spiking in Vgat cKO mice remained unchanged compared to that in control mice (Figure. 2.5e). The normal contextual tuning of the Off response in Vgat cKO mice indicates that GABA release from SACs is not required in this process. This result rules out the involvement of two synaptic loci. First, synaptic inhibition onto pDSGCs is not necessary for contextual modulation, since normal contextual sensitivity of pDSGCs persists in the absence of SAC – DSGC inhibition despite its critical role in direction selectivity. This lends further support to the important role of synaptic excitation onto pDSGCs in

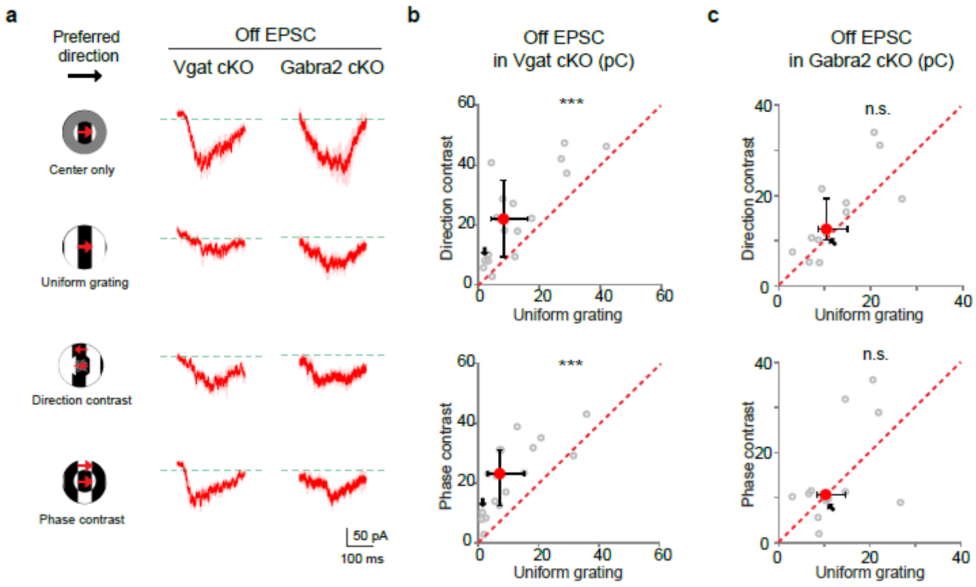

Figure 2.7: **Context-sensitive Off EPSCs of pDSGCs are unaffected in Vgat cKO mice, but disrupted in Gabra2 KO mice.**
a, Example EPSC traces of a pDSGC from a Vgat cKO mouse or a Gabra2 cKO mice during different grating stimuli.
b, Scatter plots of pDSGC Off EPSC charge transfer in Vgat cKO mice. Upper panel: Direction-contrast vs uniform grating: n = 18 cells from 13 mice, Wilcoxon signed-rank test, ***p < 0.001. Lower panel: Phase-contrast vs uniform grating: n = 17 cells from 11 mice, Wilcoxon signed-rank test, ***p < 0.001.
c, Same as **b**, but for pDSGC Off EPSC charge transfer in Gabra2 cKO mice. Upper panel: Direction-contrast vs uniform grating: n = 13 cells from 9 mice, Wilcoxon signed-rank test, p = 0.0681. Lower panel: Phase-contrast vs uniform grating: n = 13 cells from 9 mice, Wilcoxon signed-rank test, p = 0.4548.

contextual modulation as demonstrated in control mice (Figure. 2.3). Second, the reciprocal inhibition between Off SACs is not required for the stronger surround suppression of pDSGC Off response by uniform grating, excluding the possibility that Off SACs are inhibited by neighboring SACs to reduce their acetylcholine release onto pDSGCs.

We next tested whether the GABAergic inhibition from WACs to SACs plays a role in the contextual modulation. In Gabra2 cKO mice, both the Off spiking and Off EPSCs of pDSGCs were similar during uniform grating and compound gratings (Figures. 2.5b and

2.5d for spiking, Figures. 2.7a and 2.7c for EPSCs). The CMI of pDSGC Off spiking in Gabra2 cKO mice was significantly reduced compared to that in control mice (Figure. 2.5e). The disruption of Off contextual modulation in Gabra2 cKO mice was caused by diminished surround suppression during uniform grating (Figure. 2.5f). Since we have already ruled out the contribution of SAC – SAC mutual inhibition to Off contextual modulation, the reduced contextual sensitivity of pDSGCs in Gabra2 cKO mice is attributed to the feedforward inhibition from Off WACs to Off SACs (Figure. 2.5g). Indeed, Off WACs presynaptic to Off SACs have been reconstructed from a connectomic study using serial block face electron microscopy (SBEM) (Denk and Horstmann, 2004) (Figure. 2.5h) (Ding et al., 2016).

Long-range inhibition from the surround often involves spiking WACs (Baccus et al., 2008; Demb et al., 1999; Flores-Herr et al., 2001; Hoggarth et al., 2015; Roska and Werblin, 2003; Taylor, 1999). Therefore, we tested whether the contextual modulation of Off SAC acetylcholine release depends on spiking activity. When the voltage-gated Na+ channel antagonist tetrodotoxin (TTX) was applied to the control retina, the stronger suppression of pDSGC Off EPSCs during uniform gratings was completely abolished (Figures. 2.8a and 2.8b). This result indicates a prominent involvement of spiking amacrine cells in pDSGC surround suppression either by directly inhibiting Off SACs or acting upstream of the WAC – Off SAC synapse. However, we cannot rule out a role of spiking activity from bipolar cells in this process. Considering TTX affects the activity of multiple cell types in the retina (Baden et al., 2011; CUI and PAN, 2008; Saszik and DeVries, 2012), the relevant neural circuits underlying this TTX-mediated effect await further studies.

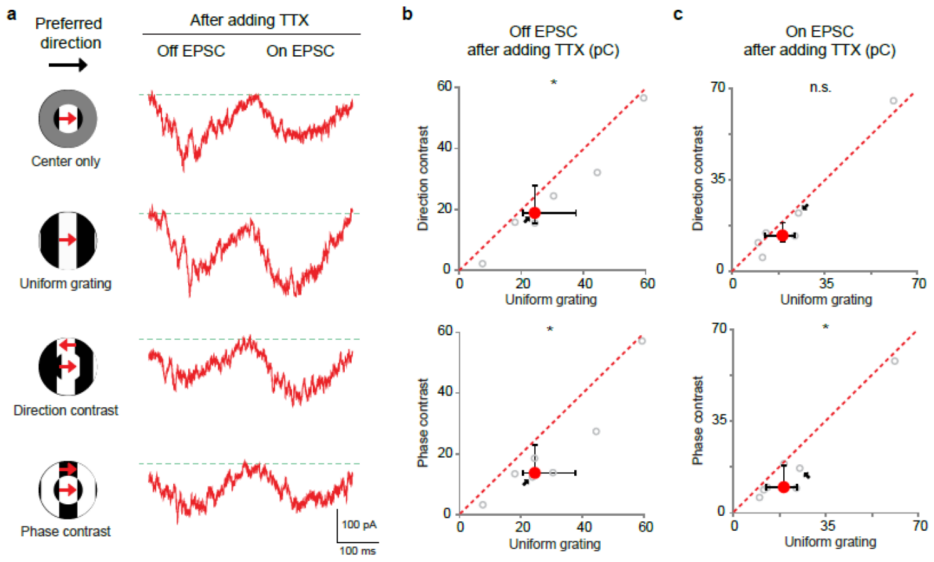

Figure 2.8: **Stronger suppression of pDSGC EPSCs during uniform grating is disrupted or masked in control mice after adding TTX.**
a, Example traces of pDSGC EPSCs in bath of TTX.
b, Scatter plots of pDSGC Off EPSC charge transfer after applying TTX, n = 7 cells from 2 mice. Upper panel: Direction-contrast vs uniform grating: Wilcoxon signed-rank test, *p = 0.0156. Lower panel: Phase-contrast vs uniform grating: Wilcoxon signed-rank test, *p = 0.156.
c, Same as **b**, but for pDSGC On EPSCs. Upper panel: Direction-contrast vs uniform grating: Wilcoxon signed-rank test, p = 0.2969. Lower panel: Phase-contrast vs uniform grating: Wilcoxon signed-rank test, *p = 0.0156.

2.4.4 Weak contextual modulation of pDSGC On responses

The preferred-direction On spiking response of pDSGC also showed contextual sensitivity (Figures. 2.9a and 2.9b; Figure. 2.2c). However, the CMI of On responses was significantly lower than that of Off responses for both direction-contrast and phase-contrast gratings (Figure. 2.9c), indicating that the On responses during uniform and compound gratings are less different. Because of the moderate contextual modulation in the On pathway, the DSI of On responses was not significantly different across stimulus conditions (Figure. 2.9d). The null-direction On spiking remained weak and did not show contextual sensitivity (Figure. 2.9e).

Similar to the Off pathway, the stronger surround suppression of pDSGC On spiking during uniform grating was due to weaker On EPSCs (Figure. 2.9f), but not enhanced On IPSCs (Figure. 2.9g). Since the main component of pDSGC On EPSCs is cholinergic (Figure. 2.4b), the contextual modulation of pDSGC On response was a result of contextually sensitive acetylcholine release from On SACs (Figure. 2.9h, Figure. 2.4d).

2.4.5 Contextual modulation of bipolar cell (BC) – On SAC synapse

Since contextually sensitive cholinergic excitation of pDSGCs from SACs underlies the stronger surround suppression of pDSGC spiking by uniform gratings in both the On and Off pathways, we next tested whether the On pathway also relies on direct inhibition of On SACs for contextual modulation. In sharp contrast to the Off response, the contextual sensitivity of pDSGC On spiking and On EPSCs is not affected by conditionally knocking out Gabra2 from SACs, and both of them remained weakly contextually sensitive like those in control mice (Figures. 2.10a and 2.10b for spiking, Figure. 2.11 for EPSCs). Therefore, direct inhibition onto On SACs is not required for the contextual modulation in the On pathway. To further rule out a role of direct inhibitory inputs onto On SACs, we examined IPSCs of On SACs during drifting grating stimuli (Figure. 2.10c). We did not detect stronger On SAC IPSCs during uniform grating, indicating that stronger suppression of acetylcholine release from On SACs by uniform grating is not due to stronger inhibitory inputs onto On SACs.

Another candidate synaptic locus for the contextual modulation of On SACs is bipolar cell terminals presynaptic to On SACs. To test if bipolar cell inputs onto On SACs are more suppressed by uniform grating than compound gratings, we performed whole-cell recordings from On SACs and measured the charge transfer of EPSCs during drifting grating stimuli.

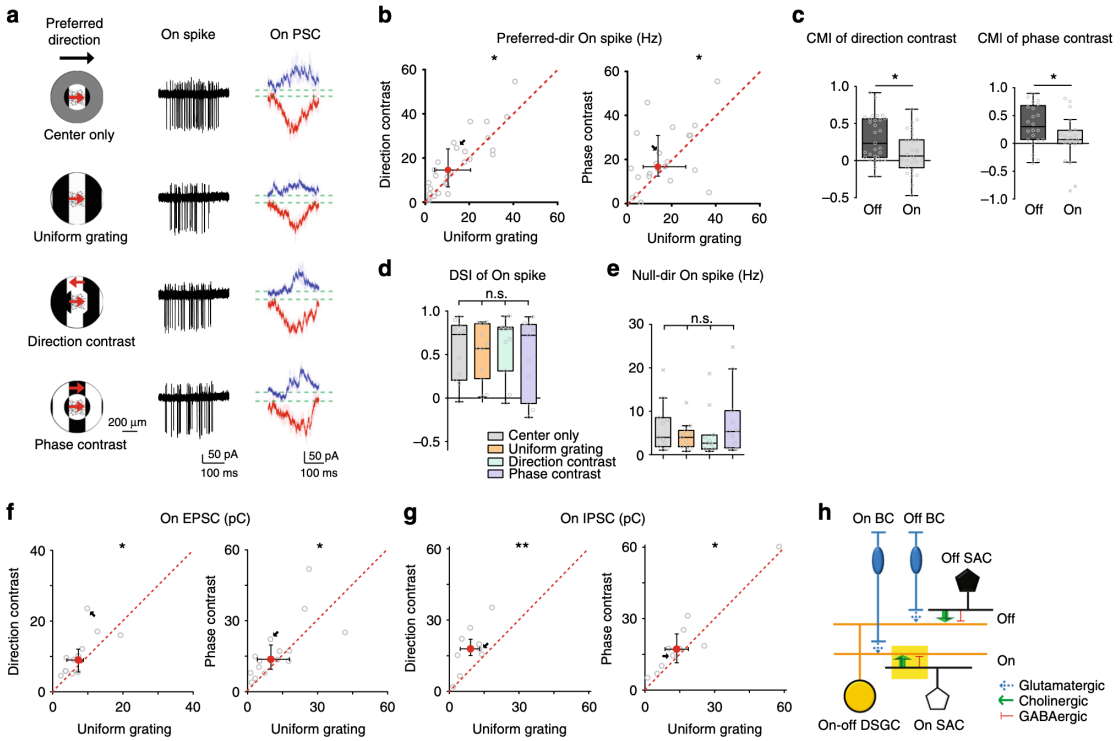

Figure 2.9: **Contextually sensitive cholinergic excitation underlies the weak contextual modulation of pDSGC On response.**

a, Left: Visual stimuli with different motion contexts. Middle: Example On spike traces of a pDSGC from a control mouse. Right: Whole-cell recording traces of On IPSCs (blue) and On EPSCs (red) from a pDSGC in a control mouse.

b, Scatter plots compare pDSGC preferred-direction On spike firing rate during uniform grating and compound gratings. Direction-contrast vs uniform grating: n = 27 cells from 10 mice, *p = 0.0361; Phase-contrast vs uniform grating: n = 22 cells from 8 mice, *p = 0.0459 (Wilcoxon signed-rank test).

c, Summary graphs compare CMI of pDSGC Off and On response in control mice. CMI of direction-contrast: *p = 0.014; CMI of phase-contrast: *p = 0.034; Wilcoxon rank-sum test, using the same sample group as Figure 2.1d and Figure 2.5b.

d, DSI of pDSGC On response under different stimulus conditions. Friedman test: n = 11 cells from 4 mice, p = 0.48.

e, pDSGC On firing rate when center gratings drift in the null direction. Friedman test: n = 11 cells from 4 mice, p = 0.43.

f, Same as **b**, but for On EPSC charge transfer. Direction-contrast vs uniform grating: n = 13 cells from 10 mice, *p = 0.017; Phase-contrast vs uniform grating: n = 15 cells from 9 mice, *p = 0.035.

g, Same as **b**, but for On IPSC charge transfer. Direction-contrast vs uniform grating: n = 9 cells from 5 mice, **p = 0.0039; Phase-contrast vs uniform grating: n = 10 cells from 6 mice, *p = 0.037.

h, Schematic diagram shows the synaptic connections modulated by motion context in the On pathway (yellow filled rectangle).

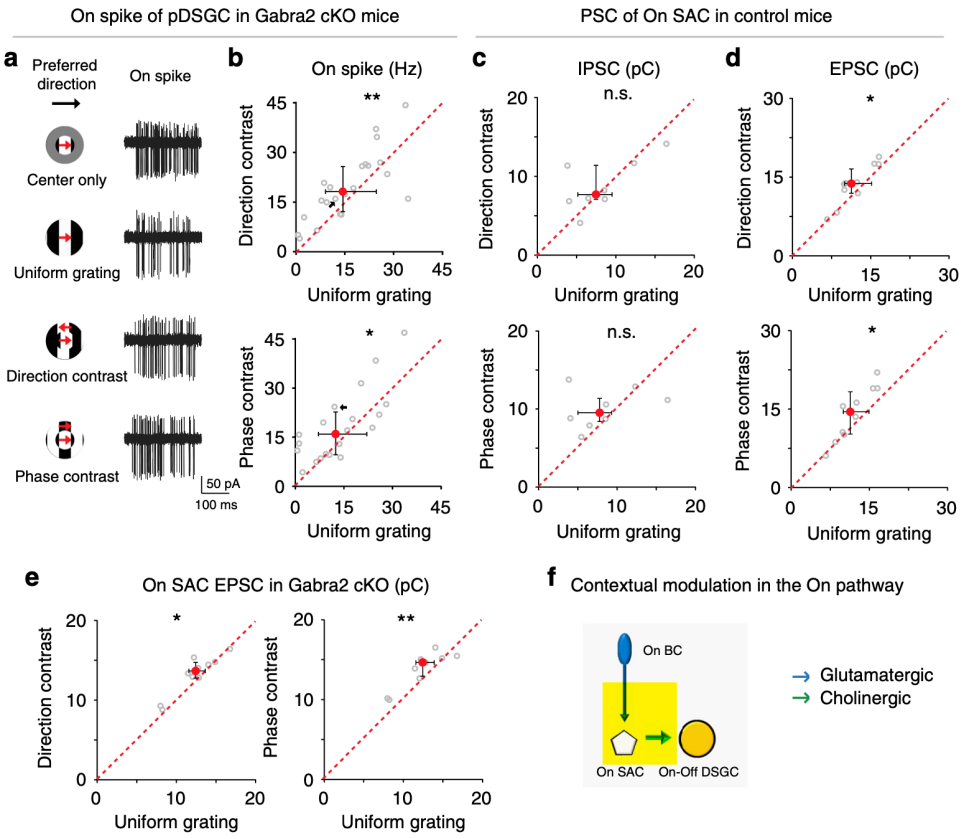

Figure 2.10: **The contextual sensitivity of pDSGCs and On SACs is mediated by the excitatory inputs but not inhibitory inputs onto On SACs.**
a, On spike traces of an example pDSGC from a Gabra2 cKO mouse under different stimulus conditions. See also Fig. 2.11a for example EPSC traces from a pDSGC in Gabra2 cKO mouse.
b, Scatter plots compare pDSGC On spike firing rate during uniform grating versus compound gratings in Gabra2 cKO mice. Direction-contrast vs uniform grating: n = 22 cells from 12 mice, **p = 0.0094; Phase-contrast vs uniform grating: n = 20 cells from 12 mice, *p = 0.0478. Wilcoxon signed-rank tests were used in this and subsequent scatter plots. See also Fig. 2.11b for comparison of On EPSC charge transfer of pDSGCs in Gabra2 cKO mice.
c, Scatter plots of On SAC inhibitory charge transfer in control mice, n = 8 cells from 4 mice. Direction-contrast vs uniform grating: p = 0.9453; Phase-contrast vs uniform grating: p = 0.1484.
d, Scatter plots of On SAC excitatory charge transfer in control mice, n = 10 cells from 4 mice. Direction-contrast vs uniform grating: *p = 0.0195; Phase-contrast vs uniform grating: *p = 0.0273.
e, Scatter plots of On SAC excitatory charge transfer in Gabra2 KO mice, n = 10 cells from 2 mice. Direction-contrast vs uniform grating: *p = 0.0371; Phase-contrast vs uniform grating: **p = 0.0098.
f, Schematic diagram shows the acetylcholine release of On SAC is contextually modulated by On BC – On SAC excitatory inputs.

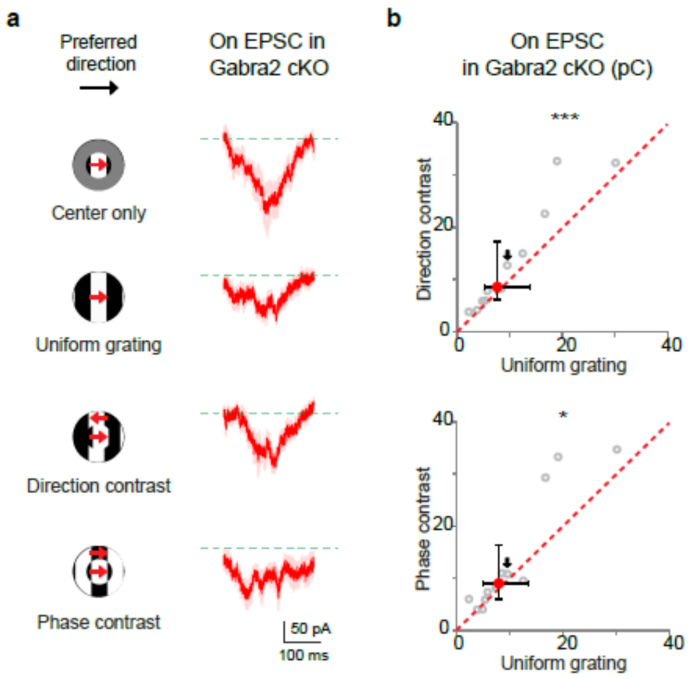

Figure 2.11: **Contextual modulation of pDSGC On EPSCs is unchanged in Gabra2 cKO mice.**
a, EPSC traces of a pDSGC from a Gabra2 cKO mouse during different motion contexts.
b, Scatter plots of pDSGC On EPSC charge transfer in Gabra2 cKO mice. Upper panel: Direction-contrast vs uniform grating: n = 12 cells from 8 mice, Wilcoxon signed-rank test, ***$p < 0.001$. Lower panel: Phase-contrast vs uniform grating: n = 12 cells from 8 mice, Wilcoxon signed-rank test, *$p = 0.0342$.

We found that EPSCs of On SACs were more suppressed by uniform grating in both control (Figure. 2.10d) and Gabra2 cKO mice (Figure. 2.10e). These results indicate that the contextual modulation in the On pathway depends on contextually modulated glutamate release of bipolar cells onto On SACs (Figure. 2.10f). Therefore, distinct microcircuits are involved in the contextual modulation in the On and Off pathways (Figures. 2.5g and 2.10f).

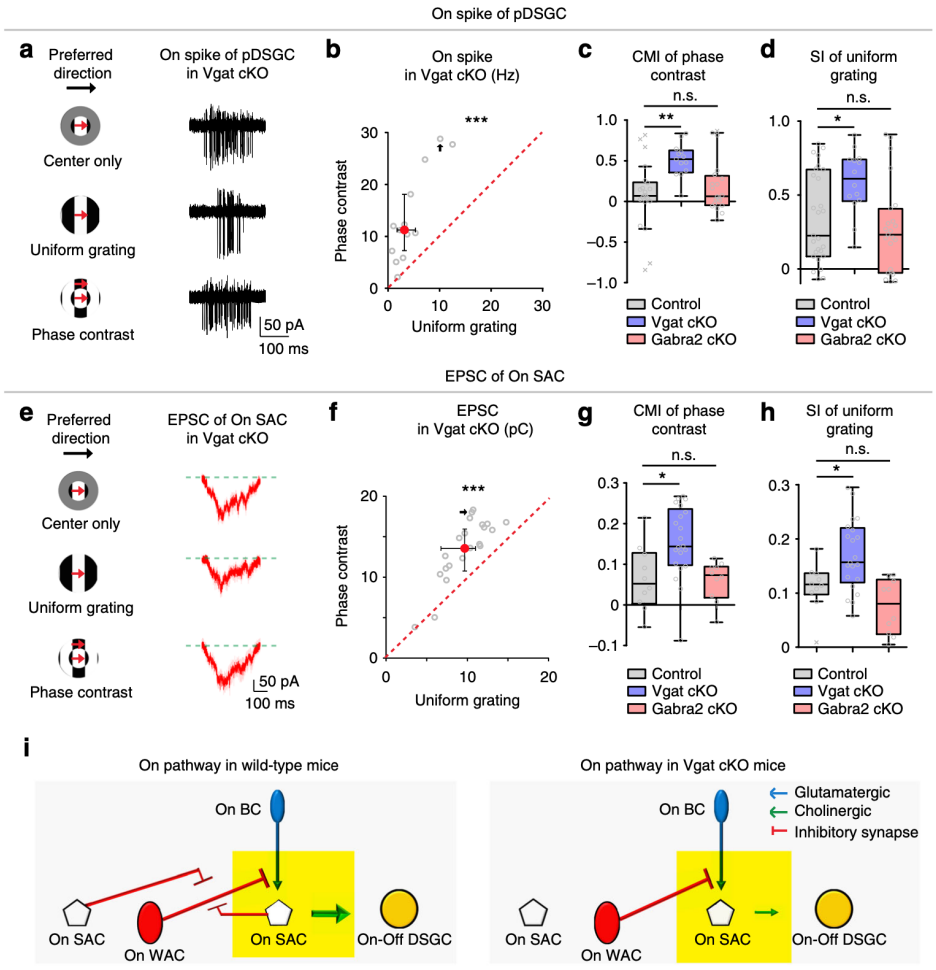

Figure 2.12: **Conditionally knocking out Vgat in SACs unmasks strong contextual modulation in the pDSGC On pathway.**
a, Example On spike traces of a pDSGC in Vgat cKO mouse.
b, Scatter plot compares pDSGC On firing rate during uniform grating and phase-contrast grating in Vgat cKO mice: n = 13 cells from 7 mice, ***p $<$ 0.001.
c, Summary graph compares CMI of phase-contrast for pDSGC On response in control, Vgat cKO and Gabra2 cKO mice: Kruskal-Wallis test: **p = 0.0016. Wilcoxon rank-sum test with Bonferroni correction: Control vs Vgat cKO: **p = 0.00080; Control vs Gabra2 cKO: p = 0.78.
d, Summary graph compares SI of pDSGC On firing rate during uniform grating between control, Vgat cKO and Gabra2 cKO mice: Kruskal-Wallis test: **p = 0.0084. Wilcoxon rank-sum test with Bonferroni correction Control vs Vgat cKO: *p = 0.014; Control vs Gabra2 cKO: p = 0.53.
e, EPSC traces of an example On SAC in Vgat cKO mouse.
f, Scatter plot of On SAC excitatory charge transfer during uniform grating versus phase-contrast in Vgat cKO mice: n = 21 cells from 5 mice, ***p $<$ 0.001. See also Figure. 2.13 for comparison of On SAC IPSC charge transfer in Vgat cKO mice.

Figure 2.12, continued.
g, Summary graph compares CMI of phase-contrast for On SAC excitatory charge transfer in control, Vgat cKO and Gabra2 cKO mice: Kruskal-Wallis test: **p = 0.0015. Wilcoxon rank-sum test with Bonferroni correction: Control vs Vgat cKO: *p = 0.0083; Control vs Gabra2 cKO: p = 0.91.
h, Summary graph compares SI of On SAC excitatory charge transfer during uniform grating between control, Vgat cKO and Gabra2 cKO mice: Kruskal-Wallis test: **p = 0.0013. Wilcoxon rank-sum test with Bonferroni correction: Control vs Vgat cKO: *p = 0.024; Control vs Gabra2 cKO: p = 0.14.
i, Schematic diagrams show the synaptic connections involved in contextual modulation in the On pathway of the direction selective circuit in wild type and Vgat cKO mice (Yellow rectangles).

2.4.6 Enhanced contextual sensitivity of On pathway in Vgat cKOs

Compared to the weakly modulated pDSGC On responses in control (Figure. 2.9b) and Gabra2 cKO mice (Figure. 2.10b), pDSGC On responses in Vgat cKO mice showed enhanced sensitivity to phase-contrast gratings (Figures. 2.12a-2.12c). Such enhancement of On contextual modulation in Vgat cKO mice was due to enhanced surround suppression during uniform grating (Figure. 2.12d). Consistent with pDSGC spiking response, the EPSCs of On SACs in Vgat cKO mice also showed enhanced contextual sensitivity to phase-contrast gratings (Figures. 2.12e-g) owing to a stronger surround suppression of EPSCs of On SACs during uniform grating (Figure. 2.12h). Residual inhibitory inputs onto On SACs from non-starburst amacrine cells (Ding et al., 2016) remained insensitive to surround motion patterns (Figure. 2.13). These results further support the participation of the BC – On SAC synapse in the contextual modulation of pDSGC On response: when the glutamatergic excitation of On SACs in Vgat cKO mice becomes more contextually sensitive to phase-contrast gratings (Figure. 2.12g), pDSGC On spiking in these mice also becomes more contextually sensitive (Figure. 2.12c).

No statistically significant enhancement of contextual modulation was detected between the uniform and direction-contrast gratings for either pDSGC On spiking activity or On SAC

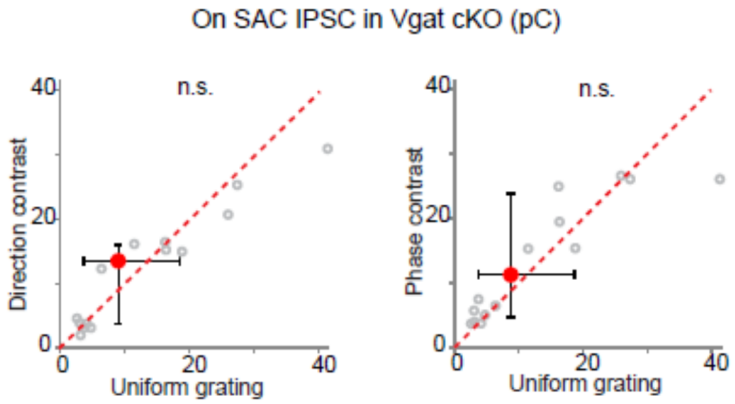

Figure 2.13: **In Vgat cKO mice, IPSC of On SAC during uniform grating is similar to that during compound gratings.**
Scatter plots of On SAC inhibitory charge transfer in Vgat cKO mice, n = 14 cells from 5 mice.
Left: Direction-contrast vs uniform grating: Wilcoxon signed-rank test, p = 0.3575.
Right: Phase-contrast vs uniform grating: Wilcoxon signed-rank test, p = 0.2676.

EPSCs in Vgat cKO mice (Figure. 2.14). We reason that the white moving edges in the center and surround regions during the direction-contrast grating stimulus show time-dependent perpendicular distance, while the center and surround white edges of the phase-contrast grating remain maximally separated by the width of the white bar (206 μm) (see schematic in Figure. 2.9a). Therefore, the enhanced sensitivity to discontinuous edges in Vgat cKO mice may be more readily revealed by the phase-contrast grating than by the direction-contrast grating.

Why is contextual sensitivity in the On pathway enhanced in Vgat cKO mice? We hypothesize that GABA released from On SACs normally inhibits the contextually sensitive amacrine cell (AC) – BC – On SAC microcircuit (Figure. 2.12i, wild type). Disrupting GABA release from SACs in Vgat cKO mice unmasks this contextually sensitive AC – BC presynaptic inhibition, and allows for stronger contextual modulation of acetylcholine release from On SACs to pDSGCs (Figure. 2.12i, Vgat cKO). Functional and connectomic analysis has revealed two postsynaptic targets of On SACs: neighboring On SACs and a class

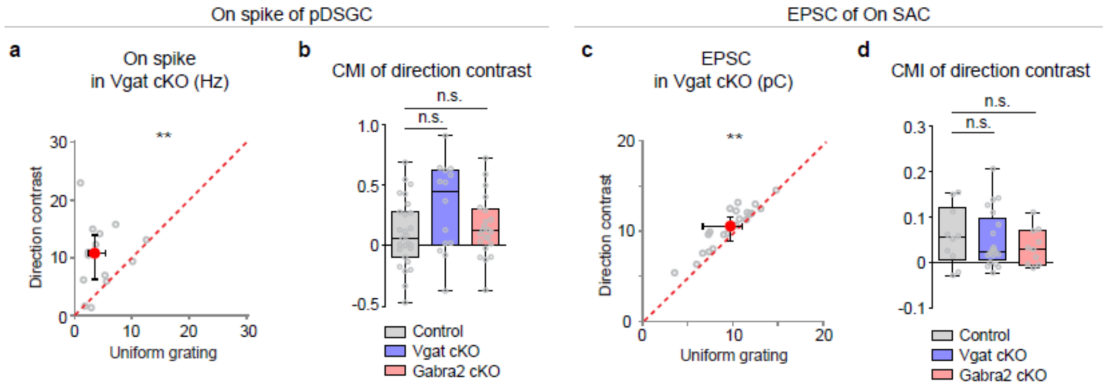

Figure 2.14: **Differential responses during uniform grating and direction-contrast gratings are not significantly enhanced in Vgat cKO mice.**
a, Scatter plot compares pDSGC On spike firing rate during uniform grating and direction-contrast in Vgat cKO mice: n = 14 cells from 8 mice, Wilcoxon signed-rank test, **p = 0.0065.
b, Summary graph compares CMI of direction-contrast for pDSGC On response in control, Vgat cKO and Gabra2 cKO mice: the same sample group as Figure 2.9b (control), Figure 2.14a (Vgat cKO) and Figure 2.10b (Gabra2 cKO), Kruskal-Wallis test, p = 0.14.
c, Scatter plot of On SAC EPSC charge transfer during uniform grating versus direction-contrast grating in Vgat cKO mice: n = 21 cells from 5 mice, Wilcoxon signed-rank test, **p = 0.0015.
d, Summary graph compares CMI of direction-contrast for EPSC charge transfer of On SAC in control, Vgat cKO and Gabra2 cKO mice: the same sample group as Figure 2.10d (control), Figure 2.14c (Vgat cKO) and Figure 2.10e (Gabra2 cKO), Kruskal-Wallis test, p = 0.80.

of WACs (Ding et al., 2016; Lee and Zhou, 2006). Since On SACs do not directly inhibit BCs, the WACs postsynaptic to On SACs are the best candidate for conferring contextual sensitivity in the On pathway.

To determine if the above circuit model (Figure. 2.12i) based on functional measurements is supported by anatomy, we performed connectomic reconstruction of the synaptic circuit postsynaptic to On SACs. We traced the amacrine cells postsynaptic to a wedge of an On SAC and focused on 3 WACs that tightly co-stratify with the ON SAC dendrites (Figures. 2.15a and 2.15b). Two WACs had displaced somas and one had a soma in the

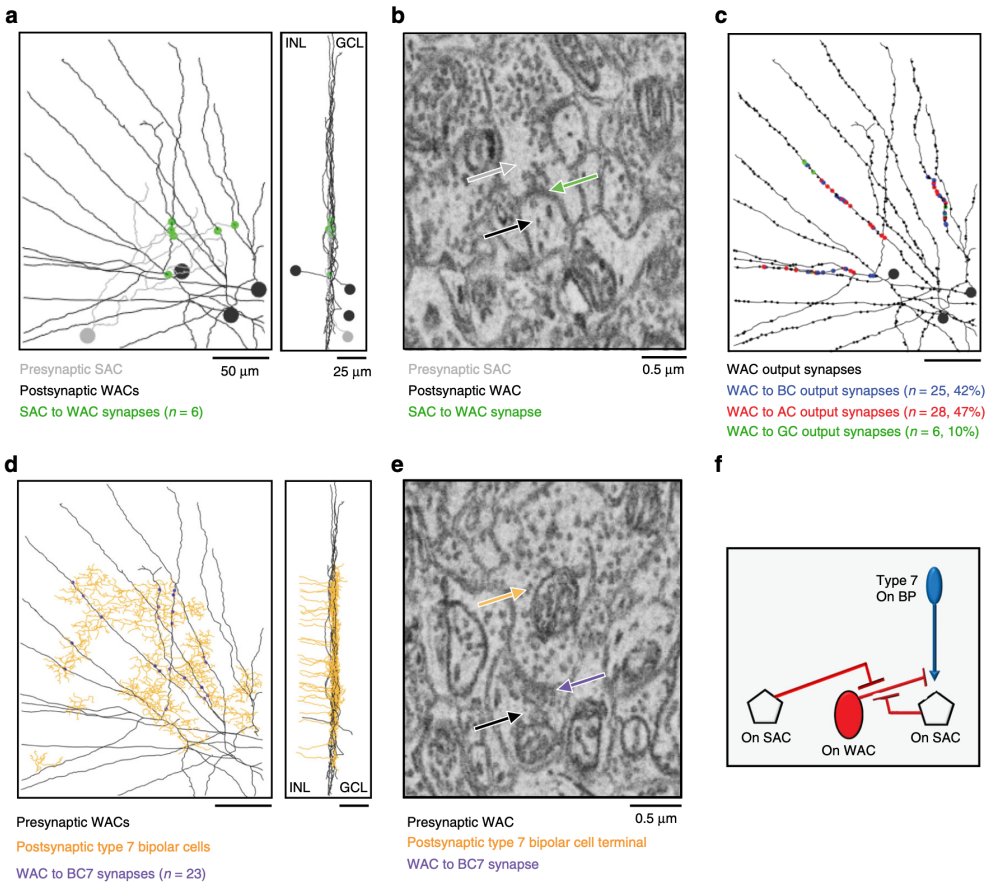

Figure 2.15: **On SAC – On WAC – On BC – On SAC synaptic motif is detected by connectomic tracing.**
a, Connectomic reconstruction of an On SAC dendritic sector (grey) and 3 of its postsynaptic On WACs (black). Spheres indicate the soma locations of the SAC (grey) and On WACs (black).
b, An electron microscopy (EM) example of On SAC – On WAC synapse.
c, Identity of the output synapses from the On WACs reconstructed in a. Color code indicates the n=59 sampled synapses in which the postsynaptic partner was classified as either bipolar cell (BC), amacrine cell (AC), or ganglion cell (GC).
d, Type 7 bipolar cells previously reconstructed in the volume (orange) and the On WACs reconstructed in a (black). Small blue spheres indicated On WAC – BC7 synapses.
e, An electron microscopy (EM) example of On WAC – BC7 synapse.
f, Schematic summarizes the On SAC – On WAC – On BC7 – On SAC synaptic connections reconstructed by connectomic tracing.

inner nuclear layer (INL). We identified 6 synapses between the presynaptic On SAC wedge and the 3 WACs. Notably, all 3 WACs postsynaptic to the On SAC (Figure. 2.15a), as well as the previously traced WACs that inhibit Off SACs (Figure. 2.5h) (Ding et al., 2016), have straight, unbranched dendritic segments extending distances of hundreds of microns, making them strong candidates for detecting continuous edges (also see Discussion). Next, the output synapses of the 3 WACs were traced, and 20 synapses from each WAC were selected for further tracing of their postsynaptic partners. We found 42% of the output synapses of the WACs were made onto bipolar cell terminals (Figure. 2.15c). Next, we asked whether the postsynaptic bipolar cells targeted by these WACs contain bipolar cell types that are known to synapse onto On SACs. We identified 23 synapses from these three WACs to type 7 bipolar cells (Figures. 2.15d and 2.15e), which are well characterized as a major bipolar cell type synapsing onto On SACs (Ding et al., 2016). Therefore, both the electrophysiological results and connectomic reconstruction support the On SAC – WAC – BC – On SAC microcircuit motif underlying the On contextual sensitivity of pDSGCs (Figure. 2.15f).

Similar to the Off pathway, the stronger suppression of On responses during uniform grating was eliminated or masked by new effects after applying TTX to the control retina (Figures. 2.8a and 2.8c), indicating that spiking cells are involved either as the WACs or indirectly upstream of this microcircuit motif to influence center-surround interactions.

2.4.7 A circuit model of pDSGC contextual modulation

Based on the above results, we propose a circuit model of pDSGC contextual modulation (Figure. 2.16). Since uniform grating generates stronger surround suppression of pDSGC responses than gratings with phase-contrast or direction-contrast, we hypothesize that the contextually sensitive WACs with straight, unbranched dendrites are preferentially activated

by a continuous moving contour extending across the center and surround regions. Gratings with direction-contrast or phase-contrast introduce discontinuities between the center and surround regions, and therefore weaken the WAC activation.

Although the center and surround edges in gratings with direction-contrast and phase-contrast are discontinuous, their orientations are always the same. We next used a drifting grating stimulus in which the surround grating drifted in the orthogonal directions relative to the center grating (surround-in-orthogonal, Figure. 2.17a, schematics). Under this condition, the orientations of center and surround contours differ at all times. Notably, we found that this surround-in-orthogonal grating did not evoke significant surround suppression of pDSGC response relative to the center-only response (Figure. 2.17c). As a result, the spike response of pDSGC during the surround-in-orthogonal grating was greater than that during the direction-contrast grating (renamed as surround-in-opposite in Figures. 2.17a and 2.17b). Together, these results indicate that the activation of the WACs is maximal during the movement of a continuous edge spanning the center and surround, and is minimal when center and surround edges are moving in orthogonal directions.

Finally, we tested whether contextual modulation of pDSGC responses can also occur in the absence of motion. We presented three types of stationary contrast-reversing grating patterns to each pDSGC (Figure. 2.17d): 1) a uniform grating with center and surround gratings in the same phase (uniform), 2) a compound grating with a 180-degree center/surround phase shift (antiphase), and 3) a compound grating where the edges in the center and the surround are orthogonal to each other (surround-in-orthogonal). We found no statistically significant difference in pDSGC spiking activity between uniform and antiphase contrast-reversing gratings (Figure. 2.17e), in contrast to the differential responses of pDSGCs to drifting uniform and compound gratings with parallel edges (Figures. 2.1d and 2.9b). We

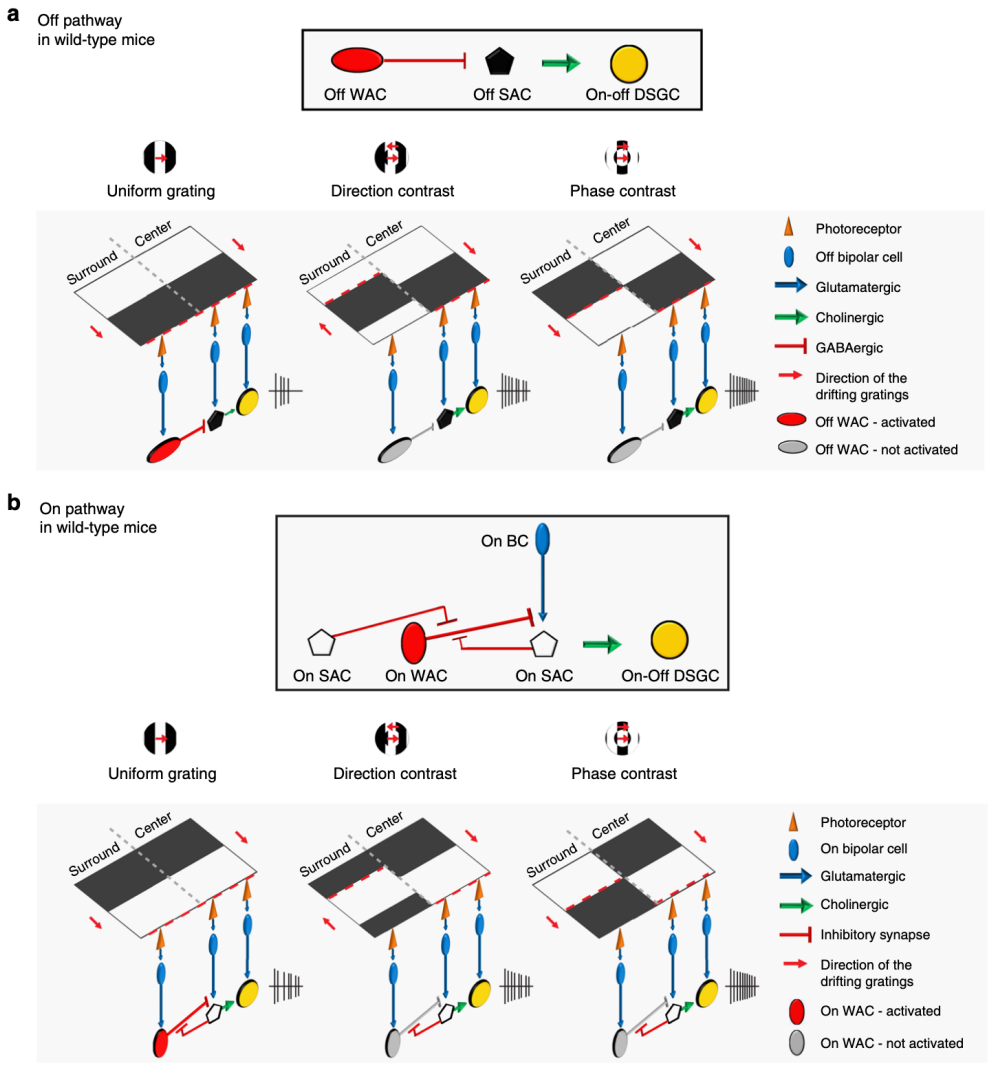

Figure 2.16: **Divergent synaptic circuits implement contextual modulation in the Off and On pathways of pDSGCs.**
a, A model of the synaptic mechanism underlying contextual modulation in the Off pathway. Box at the top: Schematic shows the synaptic motif in the Off pathway that participate in contextual modulation. Off WACs provide direct GABAergic inhibition onto Off SACs to suppress the cholinergic excitation from these Off SACs onto pDSGCs. Schematics in the bottom: Activation of the contextually modulated synaptic circuitry in wild type mice under different stimulus conditions. The leading edges of the black bars of the drifting gratings are labeled with red dashed lines. During uniform grating, Off WAC – Off SAC inhibition is maximally activated by the continuous dark contour and causes the strongest suppression of DSGC response. This inhibitory connection is less activated when discontinuities are present between center and surround contours during compound gratings (direction-contrast and phase-contrast). As a result, DSGC response is less suppressed during the compound gratings. Such difference between uniform grating and compound gratings is disrupted in Gabra2 KO mice in which Off WAC – Off SAC inhibition is removed.

Figure 2.16, continued.
b, A model of the synaptic mechanism underlying contextual modulation in the On pathway. Box at the top: Schematic shows the relevant synaptic connections in the On pathway. On WACs provide contextually sensitive inhibitory inputs onto bipolar cells (BCs) presynaptic to On SACs. In wild type mice, this inhibitory connection is suppressed by the GABAergic inhibition from On SACs. Schematics in the bottom: The leading edges of the white bars of the drifting gratings are labeled with red dashed lines. Because of the On SAC – On WAC – On BC – On SAC synaptic motif, the pDSGC On response is weakly modulated by stimulus contexts. Such weak contextual modulation is enhanced in Vgat cKO mice in which On SAC – On WAC inhibition is disrupted, but not affected in Gabra2 cKO mice in which GABA-A receptors of SACs are disrupted.

postulate that such motion sensitivity of DSGC contextual modulation likely reflects the fact that uniform drifting gratings contain continuous edges that sweep across the entire visual stimulation area, and are therefore effective in activating many WAC dendrites in the area. The continuous/discontinuous edges of the stationary uniform/antiphase gratings in our study, by contrast, are confined to fixed spatial locations, and therefore may not be as effective in differentially activating WAC dendrites as drifting gratings. However, we did find that surround-in-orthogonal contrast-reversing grating triggered a higher firing rate of the pDSGC than contrast-reversing uniform gratings (Figure. 2.17f). Therefore, even though the WAC-mediated circuitry plays important roles in the contextual modulation of moving stimuli, it can also contribute the center-surround interactions evoked by other non-motion visual stimuli.

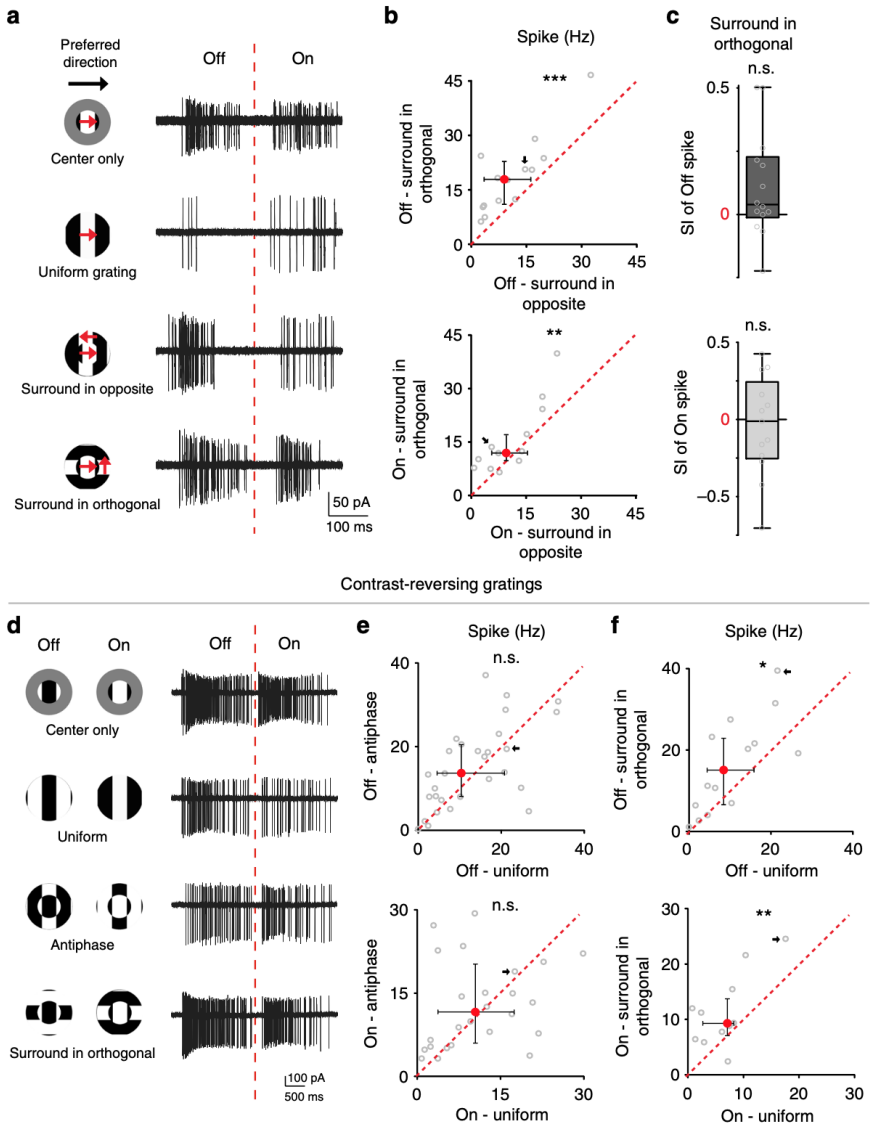

Figure 2.17: **Contextual modulation of pDSGCs is sensitive to the relative orientation of center and surround contours.**

a, Example spike traces of a pDSGC from a control mouse evoked by the visual stimuli shown on the left. The red dashed line shows the boundary of the Off and On responses.

b, Comparison of pDSGC firing rate during surround-in-orthogonal versus surround-in-opposite gratings, pairwise comparison was performed using Wilcoxon signed-rank test. Off response: n = 14 cells from 8 mice, ***$p < 0.001$; On response: n = 13 cells from 7 mice, **$p = 0.0081$.

c, Upper panel: SI of Off spike during surround-in-orthogonal: Wilcoxon signed-rank test was used to test whether the SI of surround-in-orthogonal is significantly higher than 0: $p = 0.091$. Lower panel: SI of On spike during surround-in-orthogonal: $p = 0.32$. The same sample groups as Figure 2.17b.

Figure 2.17, continued.
d-f, Loose-patch recording of pDSGC under contrast-reversing stationary gratings.
d, Left: Schematics show the contrast-reversing stationary grating stimuli. Right: Spiking responses of an example pDSGC from a control mouse. Red dashed line labels the boundary of Off and On spiking.
e, Scatter plots compares pDSGC spike firing rate during uniform contrast-reversing gratings and antiphase contrast-reversing gratings. Off response: n = 29 cells from 7 mice, p = 0.1385; On response: n = 26 cells from 7 mice, p = 0.6964.
f, Same as **e**, but comparing pDSGC spike firing rate during uniform contrast-reversing gratings versus surround-in-orthogonal contrast-reversing gratings. Off response: n = 14 cells from 4 mice, *p = 0.0203; On response: n = 11 cells from 4 mice, **p = 0.0098.

2.5 Discussion

Our study reveals that the responses of pDSGCs to bright and dark stimuli are differentially modulated by motion patterns in the surround owing to the divergent inhibitory microcircuits in the On and Off pathways. Although our study focuses on the posterior subtype of mouse On-Off DSGCs, we speculate that the mechanisms we reported here may contribute to the contextual modulation in all subtypes of On-Off DSGCs because of the following reasons. First, contextual modulation of On-Off DSGCs spiking was reported in the rabbit retina (Chiao and Masland, 2003), which sampled all four subtypes. No difference was reported among subtypes of On-Off DSGCs. Second, from our study, the mechanisms of pDSGC contextual modulation in both On and Off pathways act on SACs, which contribute to the spiking activity of all four types of On-Off DSGCs (reviewed by (Vaney et al., 2012)).

Distinct microcircuits for contextual modulation were revealed in the On and Off pathways of the direction-selective circuit. In the Off pathway, contextual sensitivity of pDSGCs depends on the GABAergic connection from WACs to Off SACs, which in turn maximally reduces cholinergic excitation from Off SACs to pDSGCs (Fig. 8a). However, a mirror symmetric motif was not found for On SACs, and the moderate contextual modulation in the On pathway is mediated by a On SAC – WAC – BC – On SAC motif. This asymmetry may reflect

the fact that On SACs also synapse onto On DSGCs (Brombas et al., 2017; Yonehara et al., 2011), which signal global image shift rather than moving objects against their backgrounds (Dhande et al., 2013; Vaney et al., 2001). The contextual sensitivity of On DSGCs to motion coherence has not been determined, and remains an interesting topic for future investigation.

A new function of On SACs was demonstrated here: GABA release from On SACs inhibits a population of WACs that provide contextual sensitivity to On SACs (Fig. 8b). Functional and connectomic data both support a previously unidentified On SAC – WAC – BC – On SAC circuit motif underlying this contextual modulation. In contrast, Off SACs do not make considerable synapses onto WACs (Ding et al., 2016). These results together highlight the power of combining functional and connectomic methods in neural circuit analysis.

Despite distinct postsynaptic targets of WACs in the On and Off pathways for pDSGC contextual modulation (Fig. 8), the WACs synaptically connected to On and Off SACs show pronounced similarities in their dendritic morphology: they all have straight, unbranched dendritic segments extending over long distances. This morphological feature, in contrast to a more branched and space-filling dendritic arbor such as those of pDSGCs, is uniquely suitable for detecting continuities of contours in visual stimuli. A continuous moving edge over the retina likely activates the BCs presynaptic to these WAC dendritic branches simultaneously, resulting in strong dendritic activation. In contrast, these WAC dendrites receive less synchronized excitation when the contours contain discontinuities, and thereby reduce the inhibitory control of their postsynaptic targets. An analogous mechanism has been implicated in the salamander retina, in which the long, straight axons of polyaxonal amacrine cells exert stronger inhibition during global motion than during differential motion (Baccus et al., 2008). It is noteworthy that although the WAC circuitry underlies motion-evoked contextual sensitivity of pDSGCs, motion is not exclusively required for the differential activation

of these WACs, since contextual modulation of pDSGCs is also present during stationary contrast-reversing gratings (Fig. 9f). Future development of novel tools and methods for directly recording these WACs will provide deeper insights into their RF properties.

Connectomic analysis shows that On WACs provide inputs to multiple cell types including BCs, ACs and ganglion cells. Therefore, it is possible that these "continuity detectors" participate in visual processing of multiple retinal circuits besides the direction-selective circuit. Furthermore, since On SACs inhibit the WACs in the On pathway, our study raises an interesting possibility that On SACs may be involved in the contextual sensitivity of multiple retinal ganglion cell types in addition to its renowned role in generating direction selectivity in DSGCs. We noted that a small fraction of presynaptic inputs from On WACs to On SACs (5%) was also reported by a previous study(Ding et al., 2016). However, contextual sensitivity of pDSGC On responses is not affected in Gabra2 cKO mice, suggesting that these On WACs-On SAC connections alone are not sufficient to modulate contextual sensitivity of pDSGCs. It is not clear how these WACs contribute to pDSGC responses, and if these WACs are also inhibited by On SACs. Future connectomic analysis will provide deeper insights into this question.

Are direction selectivity and contextual sensitivity of On-Off DSGCs independent of each other? Our study shows that this question needs to be addressed separately for On and Off pathways. The Off response of pDSGCs shows pronounced contextual sensitivity at the expense of robust direction selectivity, because the preferred-, but not null-direction Off response is more drastically suppressed by uniform grating than by compound gratings. On the other hand, the On response of pDSGCs maintains robust direction selectivity at the expense of contextual sensitivity, because the preferred-direction On response is moderately and similarly suppressed by compound gratings and uniform grating, leading to similar DSI

values of pDSGC On responses across these stimulus conditions.

We postulate that these divergent RF properties of pDSGC On and Off responses may reflect the adaptation to the light/dark asymmetries in the natural environment (Ratliff et al., 2010). Enhanced sensitivity to image discontinuities in the Off pathway and robust direction selectivity in the On pathway may also confer an advantage in information encoding of On-Off DSGCs by reducing the redundancy of information in the On and Off channels. Indeed, asymmetries between the On and Off pathways of the retina have been implicated in efficient motion estimation of natural scenes in both humans and flies (Clark et al., 2014; Fitzgerald and Clark, 2015).

On-Off DSGCs in the mouse retina innervate the superior colliculus (SC) and the dorsal lateral geniculate nucleus (dLGN) (Cruz-Martín et al., 2014; Huberman et al., 2009; Kay et al., 2011; Rivlin-Etzion et al., 2011), two major nuclei involved in the image-forming pathway and visually guided behavior. In the superior colliculus, the direction selectivity of collicular neurons originates from direction-selective inputs from DSGCs, and selective ablation of retinal direction selectivity leads to a loss of collicular direction selectivity (Shi et al., 2017). However, although collicular neurons inherit their direction selectivity from On-Off DSGC inputs, they do not inherit exactly the same contextual modulation pattern of On-Off DSGCs (Barchini et al., 2018). Differential contextual effects of surround motion in retinal and collicular direction-selective neurons provide a remarkable example of signal transformation along the visual pathways, and a starting point for investigating the input-output relationships for complex motion stimuli in higher visual circuits.

Finally, we noted that the contextual modulation of On-Off DSGCs exhibits interesting mechanistic similarities to that of visual cortical neurons. It has been well-documented in

V1 neurons that surround suppression is selectively engaged by statistical redundancy between center and surround images (Blakemore and Tobin, 1972; Cavanaugh et al., 2002; Gilbert and Wiesel, 1990). The suppression of spiking activity for visual cortical neurons is accompanied by reduced excitatory drive and a concomitant reduction of inhibition (Ozeki et al., 2009; Priebe and Ferster, 2006), similar to what was observed in On-Off DSGCs in the retina (Fig. 2). It is yet to be explored if a unified model can account for contextual modulation in multiple visual areas despite the differences in their detailed cellular and synaptic organizations.

2.6 References

Albright, T.D., and Stoner, G.R. (2002). Contextual Influences on Visual Processing. Annual Review of Neuroscience 25, 339–379.

Auferkorte, O.N., Baden, T., Kaushalya, S.K., Zabouri, N., Rudolph, U., Haverkamp, S., and Euler, T. (2012). GABA(A) receptors containing the $\alpha 2$ subunit are critical for direction-selective inhibition in the retina. PloS One 7, e35109.

Baccus, S. A, Olveczky, B.P., Manu, M., and Meister, M. (2008). A retinal circuit that computes object motion. The Journal of Neuroscience: The Official Journal of the Society for Neuroscience 28, 6807–6817.

Baden, T., Esposti, F., Nikolaev, A., and Lagnado, L. (2011). Spikes in Retinal Bipolar Cells Phase-Lock to Visual Stimuli with Millisecond Precision. Current Biology 21, 1859–1869.

Barchini, J., Shi, X., Chen, H., and Cang, J. (2018). Bidirectional encoding of motion contrast in the mouse superior colliculus. ELife 7.

Barlow, H.B., and Levick, W.R. (1965). The mechanism of directionally selective units in rabbit's retina. The Journal of Physiology 178, 477–504.

Blakemore, C., and Tobin, E.A. (1972). Lateral inhibition between orientation detectors in the cat's visual cortex. Experimental Brain Research 15, 439–440.

Brainard, D.H. (1997). The Psychophysics Toolbox. Spatial Vision 10, 433–436.

Brandstätter, J.H., Greferath, U., Euler, T., and Wässle, H. (2009). Co-stratification of GABAA receptors with the directionally selective circuitry of the rat retina. Visual Neuroscience 12, 345.

Briggman, K.L., Helmstaedter, M., and Denk, W. (2011). Wiring specificity in the direction-selectivity circuit of the retina. Nature 471, 183–188.

Brombas, A., Kalita-de Croft, S., Cooper-Williams, E.J., and Williams, S.R. (2017). Dendro-dendritic cholinergic excitation controls dendritic spike initiation in retinal ganglion cells. Nature Communications 8, 15683.

Cavanaugh, J.R., Bair, W., and Movshon, J.A. (2002). Selectivity and Spatial Distribution of Signals From the Receptive Field Surround in Macaque V1 Neurons. Journal of Neurophysiology 88, 2547–2556.

Chen, Q., and Wei, W. (2018). Stimulus-dependent engagement of neural mechanisms for reliable motion detection in the mouse retina. Journal of Neurophysiology jn.00716.2017.

Chen, Q., Pei, Z., Koren, D., and Wei, W. (2016). Stimulus-dependent recruitment of lateral inhibition underlies retinal direction selectivity. ELife 5.

Chiao, C.-C., and Masland, R.H. (2003). Contextual tuning of direction-selective retinal ganglion cells. Nature Neuroscience 6, 1251–1252.

Clark, D.A., Fitzgerald, J.E., Ales, J.M., Gohl, D.M., Silies, M.A., Norcia, A.M., and Clandinin, T.R. (2014). Flies and humans share a motion estimation strategy that exploits natural scene statistics. Nature Neuroscience 17, 296–303.

Cruz-Martín, A., El-Danaf, R.N., Osakada, F., Sriram, B., Dhande, O.S., Nguyen, P.L., Callaway, E.M., Ghosh, A., and Huberman, A.D. (2014). A dedicated circuit links direction-selective retinal ganglion cells to the primary visual cortex. Nature 507, 358–361.

CUI, J., and PAN, Z.-H. (2008). Two types of cone bipolar cells express voltage-gated Na+ channels in the rat retina. Visual Neuroscience 25, 635.

Demb, J.B., Haarsma, L., Freed, M.A., and Sterling, P. (1999). Functional circuitry of the retinal ganglion cell's nonlinear receptive field. The Journal of Neuroscience: The Official Journal of the Society for Neuroscience 19, 9756–9767.

Denk, W., and Horstmann, H. (2004). Serial block-face scanning electron microscopy to reconstruct three-dimensional tissue nanostructure. PLoS Biology 2, e329.

Dhande, O.S., Estevez, M.E., Quattrochi, L.E., El-Danaf, R.N., Nguyen, P.L., Berson, D.M., and Huberman, A.D. (2013). Genetic dissection of retinal inputs to brainstem nuclei controlling image stabilization. The Journal of Neuroscience: The Official Journal of the Society for Neuroscience 33, 17797–17813.

Ding, H., Smith, R.G., Poleg-Polsky, A., Diamond, J.S., and Briggman, K.L. (2016). Species-specific wiring for direction selectivity in the mammalian retina. Nature 535, 105–110.

Euler, T., Detwiler, P.B., and Denk, W. (2002). Directionally selective calcium signals in dendrites of starburst amacrine cells. Nature 418, 845–852.

Famiglietti, E. V (1991). Synaptic organization of starburst amacrine cells in rabbit retina: analysis of serial thin sections by electron microscopy and graphic reconstruction. The Journal of Comparative Neurology 309, 40–70.

Famiglietti, E. V. (1992). Dendritic Co-stratification of ON and ON-OFF directionally selective ganglion cells with starburst amacrine cells in rabbit retina. The Journal of Comparative Neurology 324, 322–335.

Farrow, K., Teixeira, M., Szikra, T., Viney, T.J.J., Balint, K., Yonehara, K., and Roska, B. (2013). Ambient illumination toggles a neuronal circuit switch in the retina and visual perception at cone threshold. Neuron 78, 325–338.

Fitzgerald, J.E., and Clark, D.A. (2015). Nonlinear circuits for naturalistic visual motion estimation. ELife 4, e09123.

Flores-Herr, N., Protti, D.A., and Wässle, H. (2001). Synaptic Currents Generating the Inhibitory Surround of Ganglion Cells in the Mammalian Retina. Journal of Neuroscience 21.

Fried, S.I., Münch, T.A., and Werblin, F.S. (2002). Mechanisms and circuitry underlying directional selectivity in the retina. Nature 420, 411–414.

Gilbert, C.D., and Wiesel, T.N. (1990). The influence of contextual stimuli on the orientation selectivity of cells in primary visual cortex of the cat. Vision Research 30, 1689–1701.

Helmstaedter, M., Briggman, K.L., and Denk, W. (2011). High-accuracy neurite reconstruction for high-throughput neuroanatomy. Nature Neuroscience 14, 1081–1088.

Hoggarth, A., McLaughlin, A.J.J., Ronellenfitch, K., Trenholm, S., Vasandani, R., Sethuramanujam, S., Schwab, D., Briggman, K.L.L., and Awatramani, G.B.B. (2015). Specific

Wiring of Distinct Amacrine Cells in the Directionally Selective Retinal Circuit Permits Independent Coding of Direction and Size. Neuron 86, 276–291.

Huberman, A.D., Wei, W., Elstrott, J., Stafford, B.K., Feller, M.B., and Barres, B.A. (2009). Genetic identification of an On-Off direction-selective retinal ganglion cell subtype reveals a layer-specific subcortical map of posterior motion. Neuron 62, 327–334.

Jacoby, J., and Schwartz, G.W. (2017). Three Small-Receptive-Field Ganglion Cells in the Mouse Retina Are Distinctly Tuned to Size, Speed, and Object Motion. The Journal of Neuroscience 37, 610–625.

Kay, J.N., De la Huerta, I., Kim, I.-J., Zhang, Y., Yamagata, M., Chu, M.W., Meister, M., and Sanes, J.R. (2011). Retinal ganglion cells with distinct directional preferences differ in molecular identity, structure, and central projections. The Journal of Neuroscience: The Official Journal of the Society for Neuroscience 31, 7753–7762.

Kuhn, N.K., and Gollisch, T. (2016). Joint Encoding of Object Motion and Motion Direction in the Salamander Retina. Journal of Neuroscience 36, 12203–12216.

Lee, S., and Zhou, Z.J. (2006). The synaptic mechanism of direction selectivity in distal processes of starburst amacrine cells. Neuron 51, 787–799.

Lee, S., Kim, K., and Zhou, Z.J. (2010). Role of ACh-GABA cotransmission in detecting image motion and motion direction. Neuron 68, 1159–1172.

Ölveczky, B.P., Baccus, S.A., and Meister, M. (2003). Segregation of object and background motion in the retina. Nature 423, 401–408.

Ozeki, H., Finn, I.M., Schaffer, E.S., Miller, K.D., and Ferster, D. (2009). Inhibitory Stabilization of the Cortical Network Underlies Visual Surround Suppression. Neuron 62, 578–592.

Pearson, J.T., and Kerschensteiner, D. (2015). Ambient illumination switches contrast preference of specific retinal processing streams. Journal of Neurophysiology 114, jn.00360.2015.

Pei, Z., Chen, Q., Koren, D., Giammarinaro, B., Acaron Ledesma, H., and Wei, W. (2015). Conditional Knock-Out of Vesicular GABA Transporter Gene from Starburst Amacrine Cells

Reveals the Contributions of Multiple Synaptic Mechanisms Underlying Direction Selectivity in the Retina. The Journal of Neuroscience: The Official Journal of the Society for Neuroscience 35, 13219–13232.

Priebe, N.J., and Ferster, D. (2006). Mechanisms underlying cross-orientation suppression in cat visual cortex. Nature Neuroscience 9, 552–561.

Ratliff, C.P., Borghuis, B.G., Kao, Y.-H., Sterling, P., and Balasubramanian, V. (2010). Retina is structured to process an excess of darkness in natural scenes. Proceedings of the National Academy of Sciences 107, 17368–17373.

Rivlin-Etzion, M., Zhou, K., Wei, W., Elstrott, J., Nguyen, P.L., Barres, B.A., Huberman, A.D., and Feller, M.B. (2011). Transgenic mice reveal unexpected diversity of on-off direction-selective retinal ganglion cell subtypes and brain structures involved in motion processing. The Journal of Neuroscience: The Official Journal of the Society for Neuroscience 31, 8760–8769.

Roska, B., and Werblin, F. (2003). Rapid global shifts in natural scenes block spiking in specific ganglion cell types. Nature Neuroscience 6, 600–608.

Sabbah, S., Gemmer, J.A., Bhatia-Lin, A., Manoff, G., Castro, G., Siegel, J.K., Jeffery, N., and Berson, D.M. (2017). A retinal code for motion along the gravitational and body axes. Nature 546, 492–497.

Saszik, S., and DeVries, S.H. (2012). A mammalian retinal bipolar cell uses both graded changes in membrane voltage and all-or-nothing Na+ spikes to encode light. The Journal of Neuroscience: The Official Journal of the Society for Neuroscience 32, 297–307.

Sethuramanujam, S., McLaughlin, A.J., deRosenroll, G., Hoggarth, A., Schwab, D.J., and Awatramani, G.B. (2016). A Central Role for Mixed Acetylcholine/GABA Transmission in Direction Coding in the Retina. Neuron 90, 1243–1256.

Sethuramanujam, S., Awatramani, G.B., and Slaughter, M.M. (2018). Cholinergic excitation complements glutamate in coding visual information in retinal ganglion cells. The Journal

of Physiology.

Shi, X., Barchini, J., Ledesma, H.A., Koren, D., Jin, Y., Liu, X., Wei, W., and Cang, J. (2017). Retinal origin of direction selectivity in the superior colliculus. Nature Neuroscience 20, 550–558.

Taylor, W.R. (1999). TTX attenuates surround inhibition in rabbit retinal ganglion cells. Visual Neuroscience 16, 285–290.

Taylor, W.R., and Vaney, D.I. (2002). Diverse synaptic mechanisms generate direction selectivity in the rabbit retina. The Journal of Neuroscience: The Official Journal of the Society for Neuroscience 22, 7712–7720.

Tikidji-Hamburyan, A., Reinhard, K., Seitter, H., Hovhannisyan, A., Procyk, C.A., Allen, A.E., Schenk, M., Lucas, R.J., and Münch, T.A. (2014). Retinal output changes qualitatively with every change in ambient illuminance. Nature Neuroscience 18, 66–74.

Trenholm, S., Johnson, K., Li, X., Smith, R.G., and Awatramani, G.B. (2011). Parallel mechanisms encode direction in the retina. Neuron 71, 683–694.

Vaney, D., He, S., Taylor, W., and Levick, W. (2001). Direction-selective ganglion cells in the retina. Motion Vision.

Vaney, D.I., Sivyer, B., and Taylor, W.R. (2012). Direction selectivity in the retina: symmetry and asymmetry in structure and function. Nature Reviews. Neuroscience 13, 194–208.

Wei, W., Hamby, A.M., Zhou, K., and Feller, M.B. (2011). Development of asymmetric inhibition underlying direction selectivity in the retina. Nature 469, 402–406.

Yonehara, K., Balint, K., Noda, M., Nagel, G., Bamberg, E., and Roska, B. (2011). Spatially asymmetric reorganization of inhibition establishes a motion-sensitive circuit. Nature 469, 407–410.

CHAPTER 3

TEMPORAL CONTEXTUAL MODULATION IN THE RETINAL DIRECTION SELECTIVE CIRCUIT

This Chapter is a full reprint of Huang et al., bioRxiv, in which I am the primary author. The work is included with permission from all authors. To be noted, the manuscript here have not yet been formally peer-reviewed and may undergo revision.

Relevant Publication

Xiaolin Huang, Alan Jaehyun Kim, Hector Acaron Ledesma, Jennifer Ding, Robert G Smith, Wei Wei. 2021 "**Visual stimulation induces distinct forms of sensitization of On-Off direction-selective ganglion cell responses in the dorsal and ventral retina.**" bioRxiv, doi: https://doi.org/10.1101/2021.06.19.449131

For supplementary multimedia documents, please refer to

`https://doi.org/10.1101/2021.06.19.449131`

3.1 Abstract

Experience-dependent modulation of neuronal responses is a key attribute in sensory processing. In the mammalian retina, the On-Off direction-selective ganglion cell (On-Off DSGC) is well known for its robust direction selectivity. However, how the On-Off DSGC light responsiveness dynamically adjusts to the changing visual environment is underexplored. Here, we report that the On-Off DSGC can be transiently sensitized by prior stimuli. Notably, distinct sensitization patterns are found in dorsal and ventral DSGCs that receive visual inputs from lower and upper visual fields respectively. Although responses of both dorsal and ventral DSGCs to dark stimuli (Off responses) are sensitized, only dorsal cells show sensitization of responses to bright stimuli (On responses). Visual stimulation to the dorsal retina poten-

tiates a sustained excitatory input from Off bipolar cells, leading to tonic depolarization of dorsal DSGCs. Such tonic depolarization propagates from the Off to the On dendritic arbor of the DSGC to sensitize its On response. We also identified a previously overlooked feature of DSGC dendritic architecture that can support direct electrotonic propagation between On and Off dendritic layers. By contrast, ventral DSGCs lack a sensitized tonic depolarization and thus do not exhibit sensitization of their On responses. Our results highlight a topographic difference in Off bipolar cell inputs underlying divergent sensitization patterns of dorsal and ventral On-Off DSGCs. Moreover, substantial crossovers between dendritic layers of On-Off DSGCs suggest an interactive dendritic algorithm for processing On and Off signals before they reach the soma.

3.2 Significance statement

Visual neuronal responses are dynamically influenced by the prior visual experience. This form of plasticity reflects the efficient coding of the naturalistic environment by the visual system. We found that a class of retinal output neurons, On-Off direction-selective ganglion cells, transiently increase their responsiveness after visual stimulation. Cells located in dorsal and ventral retina exhibit distinct sensitization patterns due to different adaptive properties of Off bipolar cell signaling. A previously overlooked dendritic morphological feature of the On-Off direction-selective ganglion cell is implicated in the crosstalk between On and Off pathways during sensitization. Together, these findings uncover a topographic difference in the adaptive encoding of upper and lower visual fields and the underlying neural mechanism in the dorsal and ventral retina.

3.3 Introduction

Visual perception and visual neuronal responses are dynamically influenced by prior visual stimuli. Such short-term modulation is thought to underlie some visual perceptual phenomena such as saliency-based bottom-up visual attention and a rich repertoire of aftereffects and illusions(Clifford et al., 2000; Kohn, 2007; Schwartz et al., 2007; Theeuwes, 2013; Kamkar et al., 2018; Akyuz et al., 2020). In the early stage of the vertebrate visual system, retinal ganglion cells (RGCs) already show short-term adjustments of their responsiveness. Previous studies have mainly focused on adaptation, which refers to the decrease of sensitivity after a period of strong stimulus(Kim and Rieke, 2001; Demb, 2008; Rieke and Rudd, 2009; Wark et al., 2009; Khani and Gollisch, 2017; Matulis et al., 2020). However, sensitization, the enhanced responsiveness after a strong stimulus, has been documented more recently. Studies in zebrafish, salamander, mouse and primate show that subpopulations of RGCs transiently increase their sensitivity after a period of high contrast stimulation(Kastner and Baccus, 2011; Nikolaev et al., 2013; Appleby and Manookin, 2019). That the phenomenon of RGC sensitization is conserved across species implies its functional significance. Sensitization has been proposed to complement adaptation for maintaining the responsiveness of the overall RGC population and improving the information encoding capacity and fidelity, and to contribute to the prediction of future visual inputs(Kastner and Baccus, 2011, 2013; Appleby and Manookin, 2019; Kastner et al., 2019).

The RGC population consists of diverse cell types, each conveying a distinct feature to the brain(Sanes and Masland, 2015). Delineating the sensitization or adaptation patterns of specific RGC types is thus necessary for a more comprehensive understanding of the retina's neural code. In the mammalian retina, On-Off direction-selective ganglion cells (On-Off DSGC) are well-defined encoders of direction of motion, exhibiting a strong response to motion in their preferred direction and but weak response to motion in the opposite direction

(null direction)(Barlow and Levick, 1965). However, how the light sensitivity of these cells is shaped by prior visual stimuli is not fully understood.

The On and Off responses of On-Off DSGCs are generated in different layers of their bistratified dendritic arbors, which are embedded in the On and Off sublaminae of the inner plexiform layer (IPL). The synaptic inputs onto each dendritic layer consist of glutamatergic inputs from On or Off bipolar cells, cholinergic inputs and asymmetric GABAergic inputs from On or Off starburst amacrine cells. The GABAergic inhibition is strongest when motion is in the null direction but weakest and delayed in the preferred direction, and thus plays an essential role in the direction tuning of DSGCs(Barlow and Levick, 1965). Although mechanisms underlying direction selectivity have been extensively studied, the adaptation or sensitization properties of the DSGC's synaptic inputs and the resulting impacts on its spiking activity are unknown.

In this study, we address these outstanding questions by monitoring the synaptic inputs and spiking activity of On-Off DSGCs before and after a period of visual stimulation. We found that a set of iso-contrast stimuli can induce sensitization of synaptic inputs onto DSGCs and cause enhanced spiking responses. Surprisingly, we found that dorsal and ventral DSGCs exhibit distinct sensitization patterns that originate from the Off pathway. In contrast to the conventional view of segregated signal processing in the On and Off dendritic layers of the DSGC, we noted substantial dendritic crossovers between layers that may contribute to the relay of sensitization from the Off to the On pathway in the dorsal DSGC. Together, these results reveal location-dependent synaptic mechanisms underlying the divergent sensitization patterns of On-Off DSGCs receiving inputs from the upper and the lower visual fields.

3.4 Materials and Methods

3.4.1 Animals

Drd4-GFP mice of ages P12-13 or P22-P53 of either sex were used in this study to label On-Off DSGCs that prefer motion in the posterior direction (pDSGCs). This mouse line was originally developed by MMRRC (`http://www.mmrrc.org/strains/231/0231.html`) in the Swiss Webster background and subsequently backcrossed to C57BL/6 background. All procedures for mouse maintenance and use were in accordance with the University of Chicago Institutional Animal Care and Use Committee (Protocol number ACUP 72247) and in conformance with the NIH Guide for the Care and Use of Laboratory Animals and the Public Health Service Policy.

3.4.2 Whole-mount retina preparation

Mice were dark adapted for more than 30 min, anesthetized with isoflurane and then euthanized by decapitation. Under infrared light, retinas were isolated from the pigment epithelium layers and cut into halves at room temperature in Ames' medium (Sigma-Aldrich, St. Louis, MO) bubbled with 95% O2/5% CO2. The retinas were then mounted with ganglion-cell-layer up on top of a ~ 1.5 mm^2 hole in a small piece of filter paper (Millipore, Billerica, MA). Cells in the center of the hole were used for experiments.

3.4.3 Visual stimulation

A white organic light-emitting display (OLEDXL, eMagin, Bellevue, WA; 800 $\times$ 600 pixel resolution, 60 Hz refresh rate) was controlled by an Intel Core Duo computer with a Windows 7 operating system and presented to the retina at a resolution of 1.1 μm/pixel. To be

noted, the light spectrum of the OLED does not cover the absorption spectrum of S opsin and thus only activates rhodopsin and M opsins(Rosa et al., 2016; Warwick et al., 2018). In this context, our light stimuli evoked DSGC EPSCs with comparable amplitudes in the dorsal and the ventral regions (data not shown), consistent with the even distribution of M-opsin expressing cones on the vertical axis(Applebury et al., 2000; Rosa et al., 2016). All visual stimuli were generated using MATLAB and Psychophysics Toolbox(Brainard, 1997), projected through the condenser lens of the two-photon microscope focused on the photoreceptor layer, and centered on the neuron somas.

The light response of pDSGCs was measured during multiple trials of stationary flashing spots ("the test spot"). For each trial, a white spot of 220 μm in diameter was shown for 1s, followed by 2.5 s of darkness. To measure the baseline light responsiveness, 5 trials of test spots were presented. And then 5 trials of one of the following induction stimuli were presented: 1) moving spots (same size and luminance as the test spot; moving area 660 μm in diameter; speed 300 μm/s; 3 s motion duration and 2.5 s inter-motion wait); 2) 100% contrast square wave drifting gratings (covering area 220 μm in diameter; spatial frequency 0.1 cycle/degree; temporal frequencies 1.5 Hz; 4 s motion duration and 1.5 s inter-motion wait); 3) contrast reversing square gratings (covering area 220 μm in diameter; spatial frequency 0.1 cycle/degree; temporal frequencies 1.5 Hz; 4 s contrast reversing and 1.5 s inter-stimulus wait). After that, test spots were presented for another 10-60 trials to measure the DSGC light responsiveness after induction stimulus. If not specifically noted, drifting grating stimulus in either the preferred or the null direction of the DSGC was used as the default induction stimulus to trigger sensitization effects in this study, as both directions had the same sensitizing effect on DSGCs. For experiments testing the time course of sensitization (Figure. 3.1D), we first presented five repetitions of the regular 3.5 s-interval test spots after the induction stimulus to confirm the degree of sensitization. Then we gradually increased the

time interval between test spots and measured the sensitization indexes accordingly. The luminance level of the black background was 335 isomerizations (R*)/rod/s, while both the spots and the bright bars of the gratings used light intensity of $\sim$ 2.6 x 10^5 isomerizations (R*)/rod/s in the photopic range.

3.4.4 Two-photon guided electrophysiology recording

Retinas were perfused with oxygenated Ames' medium with a bath temperature of $32-34\,^{\circ}$C. GFP-labelled pDSGCs in Drd4-GFP mice were targeted using a two-photon microscopy (Scientifica) and a Ti:sapphire laser (Spectra-Physics) tuned to 920 nm. Data were acquired using PCLAMP 10 software, Digidata 1550A digitizer and MultiClamp 700B amplifier (Molecular Devices, Sunnyvale, CA), low-pass filtered at 4 kHz and digitized at 10 kHz.

For loose cell-attached recordings, electrodes of 3.5–5 $M\Omega$ were filled with Ames' medium. For current-clamp whole cell recording (I = 0), electrodes were filled with a potassium-based internal solution containing 120 mM $KMeSO_4$, 10 mM KCl, 0.07 mM $CaCl_2 \cdot 2H_2O$, 0.1 mM EGTA, 2 mM adenosine 5'-triphosphate (magnesium salt), 0.4 mM guanosine 5'-triphosphate (trisodium salt), 10 mM HEPES, 10 mM phosphocreatine (disodium salt), pH 7.25. For voltage-clamp whole cell recording, electrodes were filled with a cesium-based internal solution containing 110 mM $CsMeSO_4$, 2.8 mM NaCl, 5 mM TEA-Cl, 4 mM EGTA, 4 mM adenosine 5'-triphosphate (magnesium salt), 0.3 mM guanosine 5'-triphosphate (trisodium salt), 20 mM HEPES, 10 mM phosphocreatine (disodium salt), 5 mM N-Ethyllidocaine chloride (QX314) (Sigma), pH 7.25. Light-evoked EPSCs and IPSCs of pDSGCs were isolated by holding the cells at reversal potentials (0 mV for GABAergic and -60 mV for cholinergic). Liquid junction potential ($\sim$ 10 mV) was corrected. In Figure. 3.5, to mimic the pDSGC activation pattern during drifting grating stimulus, we selected representative current-clamp

recordings of pDSGC membrane potential waveforms during drifting gratings, and used them as command potential waveforms in voltage-clamp experiments to replace the visual induction stimulus.

To investigate the contributions of different types of synaptic transmission to pDSGC sensitization, a synaptic agonist or antagonist was included in the Ames' medium: 0.008 mM Dihydro-b-erythroidine hydrobromide (DHbE; Tocris) for blocking nicotinic cholinergic receptors; 0.002 mM Atropine (Sigma) for blocking muscarinic cholinergic receptors; 0.0125 mM GABAzine (SR-95531, Tocris) for blocking GABA-A receptors; 0.001 mM Strychnine (Sigma) for blocking glycinergic receptors; 0.005 mM L-AP4 (Tocris) for activating type 6 metabotropic glutamatergic receptors (mGluR6) and blocking the On signaling pathways.

3.4.5 Analysis of electrophysiological data

For the measurement of the baseline light responsiveness, 5 repetitions of test spots were presented. Responses during the second to the fifth test spots were averaged as baseline light responses (N_{Before}) and the response during the first test spot was discarded to avoid the impact of the fast adaptation after the onset of visual stimulus from the long-term dark adaptation(Baccus and Meister, 2002). Sensitization index = $\frac{N_{After} - N_{Before}}{N_{After} + N_{Before}}$ was used to quantify the strength of sensitization, where N is the averaged pDSGC responses to the four test spots right before ((N_{Before}) and after (N_{After}) the period of stationary flash spots (same as test spots), moving spots, drifting gratings or contrast reversing gratings stimuli. A higher positive sensitization index value indicates stronger sensitization, while a negative sensitization index value indicates adaptation. N is firing rate for loose cell-attached recording data, subthreshold integral area for PSP and peak amplitude for PSC.

The time windows used to separate On, Off and sustained components were determined by the EPSC waveforms of dorsal pDSGCs which had three clear peaks. The mean of the boundary between the Off and the sustained components was $\sim$ 700 ms (n = 8 cells from 6 mice). Defining the onset of the test spot as t = 0, the On response time window was 0 – 1s; the Off response time window was 1 – 1.7 s; and the sustained component time window was 1.7 – 3 s. The same time windows were used for analyzing spiking, PSP and PSC data of both dorsal and ventral pDSGCs.

Data were analyzed using PCLAMP 10, MATLAB and GraphPad Prism. For whole-cell patch clamp recordings, membrane tests were performed to check the recording quality, and recordings with series resistances $> 25\ M\Omega$ or a ratio of input resistance to series resistance < 10 were discarded.

3.4.6 Dendritic tracing

GFP-labelled pDSGCs in Drd4-GFP mice were targeted using a two-photon microscopy and filled with 25 μM Alexa Fluo 594 (Life Technologies). DSGC dendrites were traced from z-stacked images in ImageJ using the open source software Simple Neurite Tracer (SNT). On and Off layers were identified and separated using NeuronStudio, and then dendritic length and dendritic arbor diameter(El-Danaf and Huberman, 2019) were calculated in MATLAB.

Two criteria were used to determine a dendritic segment as a crossover dendrite originating from one layer into the other: 1) The dendrite had at least 5 microns of segments remaining in the original layer before diving down. 2) The dendrite crossed over the gap between two layers and stratified into the other layer. The crossover dendrites were then classified into four subtypes labelled in different colors (Figure. 3.7). Red: Off dendrites

originated from On dendrites ("Off from On"); Yellow: On dendrites originated from Off dendrites ("On from Off"); Blue: On dendrites originated from the Red "Off from On" crossover dendrites ("On from Off (from On)"); Magenta: Off dendrites originated from the Yellow "On from Off" crossover dendrites ("Off from On (from Off)").

3.4.7 Computational simulation

A model of the pDSGC was developed from a real ganglion cell morphology (the cell in Figure. 3.7B) that had been reconstructed from 2-photon images. The dendritic diameters were adjusted by multiplying by a constant termed the "dendritic dia factor" (0.3 - 0.8; typically 0.5) to correct for enlargement of dendrite diameter during imaging. The morphology was discretized into a compartmental model (compartment size = 0.01 lambda, $\sim$ 2200 compartments; Ri=100 Ohm-cm, Rm=20,000 Ohm-cm2, Vrev= -70 mV) without voltage-gated ion channels to simulate subthreshold behavior in the pDSGC. The pDSGC model was stimulated at one dendritic location, and simultaneously the evoked membrane voltages were recorded at another set of locations. The stimulus was a single synaptic input from a presynaptic compartment that represented a bipolar cell voltage-clamped with a pulse of 100 ms duration. The postsynaptic conductance in the pDSGC was 2000 pS, with a reversal potential of 0 mV. Movies were generated by displaying the morphology as 2 separate images, each showing one of the pDSGC's dendritic arborization layers. The other layer in each image was made transparent. To show the spread of depolarization through the dendritic arbor, the dendritic membrane voltage was displayed as a heat map, with violet representing -72 mV and red representing -30 mV. The movie frame interval was 1 ms. The model simulations and movies were constructed with the simulation language Neuron-C(Smith, 1992).

3.4.8 Experimental design and statistical analysis

Experimental design and statistical analysis Sample size in each group was calculated based on preliminary data to have a power of test strong-er than 0.8. Grouped data with Gaussian distribution were presented as mean ± SEM in summary graphs with scattered dots representing individual cells. Two-sided one-sample t-test was per-formed to test whether the sensitization index value was significantly different from 0, while Two-sided two-sample t-test was used to compare two sample groups. Grouped data with non-Gaussian distribution were presented as median ± IQR in box plots, and Kolmogorov-Smirnov test was ap-plied. For multiple comparisons, p values were adjusted with false discovery rate (FDR) correc-tion(Jafari and Ansari-Pour, 2019). $P < 0.05$ was considered significant; n.s. stands for no sig-nificance; *$p < 0.05$; **$p < 0.01$; ***$p < 0.001$. The number of experimental repeats were indicated in Figure legends.

Data and code accessibility

All relevant data collected and analyzed in this study are available from the authors on reasonable request. The Neuron-C simulation package and codes for the pDSGC model are available at `ftp://retina.anatomy.upenn.edu/pub/nc.tgz`.

Acknowledgements

We thank Chen Zhang for managing the mouse colony. This work was supported by NIH R01 EY02416, R01 NS109990 and the McKnight Scholarship Award to W.W., NSF GRFP DGE-1746045 to J.D., NIH F31 EY029156 to H.E.A., and NIH EY022070 to RGS.

Author contributions

X.H. and W.W. conceived the concept, designed the experiments and wrote the paper. X.H. conducted all the physiological experiments and data analysis. A.J.K. conducted morpho-

logical analysis of pDSGCs in Figure. 3.7 and loose cell-attached recording of alpha cells in Figure. 3.12. H.E.A. conducted supporting experiments (data not shown). J.D. collected the dye-filled pDSGC morphology dataset in Figure. 3.7. R.G.S. conducted the computational modeling in Figure. 3.7-3.9 and helped edit the paper.

Conflict of interest statement

The authors declare no competing interests.

3.5 Results

3.5.1 On-Off DSGC light responses can be transiently sensitized after a set of visual stimuli

To examine the influence of prior visual stimuli on the light sensitivity of On-Off DSGCs, we targeted the On-Off DSGC subtype preferring motion in the posterior direction (pDSGCs) in the Drd4-GFP transgenic mouse line(Huberman et al., 2009) for patch clamp recording. We monitored the baseline pDSGC spiking response to a 1 second flashing spot (termed "test spot") presented every 3.5 seconds. Then, 27.5 seconds of visual stimulation (termed the "induction stimulus") was presented to induce sensitization. We tested three types of induction stimuli at the same contrast level as the test spot: preferred direction moving spots, preferred direction drifting gratings, and contrast reversing gratings (5 repetitions of 5.5 s trials, also see Materials and Methods) (Figure. 3.1A). Immediately after the induction stimulus, the pDSGC firing rate was monitored by trials of the same test spots as those before the induction stimulus. The average firing rates of the pDSGC to the test spot before and after the induction stimulus were then used to calculate a sensitization index, which was defined as $(Firing\ rate_{After} - Firing\ rate_{Before})/(Firing\ rate_{After} + Firing\ rate_{Before})$. Sensitized pDSGC responses are represented as positive sensitization index values, while adapted responses give negative values.

We found that pDSGC spiking responses to test spots were significantly sensitized by all three patterns of induction stimuli. As a control, continuous presentation of test spot trials did not induce sensitization (Figures. 3.1A and 3.1B). For the rest of this study, we used drifting gratings as the induction stimulus to study the mechanism underlying pDSGC sensitization. Since DSGCs are direction-selective, we also tested if pDSGCs can be sensitized by drifting gratings moving in the null direction. We found that motion in both preferred

and null directions can induce similar levels of sensitization in pDSGCs (Figure. 3.1C).

We next investigated the time course of the sensitization and found the following two properties. First, the sensitization is a short-term, reversible phenomenon. We were able to repeatedly induce sensitization in 82% of pDSGCs (14/17 cells) (See Figure. 3.2 for an example cell). Second, the sensitization was maintained without decay as long as test spots were presented at an inter-spot interval of 3.5 seconds used in our protocol (Comparing the third trial versus the first two trials in Figure. 3.2). In our longest experiment, the pDSGC firing rate to test spots remained sensitized for 210 s. However, in the absence of continuous presentation of test spots, pDSGC light responses decayed back to the baseline level within 5-20 s after the induction of sensitization (Figure. 3.1D, see Materials and Methods).

Moreover, we found that the pDSGC's response to moving stimuli can also be sensitized. We monitored the spiking activity of pDSGCs during repeated presentation of moving bar trials at the same frequency as the test spots (3.5 s each trial) in either preferred or null directions in a pseudorandom manner. We found that pDSGC firing rates in both directions show sensitization during the first 6 trials of moving bar stimulation before reaching a stable level while the direction selectivity index of the cell remains unchanged (Figure. 3.1E and 3.1F).

3.5.2 Spiking activities of pDSGCs from the dorsal and the ventral retina show differential patterns of sensitization

Despite an overall increase of spiking activity in all pDSGCs, we noticed that pDSGCs in the dorsal and ventral regions of the retina show distinct sensitization patterns after the induction stimulus (Figures. 3.3A and 3.3B). We detected sensitized On responses only in

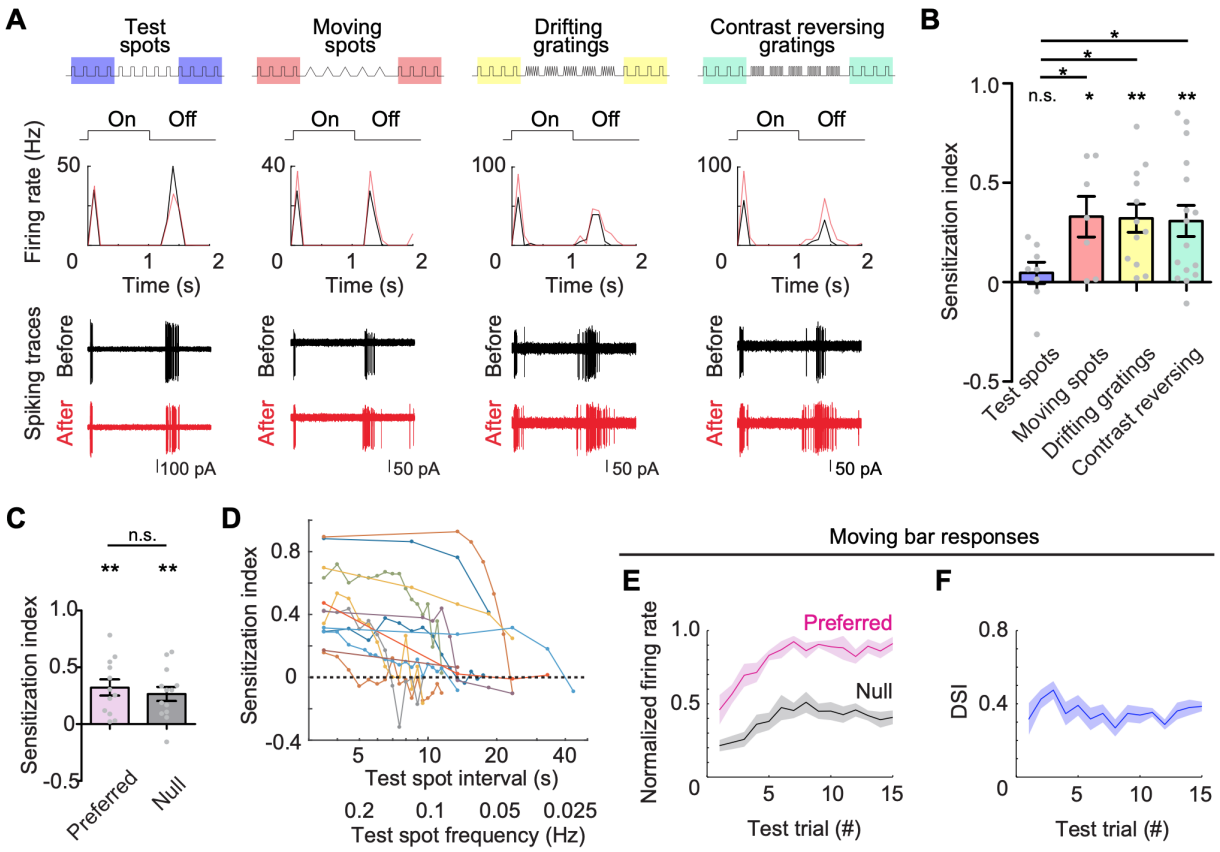

Figure 3.1: **pDSGC responses are transiently sensitized after visual stimulation.** **A**, Example pDSGC responses to 1s-duration flashing spot stimuli ("test spot") before and after 5 repetitions of test spots, moving spots, drifting or contrast reversing gratings stimuli. Top: schematics of the stimulus protocols. Middle: Firing rates of the example cells before (black) and after (red) different stimulations. Bottom: Overlay of four repetitions of pDSGC spiking traces responding to test spots before and after different stimulations. The test spot has onset at t = 0 and offset at t = 1s.

B, Summary graph comparing sensitization indices of pDSGC responses after exposure to test spots (n = 8 cells from 4 mice), moving spots in preferred direction (n = 7 cells from 3 mice), drifting gratings in preferred direction (n = 12 cells from 6 mice) or contrast reversing gratings (n = 16 cells from 6 mice). For this and subsequent plots, data with Gaussian distribution were represented as mean ± SEM, and grey dots represent individual cells. One-sample student t-test was used to test whether the sensitization index value of pDSGCs was significantly different from 0, while two-sample t-test was used for comparison between control ("test spots") and induction visual stimulations. All p values were adjusted with FDR correction: test spots: p = 0.41; moving spots: *p = 0.031; drifting gratings: **p = 0.0056; contrast reversing gratings: **p = 0.0046; test spots vs moving spots: *p = 0.035; test spots vs drifting gratings: *p = 0.027; test spots vs contrast reversing gratings: *p = 0.044.

Figure 3.1, continued.
C, Comparison of pDSGC sensitization indices after 5 repetitions of drifting gratings in preferred (n = 12 cells from 6 mice) or null direction (n = 13 cells from 4 mice). Preferred direction: **p = 0.0024; null direction: **p = 0.0017; preferred vs null, p = 0.55.
D, Plot of sensitization indices of individual cells with increasing interval between test spots after the induction stimulus (also see Materials and Methods) (n = 13 cells from 5 mice). Individual cells are represented in different colors.
E, Normalized firing rate of pDSGCs in preferred and null directions relative to the maximal response of the cell in all trials. Mixed-effects analysis for repeated measurements (n = 6 cells from 3 mice): for preferred response, *p = 0.014; for null response, *p = 0.035.
F, Direction selectivity index (DSI) of pDSGCs monitored over test trials. Mixed-effects analysis for repeated measurements (n = 6 cells from 3 mice): p = 0.15.

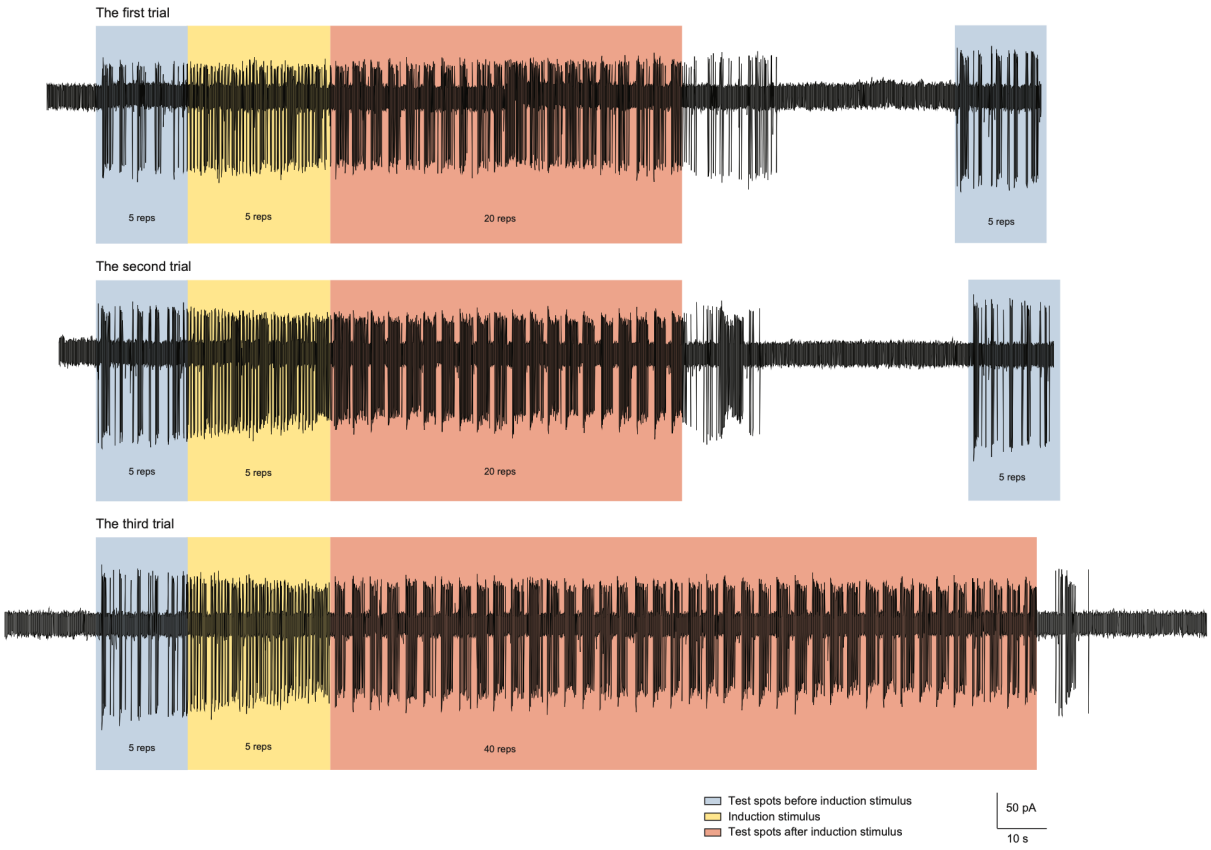

Figure 3.2: **Example spiking traces of a pDSGC represent the maintenance, extinction, and repeated induction of sensitization.**
Upper, middle and lower traces represent pDSGC spiking responses during the first, second and third trials of the induction protocol.

the dorsal, but not in the ventral pDSGCs. The Off responses of pDSGCs were sensitized in both the dorsal and ventral groups (Figure. 3.3B and 3.3C). Notably, in dorsal but not ventral pDSGCs, we also observed elevated baseline spiking activity between trials of test spots, which we termed "the sustained component" (Figures. 3.3B, left panel, and 3.3D). In summary, for pDSGCs from the dorsal retina, both On and Off responses were sensitized by the induction stimulus, and there was a sensitized sustained component of spiking between test spot trials. However, for pDSGCs from the ventral retina, there was no sustained component and only Off responses were enhanced after the induction stimulus.

3.5.3 Subthreshold membrane potentials of dorsal and ventral DSGCs show distinct sensitization patterns

We next examined membrane depolarization patterns that drive distinct firing patterns of dorsal and ventral pDSGCs using whole-cell current clamp recording. Spikes were digitally removed to reveal the subthreshold postsynaptic potentials (PSPs) of pDSGCs (see Materials and Methods). Consistent with the spiking activity, in the dorsal retina, both On and Off PSPs were sensitized after the induction stimulus, while in the ventral retina, only the Off PSPs were sensitized (Figure. 3.4B). Moreover, dorsal pDSGCs exhibit sustained depolarization of their membrane potentials between test spots after the induction stimulus (Figures. 3.4A and 3.4C), which corresponds to the sensitized sustained component in their spiking activities.

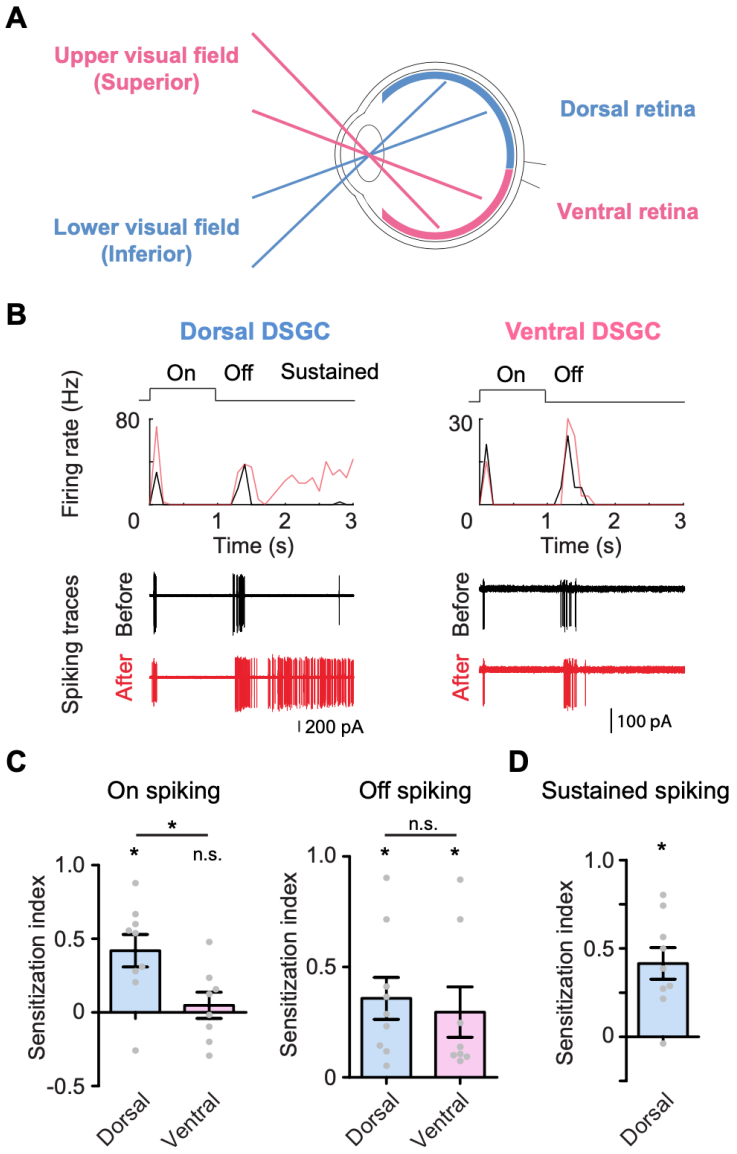

Figure 3.3: **pDSGCs from the dorsal and the ventral retina show differential patterns of sensitization.**

A, Schematic diagram showing the topographic relationship of dorsal/ventral retina and the visual fields where they receive visual inputs.

B, Firing rate plots and spiking traces of example pDSGCs from the dorsal and the ventral retina responding to test spot stimuli before (black) and after (red) the induction stimulus.

C, Summary graphs comparing the sensitization indices of On and Off spiking between pDSGCs from the dorsal and the ventral retina. Dorsal: n = 9 cells from 3 mice; ventral: n = 8 cells from 4 mice. For On spiking: dorsal: *p = 0.018; ventral: p = 0.70; dorsal vs ventral: *p = 0.037. For Off spiking: dorsal: *p = 0.013; ventral: *p = 0.049; dorsal vs ventral: p = 0.68.

D, Summary graph of sensitization index for the sustained component of dorsal pDSGC spiking activity. N = 9 cells from 3 mice, *p = 0.011.

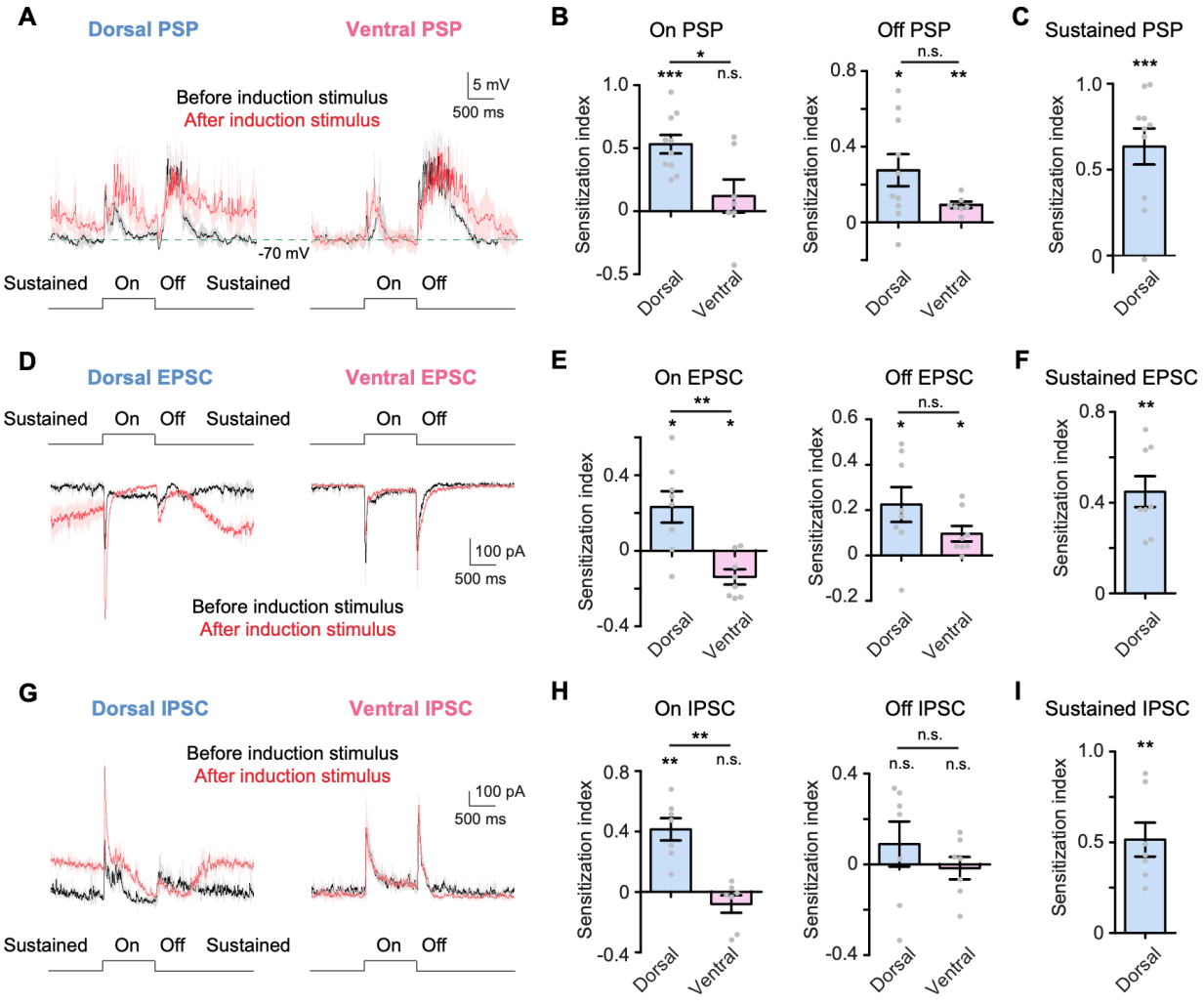

Figure 3.4: **Membrane potential and synaptic currents of dorsal and ventral pDSGCs show distinct sensitization patterns.**
A, Example PSP traces of dorsal and ventral pDSGCs evoked by test spots before (black) and after (red) induction stimulus. PSP traces represent trial average (darker traces) and SEM (lighter traces). Note that in the dorsal PSP trace, there is a sustained component of elevated depolarization that persists during the time window between the test spot offset and the onset of the next test spot.
B, Summary plots comparing the sensitization indices of PSPs between dorsal and ventral pDSGCs. Dorsal: n = 10 cells from 4 mice; ventral: n = 7 cells from 4 mice. For On PSP: dorsal: ***p < 0.001; ventral: p = 0.39; dorsal vs ventral: *p = 0.014. For Off PSP: dorsal: *p = 0.017; ventral: **p = 0.0035; dorsal vs ventral: p = 0.11.
C, Summary graph of the sensitization index of the sustained component of PSPs from dorsal pDSGCs. N = 10 cells from 4 mice, ***p < 0.001.

Figure 3.4, continued.
D, Example EPSC traces of a dorsal and a ventral pDSGC evoked by test spots before (black) and after (red) induction stimulus. PSC traces represent trial average (darker traces) and SEM (lighter traces) for this and subsequent Figures. Note that in the dorsal pDSGC EPSC, there is a sustained inward current that persists during the time window between the test spot offset and the onset of the next test spot. Such a sustained component was not observed in the ventral pDSGCs.
E, Same as **B**, but for On and Off EPSCs. Dorsal: n = 8 cells from 6 mice; ventral: n = 8 cells from 5 mice. Dorsal On EPSC peak amplitude value after sensitization is relative to the elevated baseline tonic current. For On EPSC: dorsal: *p = 0.030; ventral: *p = 0.026; dorsal vs ventral: **p = 0.0042. For Off EPSC: dorsal: *p = 0.039; ventral: *p = 0.036; dorsal vs ventral: p = 0.15.
F, Same as **C**,but for the sustained component of dorsal EPSCs. N = 8 cells from 6 mice, **p = 0.0021.
G, Same as **D**,but for IPSCs. Note that the sustained component was also observed in the IPSC traces from the dorsal pDSGC but absent from the ventral pDSGC.
H, Comparison of IPSC sensitization indices between dorsal and ventral pDSGCs. Dorsal: n = 7 cells from 3 mice; ventral: n = 7 cells from 2 mice. For On IPSC: dorsal: **p = 0.0046; ventral: p = 0.38; dorsal vs ventral: **p = 0.0014. For Off IPSC: dorsal: p = 0.47; ventral: p = 0.75; dorsal vs ventral: p = 0.50.
I, Same as **C**,but for the sustained component of IPSCs. N = 7 cells from 3 mice, **p = 0.0035.

3.5.4 Synaptic inputs of dorsal and ventral DSGCs show differential patterns of sensitization

We hypothesized that the stronger depolarization of the pDSGC membrane potential after the induction stimulus may result from enhanced excitatory inputs or reduced inhibitory inputs. To determine how the synaptic inputs of pDSGC are modulated by the induction stimulus, we measured the excitatory postsynaptic currents (EPSCs) and inhibitory postsynaptic currents (IPSCs) of dorsal and ventral pDSGCs using whole cell voltage-clamp recording. After the induction stimulus, both dorsal and ventral pDSGCs showed enhanced Off EPSC responses (Figures. 3.4D and 3.4E). The EPSCs of dorsal pDSGCs showed an enhanced On EPSC amplitude (Figures. 3.4D and 3.4E), as well as an elevated sustained component between test spots (Figures. 3.4D and 3.4F) that corresponds to the sustained

component of the spiking activity (Figures. 3.3B and 3.3D) and of the membrane depolarization (Figures. 3.4A and 3.4C).

Sensitized spiking activity was not accompanied by reduced inhibition of pDSGCs (Figures. 3.4G-3.4I). In dorsal pDSGCs, we detected an elevated sustained component of the IPSC after the induction stimulus similar to that of the EPSC, suggesting that the sensitization of a sustained excitatory drive to both pDSGCs and its presynaptic inhibitory neuron, likely starburst amacrine cells (SACs), which share common bipolar cell inputs(Duan et al., 2014; Kim et al., 2014; Sethuramanujam et al., 2017; Yu et al., 2018).

Taking the above results together, we found that pDSGCs transiently increased their firing after the induction stimulus. The sensitization of the spiking activity is accompanied by enhanced synaptic excitation and membrane depolarization, but not reduced inhibition. Furthermore, in the dorsal retina, sensitized pDSGCs acquired a sustained increase in their synaptic inputs, membrane potential and spiking activity between test spots.

3.5.5 Synaptic activity is required for the induction of pDSGC sensitization

To investigate the mechanism underlying the induction of pDSGC sensitization, we first tested whether the membrane depolarization of the pDSGC evoked by the induction stimulus is sufficient to trigger sensitization. Instead of using the drifting grating stimulus as the induction stimulus, we mimicked drifting grating-evoked membrane potential changes in dorsal pDSGCs by directly voltage clamping the membrane potential of the pDSGC using the command voltage waveform recorded during the drifting grating stimulus (Figures. 3.5A and 3.5B). We found that pDSGC EPSCs were not sensitized by this direct depolarization, indicating that sensitization requires visually evoked synaptic inputs (Figures. 3.5C and 3.5D).

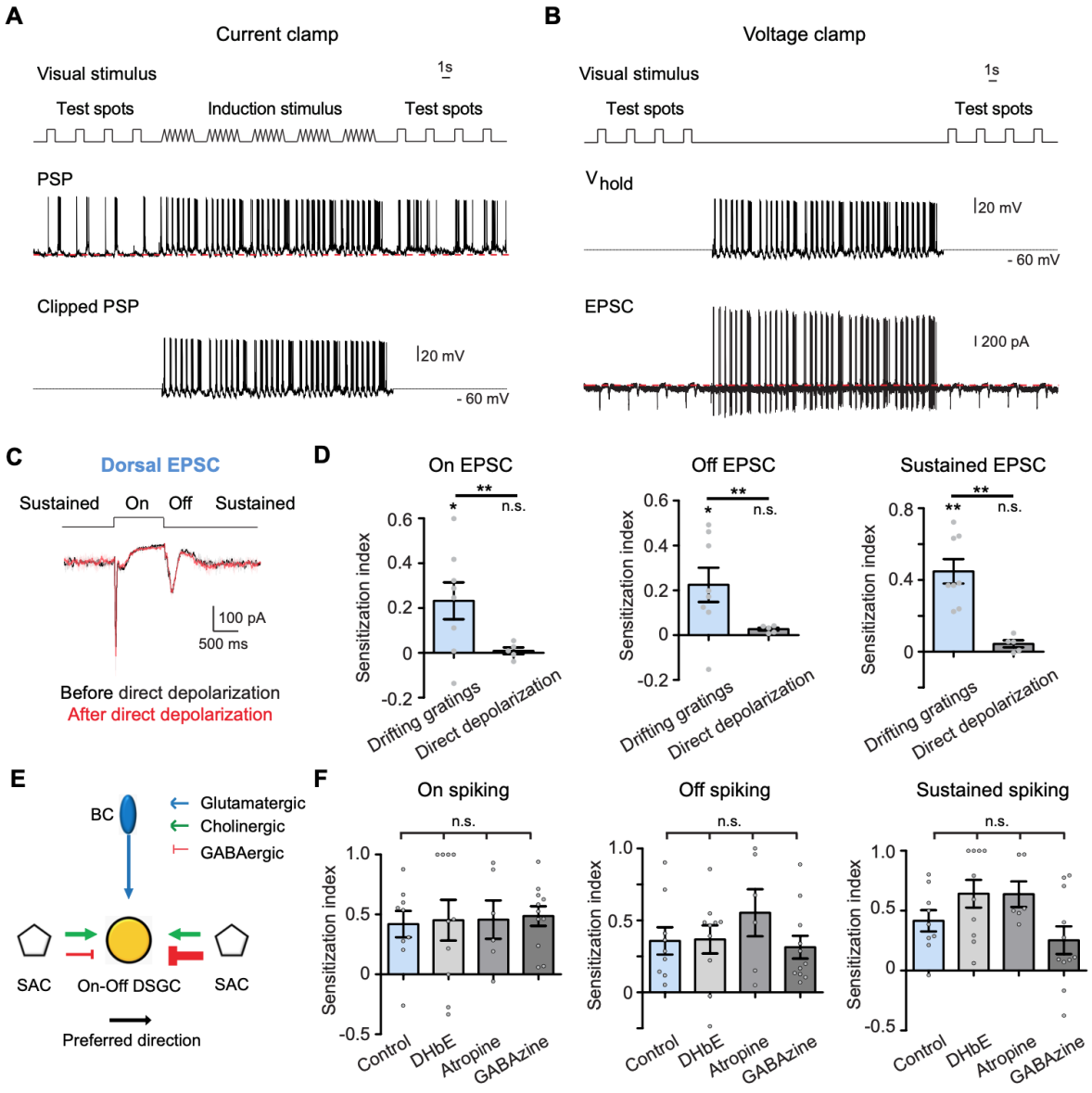

Figure 3.5: **Synaptic inputs to pDSGCs are necessary for the induction of sensitization.**

A, Top: schematic shows the complete induction protocol including test spots before and after drifting gratings as the induction stimulus. Middle: Whole-cell current clamp recording of a pDSGC from the dorsal retina during the visual stimulus shown on the top. Bottom: PSP waveform evoked by drifting gratings was clipped from the PSP trace shown above.

B, Top: schematic shows the visual stimulus protocol with only test spots but without induction stimulus (drifting gratings). Middle: Waveform of the holding potential during whole-cell voltage clamp recordings of pDSGCs. Bottom: an example EPSC trace from a dorsal pDSGC recorded with the visual stimulus protocol and the holding potential shown above.

Figure 3.5, continued.
C, Example EPSC traces of a dorsal pDSGC during test spot stimulus before (black) and after (red) direct depolarization of the pDSGC as a replacement of drifting gratings visual stimulation. This is the same EPSC recording as the one shown in **B**. Traces are averaged from four repetitions.
D, Comparison of the EPSC sensitization indices after drifting grating stimulus (n = 8 cells from 6 mice) versus after direct depolarization (no induction visual stimulation) (n = 5 cells from 2 mice). For On EPSC: Drifting gratings: *p = 0.039; direct depolarization: p = 0.60; Drifting gratings vs direct depolarization: **p = 0.0056. For Off EPSC: Drifting gratings: *p = 0.040; direct depolarization: p = 0.29; Drifting gratings vs direct depolarization: **p = 0.0018. For sustained EPSC: Drifting gratings: **p = 0.0014; direct depolarization: p = 0.11; Drifting gratings vs direct depolarization: **p = 0.0024.
E, Simplified schematic shows major types of synaptic inputs onto On-Off DSGCs. BC: bipolar cell; SAC: starburst amacrine cell.
F, Comparison of the sensitization indices for pDSGC spiking in control (Ames' solution, n = 9 cells from 3 mice) or in the presence of different receptor antagonists (DHbE: n = 10 cells from 4 mice; Atropine: n = 6 cells from 2 mice; GABAzine: n = 11 cells from 3 mice). One-way ANOVA for On spiking: p = 0.99; for Off spiking: p = 0.73; for sustained spiking: p = 0.14.

We next investigated which type(s) of synaptic signaling is required for pDSGC sensitization. A major source of synaptic inputs to pDSGCs is the SAC, which releases both acetylcholine and GABA to the DSGC (Figure. 3.5E). However, we found that pharmacological blockade of nicotinic, muscarinic, or GABA-A receptors in the retina with DHbE, atropine or gabazine respectively did not prevent the sensitization of the pDSGC spiking activity (Figure. 3.5F). This suggested that, the sensitization of the pDSGC arises from enhanced glutamate release from bipolar cells.

3.5.6 Glycinergic signaling in the Off pathway contributes to sensitized glutamatergic inputs to pDSGCs

Previous studies in the vertebrate retina indicate that enhanced bipolar cell glutamate release can result from adapted presynaptic inhibition of bipolar cell terminals(Kastner and Baccus, 2013; Nikolaev et al., 2013; Mazade and Eggers, 2016; Appleby and Manookin, 2019; Kastner et al., 2019). Since blocking GABA-A receptor signaling did not affect pDSGC sensitization (Figure. 3.5F), we next blocked another major type of presynaptic inhibition, glycinergic signaling(Diamond, 2017), by bath application of strychnine while recording from dorsal pDSGCs before and after the induction stimulus. We found that glycinergic blockade significantly reduced the sensitization of dorsal pDSGC spiking activity during On and Off responses, and between test spots (Figures. 3.6A and 3.6B). The Off and sustained component of EPSCs also showed reduced sensitization. However, the sensitization index of the On EPSC was not affected by strychnine despite the impaired sensitization of On spiking responses (Figures. 3.6C and 3.6D), indicating that the sensitization of On EPSCs by itself is not sufficient to induce sensitization of On spiking responses in dorsal pDSGCs.

Since a well-established role of glycinergic inhibition is to mediate crossover inhibition from the On to the Off pathway via glycinergic AII amacrine cells(Demb and Singer, 2012; Graydon et al., 2018), we tested whether On bipolar cell activity is required for the glycinergic signaling underlying pDSGC sensitization in the Off pathway. We bath applied the mGluR6 agonist L-AP4 to silence rod and On bipolar cells during visual stimulation. As expected, the On spiking response of the dorsal pDSGC was abolished in L-AP4. However, we still observed sensitized Off responses and sustained components after the induction stimulus (Figures. 3.6E and 3.6F). This result shows that 1) On bipolar cell activity is not involved in the sensitization of Off bipolar cell signaling, and 2) in the dorsal retina, the sustained pDSGC activity between test spots arises from the Off pathway.

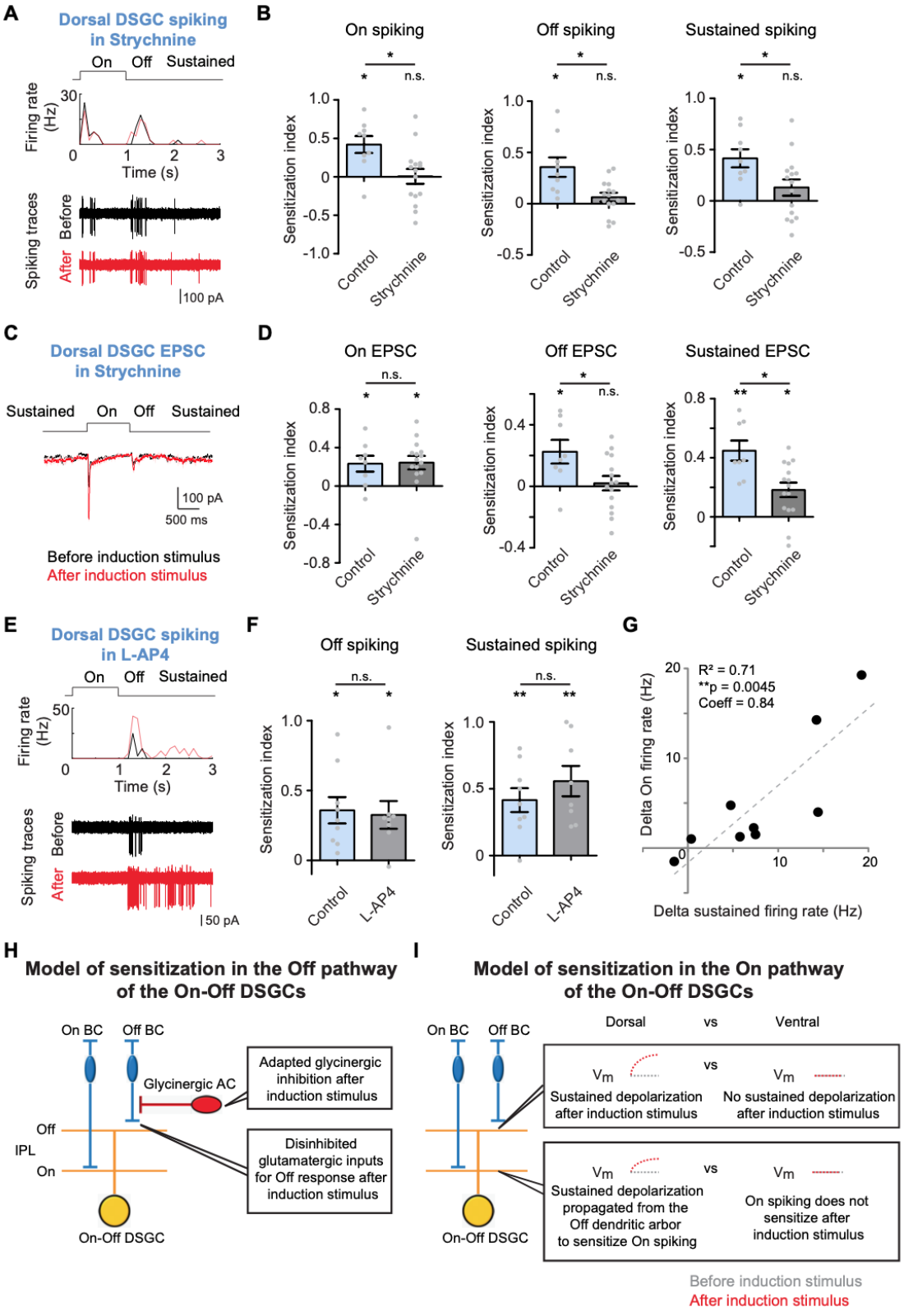

Figure 3.6: **Glycinergic signaling contributes to pDSGC sensitization.**

Figure 3.6, continued.
A, Example firing rate plot and spiking traces of a dorsal pDSGC responding to test spot stimuli before and after induction stimulus in the presence of strychnine.
B, Summary plots comparing the sensitization indices of spiking activity in control (Ames' solution, n = 9 cells from 3 mice) and in the presence of strychnine (n = 15 cells from 5 mice). For On spiking, control: *p = 0.016; strychnine: p = 0.95; control vs strychnine: *p = 0.022. For Off spiking, control: *p = 0.012; strychnine: p = 0.18; control vs strychnine: *p = 0.018. For sustained spiking, control: *p = 0.014; strychnine: p = 0.16; control vs strychnine: *p = 0.047.
C, Example EPSC traces during test spot stimulus before (black) and after (red) induction stimulus in the presence of strychnine.
D, Comparison of the EPSC sensitization indices in control (n = 8 cells from 6 mice) versus in the presence of strychnine (n = 15 cells from 8 mice). For On EPSC, control: *p = 0.033; strychnine: *p = 0.011; control vs strychnine: p = 0.93. For Off EPSC, control: *p = 0.040; strychnine: p = 0.76; control vs strychnine: *p = 0.037. For sustained EPSC, control: **p = 0.0027; strychnine: *p = 0.011; control vs strychnine: *p = 0.010.
E, Example firing rate plot and spiking traces of a dorsal pDSGC responding to test spot stimuli before and after induction stimulus in the presence of L-AP4.
F, Summary graphs comparing the sensitization indices for the Off and the sustained components of spiking activity in control (Ames' solution, n = 9 cells from 3 mice) versus in the presence of L-AP4 (n = 8 cells from 3 mice). For Off spiking, control: *p = 0.011; strychnine: *p = 0.020; control vs strychnine: p = 0.81. For sustained spiking, control: **p = 0.0096; strychnine: **p = 0.0054; control vs strychnine: p = 0.40.
G, Scatter plot comparing the increase of firing rates of the On spiking response versus that of the sustained component. Black dots represent individual cells (n = 9 cells from 3 mice), and dashed line indicates linear regression fit.
H and **I**, A mechanistic model of sensitization in the direction-selective circuit. Schematic diagrams show side views of the laminar organization of bipolar cells (BCs), glycinergic amacrine cells (ACs) and On-Off DSGCs in the inner plexiform layer (IPL). In the Off pathway, the presynaptic glycinergic AC adapts and disinhibits Off BC after induction stimulus. Therefore, the DSGC Off responses is enhanced due to higher glutamate release from Off BCs (**H**). Moreover, dorsal DSGC also gained an elevated baseline depolarization originating from Off BCs. Such sustained depolarization propagates to On dendritic arbors and enhances the subsequent On response. In contrast, ventral DSGCs do not have sustained depolarization and thus only show sensitized Off responses but not On responses after induction stimulus (**I**).

Based on the above results, our working model for the sensitization in the Off pathway is that the induction stimulus triggers synaptic depression at the glycinergic synapse from

amacrine cells to Off bipolar cells, which leads to increased glutamate release from Off bipolar cells to pDSGCs. Glycinergic disinhibition of Off bipolar cells causes sensitized pDSGC Off responses, as well as sustained depolarization of membrane potential between test spots in dorsal pDSGCs (Figure. 3.6H).

3.5.7 Off-to-On crossover excitation within the bistratified pDSGC dendrites contributes to the sensitization of the On spiking response in the dorsal retina

In dorsal pDSGCs, blocking glycinergic signaling in the retina impaired the sensitization of the On spiking response (Figures. 3.6A and 3.6B), even though the On EPSC was not affected (Figures. 3.6C and 3.6D), suggesting an alternative glycinergic mechanism underlying the sensitization of the On spiking activity in the dorsal retina. Since the sensitization of dorsal On spiking responses is associated with the presence of the sensitized sustained components, both of which are dependent on glycinergic signaling, we hypothesized that this sustained component between test spot trials tonically increases the excitability of dorsal pDSGCs to boost their On spiking responses. We reasoned that if the sustained depolarization of the pDSGC is important for the sensitization of its On spiking response, we would expect to see a positive correlation between the two. We calculated the correlation coefficient between the change of sustained firing rate and that of the On firing rate, and indeed found a strong correlation between these two components (Figure. 3.6G, R2 = 0.71, **p = 0.0045, Coeff = 0.84). These experimental results support an important role of the sustained depolarization of the dorsal pDSGC after the induction stimulus in the sensitization of its On response.

How did the sustained depolarization originating from Off bipolar cells influence the On response of the pDSGC? One route is the electrotonic spread of the depolarization in the

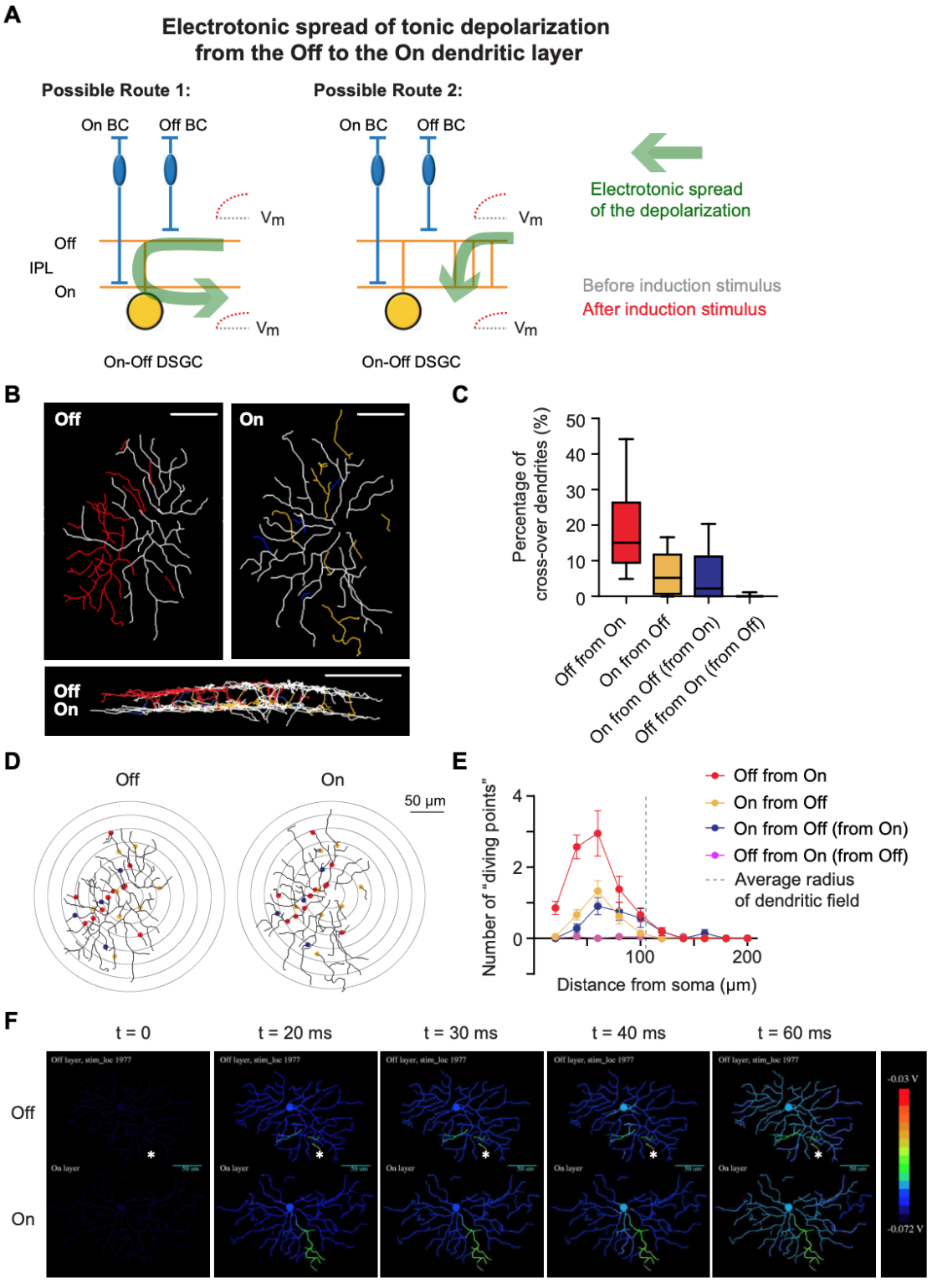

Figure 3.7: **pDSGC dendrites show extensive crossovers between On and Off layers.**

Figure 3.7, continued.
A, Schematics showing two possible routes for the electrotonic spread of depolarization from the Off to the On dendritic layers of the bistratified On-Off DSGC.
B, Dendritic morphology of an example pDSGC, including dendrites staying in one single layer (white), On dendrites crossing over to the Off layer (red), Off dendrites crossing over to the On layer (yellow), and dendrites from On to Off and then back to On layer (blue).
C, Summary box plots representing the percentages of dendritic crossovers over total dendritic lengths. Data were represented as median ± IQR (n = 21 cells).
D, The same example cell as **B**, but with labels showing the locations of the starting points where dendrites started to cross from one layer to the other ("the diving points"). The colors were coded as **B** and **C**. Concentric rings represent radial distance from soma.
E, Sholl analysis of the diving points (n = 21 cells).
F, A color map showing the membrane potentials of the pDSGC Off and On layers in response to a simulated bipolar cell input onto a location (indicated by *) in the Off layer. Model parameters: Ri = 100 Ohm-cm, dendritic dia factor = 0.5.

pDSGC Off dendritic arbor through the soma to the On dendritic arbor (Figure. 3.7A, left). Interestingly, we noted an alternative route for the Off-On crosstalk within the bistratified pDSGC dendritic morphology (Figure. 3.7A, right). By two-photon imaging of dye-filled pDSGCs, we noted frequent crossovers of dendritic branches from one dendritic layer to the other. On average, about 30% of the total dendritic arbors of a pDSGC originate from the other layer through crossover dendrites (Figure. 3.7B, 29.5 ± 3.2 % of the total dendritic length, mean ± SEM, n = 21 cells). The majority of the crossover segments branched from the On layer into the Off layer (the red dendrites in Figures. 3.7B and 3.7C). And the majority of the crossover dendrites started diving from one layer to the other at a radial distance of around 40-80 μm away from the soma (Figures. 3.7D and 3.7E), which mainly falls in the distal half of the pDSGC dendritic field radius (105.3 ± 2.0 μm, n = 21 cells).

To assess the functional importance of dendritic crossover in signal propagation between On and Off pathways, we simulated the electronic spread from one dendritic layer to the other in a detailed biophysical model of the pDSGC based on the reconstruction of a representative dye-filled cell (Figures. 3.7F, 3.8, 3.9 and Online Supplementary Video). We

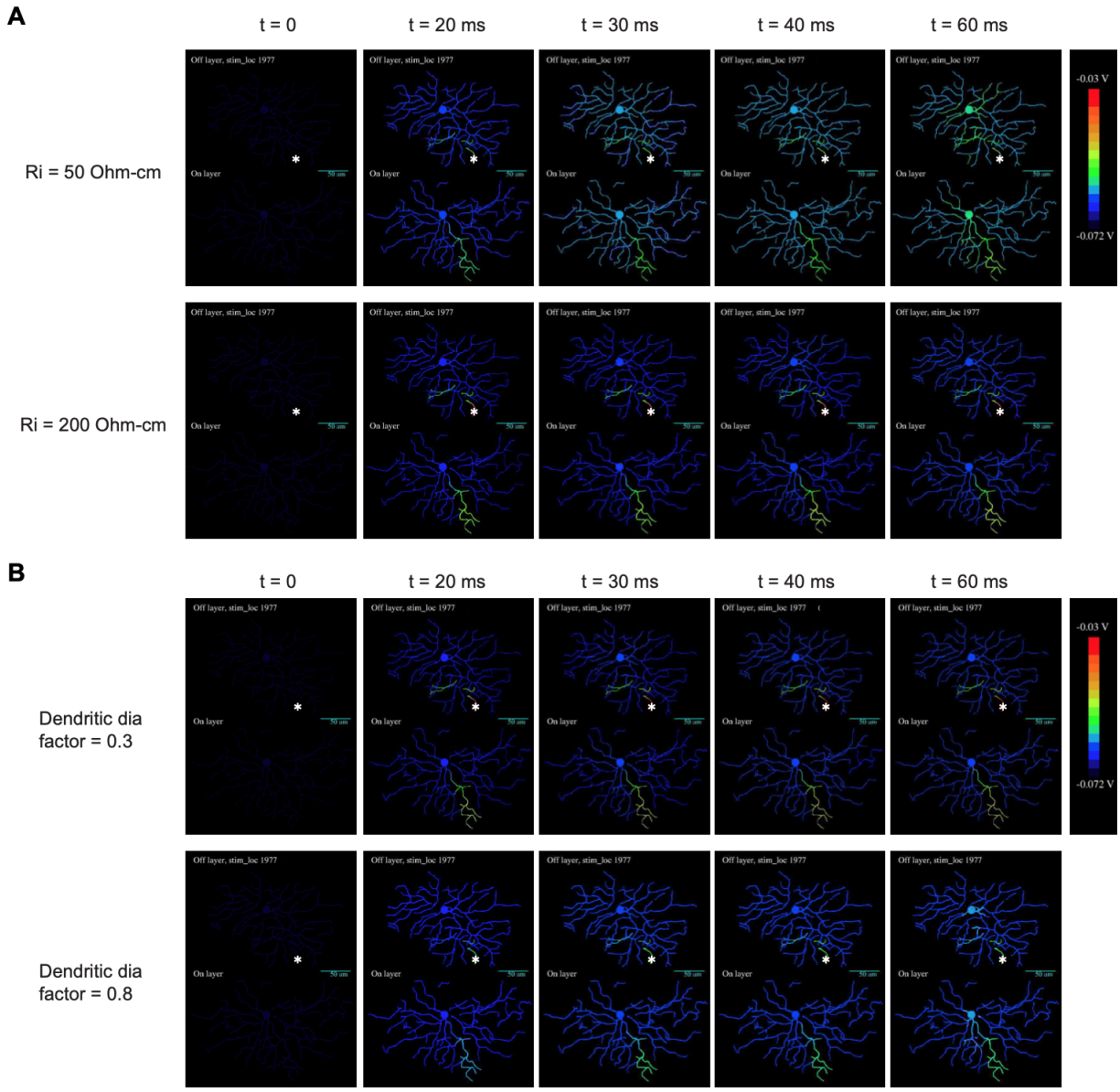

Figure 3.8: **Direct electrotonic spread of depolarization between pDSGC dendritic layers is robust in simulations with brackets of different parameters.**
A, Simulation model with different axial dendritic resistances. See also Figure. 7F for Ri = 100 Ohm-cm.
B, Simulation model with different dendritic diameter factors. See also Figure. 7F for dia factor = 0.5.

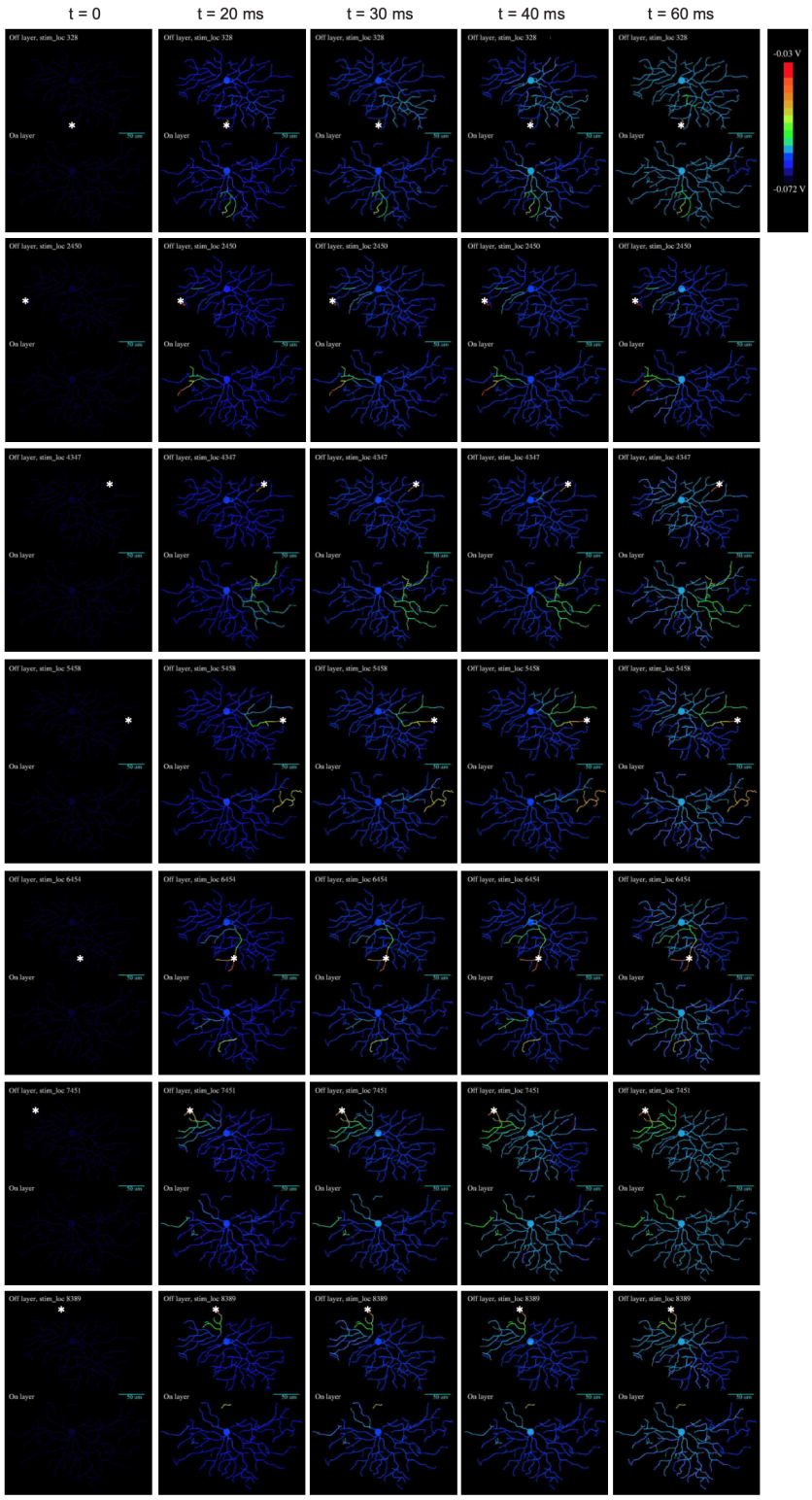

Figure 3.9: **Crossover dendrites of pDSGCs allow for direct electrotonic spread of depolarization between dendritic layers bypassing the soma.**

Figure 3.9, continued.
Color maps of pDSGC membrane potentials after stimulation at different locations in the Off layer. The stimulated locations are indicated by * in the heat map plots. For these simulation videos, Ri = 100 Ohm-cm, dendritic dia factor = 0.5.

simulated a single synaptic input from a presynaptic compartment that represented a bipolar cell voltage-clamped with a pulse of 100 ms duration. This input was placed at different locations throughout the Off dendritic arbor of the pDSGC while the membrane potential changes in both the On and Off dendritic layers were monitored. We found that dendritic crossovers provide shortcuts for fast and efficient spread of depolarization from the Off layer to the On layer bypassing the soma (Figure. 3.7F, 3.8, 3.9 and Online Supplementary Video). Therefore, the direct route through dendritic crossovers and the transomatic route together provide plausible physical substrates for the cross-layer influence of sustained Off bipolar cell inputs on the On responses of dorsal pDSGCs during sensitization.

Based on the above experimental and modeling results, our working model for the sensitized pDSGC On response in the dorsal retina is that after the induction stimulus, dorsal pDSGCs receive enhanced tonic glutamatergic inputs from Off bipolar cells, which depolarize the membrane potential and propagate to the On dendritic layers of pDSGCs, increasing the excitability of the cell. As a result, the subsequent On stimulus triggers a stronger On response (Figure. 3.6I, dorsal). In contrast, ventral pDSGCs lack the sustained depolarization after the induction stimulus, and therefore did not exhibit sensitized On responses (Figure. 3.6I, ventral).

3.5.8 Development of neural sensitization in pDSGCs

Since the sensitization of the pDSGC depends on the glycinergic circuitry that shapes the Off bipolar cell activity, we postulated that the development of the sensitization should co-

incide with the period when bipolar cell connectivity matures. Previous studies in rodents have shown that the integration of Off bipolar cells into the retinal network starts at around postnatal day 8 (P8) and continues for several weeks after the eye opening at P14(Olney, 1968; Fisher, 1979; Sassoè-Pognetto and Wässle, 1997; Tian and Copenhagen, 2001; Sherry et al., 2003; He et al., 2011; Stafford et al., 2014). We did not detect sensitization of either On or Off spiking responses of dorsal pDSGCs at the early stage of bipolar cell innervation at P12-13, nor did we detect the sustained component in dorsal pDSGCs at this stage (Figure. 3.10A and 3.10C). Therefore, the emergence of the sensitization and the sustained component of pDSGC occurs after eye opening, which overlaps with the maturation timeline of both glycinergic inhibition and bipolar cell connectivity in the rodent retina(Fisher, 1979; Sassoè-Pognetto and Wässle, 1997).

We next asked whether the visual experience after eye-opening is required for the development of pDSGC sensitization. We reared mice in dark from P8 to P36 and then compared the sensitization indices of pDSGCs from these mice to those of the controls. Dark rearing did not alter the normal pattern of sensitization: dorsal cells still exhibited sustained elevation of baseline firing and enhanced light responses to test spots after the induction stimulus (Figure. 3.10B and 3.10C). Therefore, the sensitization of pDSGCs developed after eye opening but was independent of visual experience.

3.5.9 Sensitization of other types of RGCs in the mouse retina

The sensitized Off bipolar cell inputs detected in our study may influence multiple postsynaptic targets in addition to pDSGCs. To test if other RGC types also receive sensitized Off bipolar cell inputs in the dorsal retina, we focused on alpha ganglion cells, which can be conveniently targeted by their large soma sizes for recording. On transient (tOn), On

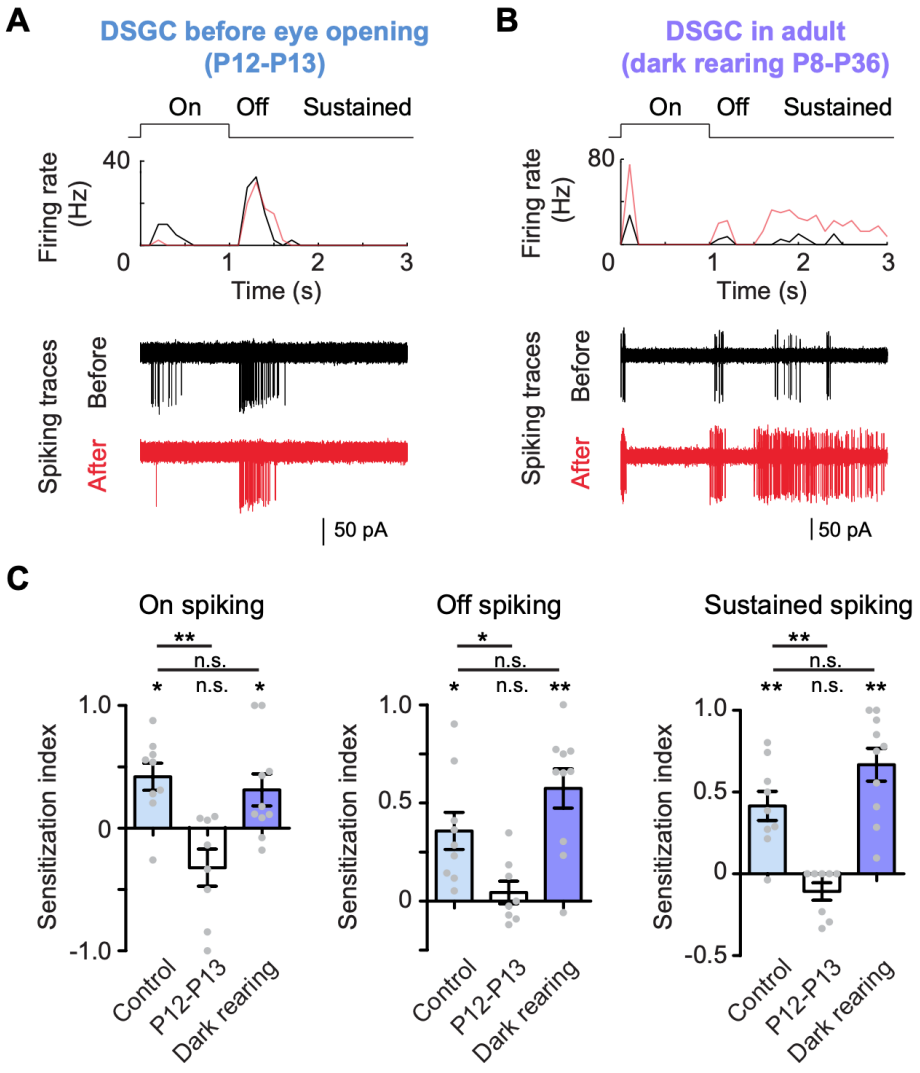

Figure 3.10: **Sensitization of pDSGC light responses develops after eye opening and persists with dark rearing.**

A, Example firing rate plot and spiking traces of a dorsal pDSGC responding to test spots before and after induction stimulus from a mouse before eye opening at P12.

B, Example firing rate plot and spiking traces of a dorsal pDSGC responding to test spots from an adult mouse dark reared during P8-P36.

C, Summary graphs comparing the sensitization indices of dorsal pDSGC spiking from control mice (n = 9 cells from 3 mice), P12-P13 mice (n = 8 cells from 2 mice) and dark-reared adult mice (n = 10 cells from 4 mice). All p values shown here were adjusted with FDR correction. For On spiking, control: *p = 0.013; P12-P13: p = 0.11; dark rearing: *p = 0.050; control vs P12-P13: **p = 0.0041; control vs dark rearing: p = 0.54. For Off spiking, control: *p = 0.012; P12-P13: p = 0.50; dark rearing: **p = 0.0015; control vs P12-P13: *p = 0.028; control vs dark rearing: p = 0.16. For sustained component: control: **p = 0.0048; P12-P13: p = 0.10; dark rearing: **p = 0.0014; control vs P12-P13: **p = 0.0015; control vs dark rearing: p = 0.11.

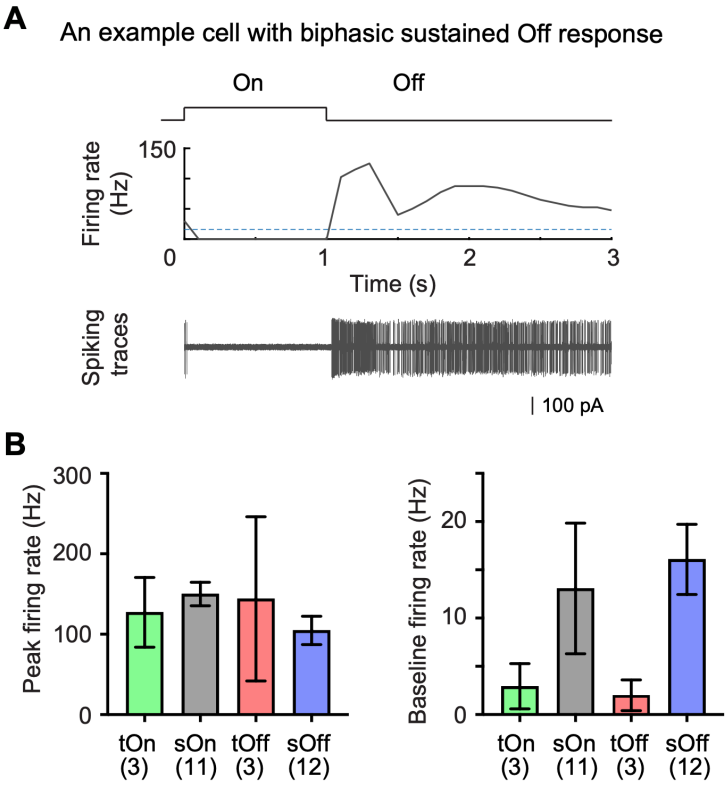

Figure 3.11: **Firing patterns of alpha ganglion cell types.**
A, Firing rate plot and spiking traces of an example cell with biphasic sustained Off response. The horizontal blue dash line in the firing rate plot indicates baseline firing rate when there was no visual stimulus, and the spiking traces includes 4 trials of spot responses. **B**, Peak firing rates and baseline firing rates of four types of alpha cells. Sample sizes were represented in the plot.

sustained (sOn), Off transient (tOff) and Off sustained (sOff) alpha cells were identified based on their large soma sizes and typical light responses as reported previously(Krieger et al., 2017). We noted a subset of RGCs with large somas had sustained Off responses but exhibited biphasic Off spiking activity (Figure. 3.11A, n = 7 cells from 5 mice). Here we tentatively classify them as sOff alpha cells. We found that these four types of alpha cells had similar levels of peak firing rate (Kruskal-Wallis test, p = 0.39) but different baseline firing rates (Kruskal-Wallis test, *p = 0.040, Figure. 3.11B), which agrees with previous descriptions(Krieger et al., 2017).

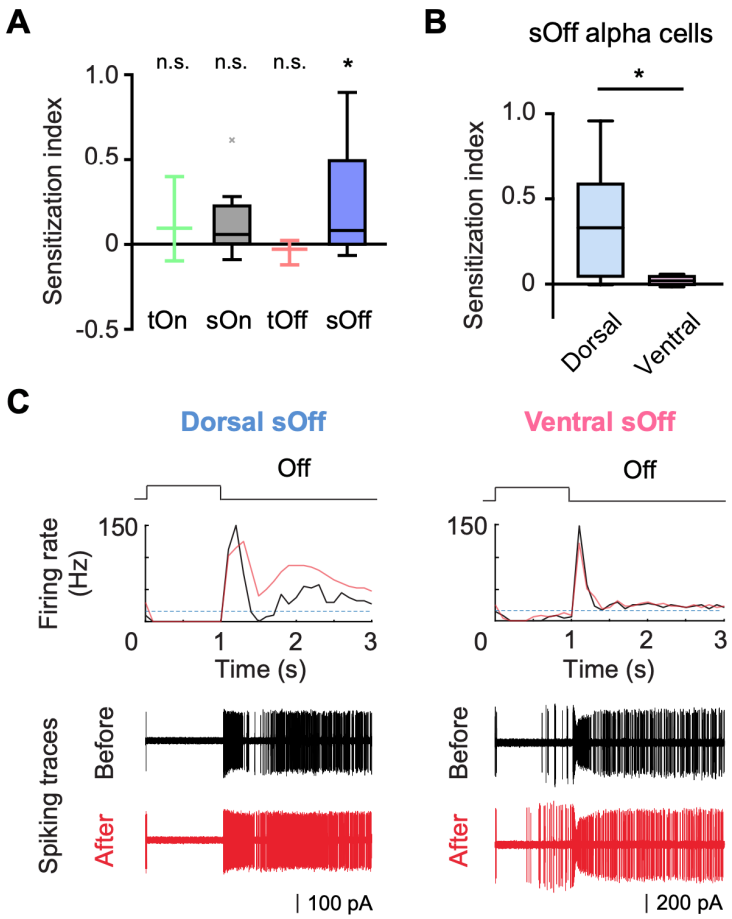

Figure 3.12: **Sensitization is detected in sustained Off alpha ganglion cells.**
A, Summary box plot of sensitization indices for four types of alpha ganglion cells. Single sample Kolmogorov-Smirnov test: tOn, n = 3 cells from 3 mice, p = 0.75; sOn, n = 11 cells from 9 mice, p = 0.084; tOff, n = 3 cells from 3 mice, p = 0.66; sOff, n =12 cells from 8 mice, *p = 0.037.
B, Comparison of the sensitization indices between dorsal (n = 8 cells from 5 mice) and ventral (n = 4 cells from 3 mice) sOff alpha cells. Two-sample Kolmogorov-Smirnov test, *p = 0.048.
C, Example firing rate plots and spiking traces of sOff alpha cells from the dorsal and the ventral retina during 1s-duration test spot stimuli before (black) and after (red) induction stimulus.

We then calculated the sensitization index of alpha cells, and found that sOff alpha cells also showed sensitization after the induction stimulus (Figure. 3.12A). We noted that the

subset of sOff alpha cells with biphasic Off responses were located exclusively in the dorsal retina (7 out of 8 dorsal cells, 0 out of 4 ventral cells, Figure. 3.12C). Moreover, only the dorsal biphasic sOff alpha cells showed sensitized responses to test spots after the induction stimulus (Figures. 3.12B and 3.12C). Sensitization of biphasic Off responses in both pDS-GCs and sOff alpha cells in the dorsal retina supports our working model of sensitized Off bipolar cell sustained signaling in this region.

3.6 Discussion

Our finding that the pDSGC responsiveness can be transiently and reversibly sensitized by visual stimulation adds to the accumulating evidence on the contextual modulation of the DSGC response in addition to its robust direction selectivity(Chiao and Masland, 2003; Rivlin-Etzion et al., 2012; Vlasits et al., 2014; Yao et al., 2018; Huang et al., 2019). Notably, dorsal and ventral pDSGCs differ in their sensitization patterns. When sensitization is induced in dorsal pDSGCs, a tonic depolarization originating from Off bipolar cells onto the DSGC Off dendrites readily spreads into the On dendritic layer, causes a prolonged increase of excitability, and boosts the subsequent On spiking responses. In contrast, ventral pDSGCs lack such a sustained elevation of dendritic excitability after induction and therefore are not subject to the relay of sensitization from the Off to the On pathway. Because this dorsal-ventral difference arises from Off bipolar cell modulation, other RGC types that share common Off bipolar cell inputs with pDSGCs may have a similar divergence of sensitization patterns between the dorsal and the ventral retinal regions. Indeed, we found a comparable dorsal-ventral difference in the sensitization pattern of sOff alpha cells, which share common inputs with On-Off DSGCs from type 2 Off bipolar cells (CBC2)(Duan et al., 2014; Yu et al., 2018).

Different adaptive properties of pDSGC responsiveness in the dorsal and the ventral retina highlight the topographic variations in the retinal code. In the mouse retina, dorsal-ventral asymmetry has been reported at multiple stages of visual processing from photoreceptor spectral sensitivity to ganglion cell sizes, densities and receptive field properties(Baden et al., 2019; Heukamp et al., 2020; Nadal-Nicolás et al., 2020; Szatko et al., 2020). These specializations on the vertical axis are thought to reflect the adaptation of the retinal circuitry to the different environments in the animal's upper and lower visual fields. However, in the direction-selective circuit, while extensive studies have focused on the robustness of

direction selectivity across the retina under diverse visual conditions, regional differences of the circuit on the vertical axis are underexplored. A decrease in On-Off DSGC dendritic field size from the dorsal to the ventral retina has been reported(El-Danaf and Huberman, 2019). Moreover, On starburst amacrine cells in the dorsal retina can reverse their contrast polarity under certain visual stimulation conditions, a phenomenon that likely originates from region-specific photoreceptor properties and may contribute to the switch of the DSGC directional preference(Rivlin-Etzion et al., 2012; Vlasits et al., 2014; Ankri et al., 2020).

In this study, we found that Off bipolar cell signaling in the dorsal and the ventral retina is differentially modulated by visual experience, which contributes to the distinct sensitization patterns of postsynaptic RGC targets including On-Off pDSGCs. An induction stimulus triggers elevated baseline firing and enhanced On and Off responses in dorsal pDSGCs, but only a transient increase of Off responses in ventral cells. Therefore, dorsal and ventral pDSGCs report the changing visual scenes differently to their downstream targets in the brain including the superficial layer of the superior colliculus and the shell region of the dLGN(Huberman et al., 2009; Kay et al., 2011; Rivlin-Etzion et al., 2011; Cruz-Martín et al., 2014). As an interesting parallel, the dorsal retina receives more balanced On and Off stimuli on the ground while the ventral retina receives predominant Off stimuli in the sky(Baden et al., 2013). These observations suggest that differential processing strategies of dorsal and ventral retinal circuits may underlie different coding principles of upper and lower visual field information, and help serve the animal's behavioral demands in its ecological niche.

Previous studies on RGC sensitization primarily focused on contrast adaptation, a condition under which induction stimuli have a higher contrast than the test stimulus(Kastner and Baccus, 2011, 2013; Nikolaev et al., 2013; Appleby and Manookin, 2019; Kastner et al., 2019). In this study, we found that the sensitization of pDSGCs can be induced by other

forms of visual stimulation, such as moving spots, drifting and contrast-reversing gratings, at the same contrast as the testing stimulus. Despite different forms of induction stimuli, our results and other studies(Kastner and Baccus, 2011, 2013; Nikolaev et al., 2013; Appleby and Manookin, 2019; Kastner et al., 2019) indicate that RGC sensitization in several species involves short-term disinhibition of bipolar cells. This common mechanistic origin implies that the phenomenon of sensitization is not bound by the category of the induction stimulus per se, but reflects the synaptic plasticity rules that permit short-term modulation of bipolar cell signaling under multiple stimulus conditions.

In the dorsal retina, the tonic elevation of Off bipolar cell inputs after sensitization permits a specific mode of crossover signaling from the Off to the On dendritic layers of the bistratified pDSGC. The electrotonic spread of sustained depolarization from the Off to the On dendritic layers depends on the dendritic architecture and membrane properties. In this context, the dendritic crossovers between the On and the Off layers of On-Off DSGCs, which are evident in published retinal studies(Rivlin-Etzion et al., 2011; Wei et al., 2011) but have not been investigated, are particularly relevant and caught our attention. Here, we provide the first quantification of this dendritic feature in mouse pDSGCs. We found that dendritic crossover is present in every pDSGC. For a given cell, a significant fraction of dendrites in one layer originates from the other layer. These direct connections between the On and the Off dendritic layers bypassing the soma indicate a more direct route for membrane depolarization to spread across dendritic layers. Therefore, elevated membrane excitability in the Off dendritic layer can be more readily relayed to the On dendritic layer to sensitize its On response. Interestingly, studies in the rabbit retina have demonstrated that spikes of On-Off DSGCs are initiated in the dendritic arbors(Oesch et al., 2005; Schachter et al., 2010). In this context, dendritic crossovers may significantly influence local spike initiation at the On layer upon sensitization. Future experimental and modeling studies will provide

more insights into functional implications of On-Off DSGC dendritic crossovers during visual processing.

3.7 References

Akyuz S, Pavan A, Kaya U, Kafaligonul H (2020) Short- and long-term forms of neural adaptation: An ERP investigation of dynamic motion aftereffects. Cortex 125:122–134.

Ankri L, Ezra-Tsur E, Maimon SR, Kaushansky N, Rivlin-Etzion M (2020) Antagonistic Center-Surround Mechanisms for Direction Selectivity in the Retina. Cell Reports 31:107608.

Applebury ML, Antoch MP, Baxter LC, Chun LLY, Falk JD, Farhangfar F, Kage K, Krzystolik MG, Lyass LA, Robbins JT (2000) The Murine Cone Photoreceptor: A Single Cone Type Expresses Both S and M Opsins with Retinal Spatial Patterning. Neuron 27:513–523.

Appleby TR, Manookin MB (2019) Neural sensitization improves encoding fidelity in the primate retina. Nature Communications 2019 10:1 10:1–15.

Baccus SA, Meister M (2002) Fast and Slow Contrast Adaptation in Retinal Circuitry. Neuron 36:909–919.

Baden T, Euler T, Berens P (2019) Understanding the retinal basis of vision across species. Nature Reviews Neuroscience 2019 21:1 21:5–20.

Baden T, Schubert T, Chang L, Wei T, Zaichuk M, Wissinger B, Euler T (2013) A Tale of Two Retinal Domains: Near-Optimal Sampling of Achromatic Contrasts in Natural Scenes through Asymmetric Photoreceptor Distribution. Neuron 80:1206–1217.

Barlow HB, Levick WR (1965) The mechanism of directionally selective units in rabbit's retina. The Journal of physiology 178:477–504.

Brainard DH (1997) The Psychophysics Toolbox. Spatial vision 10:433–436.

Chiao C-C, Masland RH (2003) Contextual tuning of direction-selective retinal ganglion cells. Nature neuroscience 6:1251–1252.

Clifford CWG, Wenderoth P, Spehar B (2000) A functional angle on some after-effects in cortical vision. Proceedings of the Royal Society of London Series B: Biological Sciences 267:1705–1710.

Cruz-Martín A, El-Danaf RN, Osakada F, Sriram B, Dhande OS, Nguyen PL, Callaway EM,

Ghosh A, Huberman AD (2014) A dedicated circuit links direction-selective retinal ganglion cells to the primary visual cortex. Nature 507:358–361.

Demb JB (2008) Functional circuitry of visual adaptation in the retina. The Journal of Physiology 586:4377–4384.

Demb JB, Singer JH (2012) Intrinsic properties and functional circuitry of the AII amacrine cell. Visual Neuroscience 29:51–60.

Diamond JS (2017) Inhibitory Interneurons in the Retina: Types, Circuitry, and Function. Annual review of vision science 3:1–24.

Duan X, Krishnaswamy A, De la Huerta I, Sanes JR (2014) Type II Cadherins Guide Assembly of a Direction-Selective Retinal Circuit. Cell 158:793–807.

El-Danaf RN, Huberman AD (2019) Sub-topographic maps for regionally enhanced analysis of visual space in the mouse retina. Journal of Comparative Neurology 527:259–269.

Fisher LJ (1979) Development of synaptic arrays in the inner plexiform layer of neonatal mouse retina. Journal of Comparative Neurology 187:359–372.

Graydon CW, Lieberman EE, Rho N, Briggman KL, Singer JH, Diamond JS (2018) Synaptic Transfer between Rod and Cone Pathways Mediated by AII Amacrine Cells in the Mouse Retina. Current Biology 28:2739-2751.e3.

He Q, Wang P, Tian N (2011) Light-evoked synaptic activity of retinal ganglion and amacrine cells is regulated in developing mouse retina. European Journal of Neuroscience 33:36–48.

Heukamp AS, Warwick RA, Rivlin-Etzion M (2020) Topographic Variations in Retinal Encoding of Visual Space. Annual review of vision science 6:237–259.

Huang X, Rangel M, Briggman KL, Wei W (2019) Neural mechanisms of contextual modulation in the retinal direction selective circuit. Nature Communications 2019 10:1 10:1–15.

Huberman AD, Wei W, Elstrott J, Stafford BK, Feller MB, Barres BA (2009) Genetic identification of an On-Off direction-selective retinal ganglion cell subtype reveals a layer-specific subcortical map of posterior motion. Neuron 62:327–334.

Jafari M, Ansari-Pour N (2019) Why, When and How to Adjust Your P Values? Cell journal 20:604–607.

Kamkar S, Moghaddam HA, Lashgari R (2018) Early Visual Processing of Feature Saliency Tasks: A Review of Psychophysical Experiments. Frontiers in Systems Neuroscience 12:54.

Kastner DB, Baccus SA (2011) Coordinated dynamic encoding in the retina using opposing forms of plasticity. Nature Neuroscience 2011 14:10 14:1317–1322.

Kastner DB, Baccus SA (2013) Spatial Segregation of Adaptation and Predictive Sensitization in Retinal Ganglion Cells. Neuron 79:541–554.

Kastner DB, Ozuysal Y, Panagiotakos G, Baccus SA (2019) Adaptation of Inhibition Mediates Retinal Sensitization. Current Biology 29:2640-2651.e4.

Kay JN, Huerta ID la, Kim I-J, Zhang Y, Yamagata M, Chu MW, Meister M, Sanes JR (2011) Retinal Ganglion Cells with Distinct Directional Preferences Differ in Molecular Identity, Structure, and Central Projections. Journal of Neuroscience 31:7753–7762.

Khani MH, Gollisch T (2017) Diversity in spatial scope of contrast adaptation among mouse retinal ganglion cells. Journal of Neurophysiology 118:3024–3043.

Kim JS, Greene MJ, Zlateski A, Lee K, Richardson M, Turaga SC, Purcaro M, Balkam M, Robinson A, Behabadi BF, Campos M, Denk W, Seung HS (2014) Space–time wiring specificity supports direction selectivity in the retina. Nature 2014 509:7500 509:331–336.

Kim KJ, Rieke F (2001) Temporal contrast adaptation in the input and output signals of salamander retinal ganglion cells. Journal of Neuroscience 21:287–299.

Kohn A (2007) Visual adaptation: physiology, mechanisms, and functional benefits. Journal of neurophysiology 97:3155–3164.

Krieger B, Qiao M, Rousso DL, Sanes JR, Meister M (2017) Four alpha ganglion cell types in mouse retina: Function, structure, and molecular signatures. PLOS ONE 12:e0180091.

Matulis CA, Chen J, Gonzalez-Suarez AD, Behnia R, Clark DA (2020) Heterogeneous Temporal Contrast Adaptation in Drosophila Direction-Selective Circuits. Current Biol-

ogy 30:222-236.e6.

Mazade RE, Eggers ED (2016) Light adaptation alters inner retinal inhibition to shape OFF retinal pathway signaling. Journal of Neurophysiology 115:2761–2778.

Nadal-Nicolás FM, Kunze VP, Ball JM, Peng BT, Krisnan A, Zhou G, Dong L, Li W (2020) True S-cones are concentrated in the ventral mouse retina and wired for color detection in the upper visual field. eLife 9:1–30.

Nikolaev A, Leung K-M, Odermatt B, Lagnado L (2013) Synaptic mechanisms of adaptation and sensitization in the retina. Nature Neuroscience 2013 16:7 16:934–941.

Oesch N, Euler T, Taylor WR (2005) Direction-selective dendritic action potentials in rabbit retina. Neuron 47:739–750.

Olney JW (1968) An electron microscopic study of synapse formation, receptor outer segment development, and other aspects of developing mouse retina. Investigative Ophthalmology 7:250–268.

Rieke F, Rudd ME (2009) The Challenges Natural Images Pose for Visual Adaptation. Neuron 64:605–616.

Rivlin-Etzion M, Wei W, Feller MB (2012) Visual Stimulation Reverses the Directional Preference of Direction-Selective Retinal Ganglion Cells. Neuron 76:518–525.

Rivlin-Etzion M, Zhou K, Wei W, Elstrott J, Nguyen PL, Barres BA, Huberman AD, Feller MB (2011) Transgenic Mice Reveal Unexpected Diversity of On-Off Direction-Selective Retinal Ganglion Cell Subtypes and Brain Structures Involved in Motion Processing. Journal of Neuroscience 31:8760–8769.

Rosa JM, Morrie RD, Baertsch HC, Feller MB (2016) Contributions of Rod and Cone Pathways to Retinal Direction Selectivity Through Development. Journal of Neuroscience 36:9683–9695.

Sanes JR, Masland RH (2015) The types of retinal ganglion cells: current status and implications for neuronal classification. Annual review of neuroscience 38:221–246.

Sassoè-Pognetto M, Wässle H (1997) Synaptogenesis in the rat retina: subcellular localization of glycine receptors, GABA(A) receptors, and the anchoring protein gephyrin. The Journal of comparative neurology 381:158–174.

Schachter MJ, Oesch N, Smith RG, Taylor WR (2010) Dendritic Spikes Amplify the Synaptic Signal to Enhance Detection of Motion in a Simulation of the Direction-Selective Ganglion Cell. PLOS Computational Biology 6:e1000899.

Schwartz O, Hsu A, Dayan P (2007) Space and time in visual context. Nature Reviews Neuroscience 2007 8:7 8:522–535.

Sethuramanujam S, Yao X, deRosenroll G, Briggman KL, Field GD, Awatramani GB (2017) "Silent" NMDA Synapses Enhance Motion Sensitivity in a Mature Retinal Circuit. Neuron 96:1099-1111.e3.

Sherry DM, Wang MM, Bates J, Frishman LJ (2003) Expression of vesicular glutamate transporter 1 in the mouse retina reveals temporal ordering in development of rod vs. cone and ON vs. OFF circuits. The Journal of Comparative Neurology 465:480–498.

Smith RG (1992) NeuronC: a computational language for investigating functional architecture of neural circuits. Journal of Neuroscience Methods 43:83–108.

Stafford BK, Park SJH, Wong KY, Demb JB (2014) Developmental Changes in NMDA Receptor Subunit Composition at ON and OFF Bipolar Cell Synapses onto Direction-Selective Retinal Ganglion Cells. Journal of Neuroscience 34:1942–1948.

Szatko KP, Korympidou MM, Ran Y, Berens P, Dalkara D, Schubert T, Euler T, Franke K (2020) Neural circuits in the mouse retina support color vision in the upper visual field. Nature Communications 11:1–14.

Theeuwes J (2013) Feature-based attention: it is all bottom-up priming. Philosophical transactions of the Royal Society of London Series B, Biological sciences 368.

Tian N, Copenhagen DR (2001) Visual Deprivation Alters Development of Synaptic Function in Inner Retina after Eye Opening. Neuron 32:439–449.

Vlasits AL, Bos R, Morrie RD, Fortuny C, Flannery JG, Feller MB, Rivlin-Etzion M (2014) Visual Stimulation Switches the Polarity of Excitatory Input to Starburst Amacrine Cells. Neuron 83:1172–1184.

Wark B, Fairhall A, Rieke F (2009) Timescales of Inference in Visual Adaptation. Neuron 61:750–761.

Warwick RA, Kaushansky N, Sarid N, Golan A, Rivlin-Etzion M (2018) Inhomogeneous Encoding of the Visual Field in the Mouse Retina. Current Biology 28:655-665.e3.

Wei W, Hamby AM, Zhou K, Feller MB (2011) Development of asymmetric inhibition underlying direction selectivity in the retina. Nature 469:402–406.

Yao X, Cafaro J, McLaughlin AJ, Postma FR, Paul DL, Awatramani G, Field GD (2018) Gap Junctions Contribute to Differential Light Adaptation across Direction-Selective Retinal Ganglion Cells. Neuron 100:216-228.e6.

Yu W-Q, El-Danaf RN, Okawa H, Pacholec JM, Matti U, Schwarz K, Odermatt B, Dunn FA, Lagnado L, Schmitz F, Huberman AD, Wong ROL (2018) Synaptic Convergence Patterns onto Retinal Ganglion Cells Are Preserved despite Topographic Variation in Pre- and Postsynaptic Territories. Cell Reports 25:2017-2026.e3.

CHAPTER 4

CONCLUSIONS AND PERSPECTIVES

4.1 Delineating both spatial and temporal contextual modulation of retinal neuronal response

In this thesis, we report that in the mouse retina, DSGC responses can be flexibly modulated depending on spatial and temporal environments of the target visual stimulus. In spatial domain, DSGC responses are strongly reduced by continuous contours across the center and surround regions of the receptive field, but less suppressed when there is discontinuity between the center and surround. In temporal domain, DSGC responses are remarkably enhanced after several types of induction stimuli, which are "strong" stimuli that can depress the upstream glycinergic inhibition. Together, this thesis made a comprehensive exploration of contextual modulation in the direction-selective circuit across both spatial and temporal domains.

The direction-selective circuit provides a convenient and reliable platform for us to study spatial and temporal contextual modulation in the same subject. And we found spatial and temporal contextual modulations show similarities across several aspects. They are both reflected by changes in the mean firing rate and both exhibit sensitivity to visual saliency (center stimulus discontinuous from the background; stronger stimulus compared to prior visual experience). Moreover, both spatial and temporal contextual modulations in the retina may reflect the demand of sensory neural circuits to meet the statistical attributes of visual inputs from the natural environment (asymmetric spatial contextual modulation in retinal On/Off pathways parallels with unbalanced bright/dark stimulus from the natural visual scenes; dorsal/ventral distinct sensitization parallels with uneven distribution of visual contrast from the ground and the sky). These similarities between spatial and temporal

contextual modulations point to the future direction of investigating them simultaneously, a necessary next step for understanding motion processing in the complex natural environment.

4.2 Multilayered network for sensory encoding under complex contexts

4.2.1 Extending the canonical direction-selective circuit into a broader network

The direction-selective circuit is one of the canonical circuits used to study neural encoding of certain visual feature, which specifically refers to motion direction here. The main constituents of the direction-selective circuit include the output neuron On-Off DSGC, as well as the upstream bipolar cell (BC) and starburst amacrine cell (SAC) (Figure 2.1a). On-Off DSGC acquires glutamatergic inputs from BC, cholinergic and GABAergic inputs from SAC (Figure 2.1b). In this thesis, we revealed an extensive network for contextual modulation beyond the three sources of synaptic inputs onto On-Off DSGCs (Figure 4.1). For temporal contextual modulation, there is glycinergic signaling in the Off pathway disinhibiting the glutamatergic inputs from Off BC onto On-Off DSGC (Figure 4.1 left portion). For spatial contextual modulation, there are wide-field amacrine cells (WACs) directly (Off WAC) or indirectly (On WAC) suppressing the cholinergic inputs from SAC onto On-Off DSGC (Figure 4.1 right portion). Our findings therefore put the direction-selective circuit into a broader retinal neural network involving new types of amacrines contributing to context-dependent coding.

To be noted, contextual modulation of On-Off DSGC is not only accomplished by the extensive circuit wiring, but also powerfully shaped by short-term synaptic plasticity and

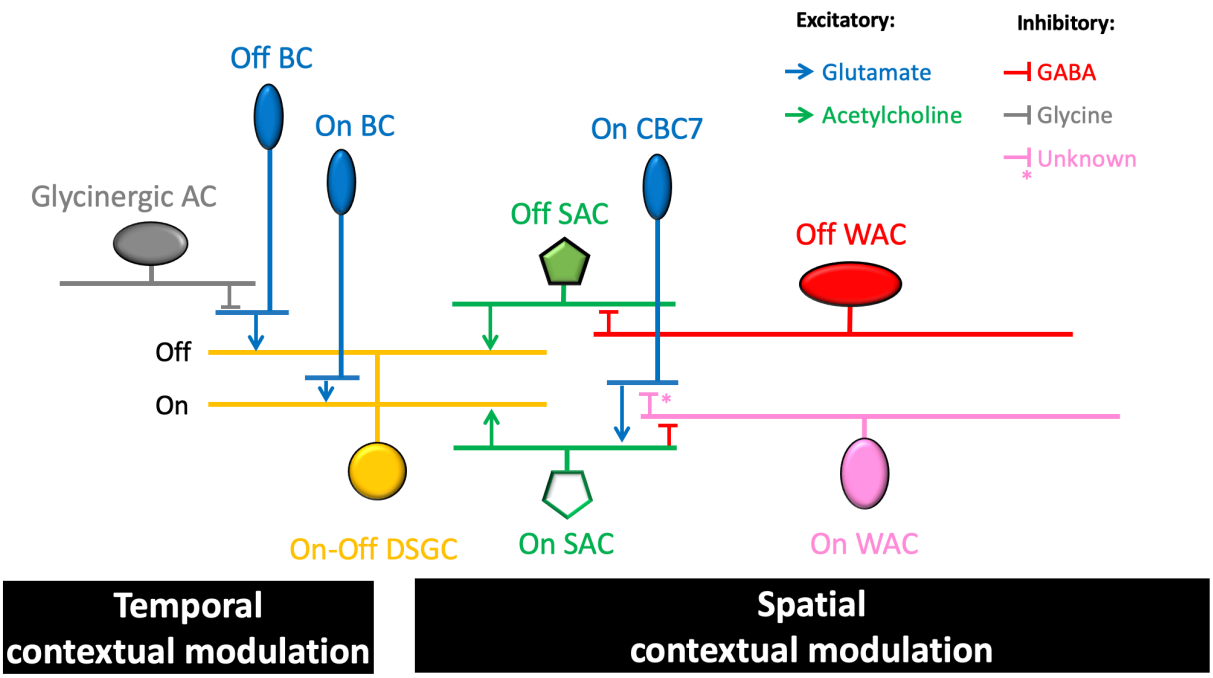

Figure 4.1: **A multilayered neural network for context-dependent coding in the direction-selective circuit.**
For more details of the circuit motifs, refer to Figure 3.6 and Figure 3.7 for temporal contextual modulation, Figure 2.5, Figure 2.12 and Figure 2.15 for spatial contextual modulation.

the morphology of neurons within the network. One example is the crossover dendritic process that connects the two strata of On-Off DSGC, which allows for travel of sustained depolarization from the Off layer to the On layer. Another example is the long and straight dendrites of WACs, which may work as potential detector for contour continuity. Both cases prove again how dendritic architecture can shape signal integration and neural encoding.

4.2.2 Potential ubiquitous mechanisms of contextual modulation

in the retinal circuits

The contextual modulation mechanisms we found in the direction-selective circuit may not be specifically limited to DSGCs, but generally exist among retinal ganglion cell (RGC) populations. And such speculation is not only inferred from the commonality of the circuit locus for signal modulation, but also supported by physiological or anatomical evidences. For instance, the glycinergic mechanism underlying temporal contextual modulation is implemented by adjusting BC output (Figure 4.1 left portion), which will also apply to other RGCs sharing the common BC inputs. Consistent with that, we found similar patterns of temporal contextual modulation in On-Off DSGC and sustained Off alpha cells, both of which obtain glutamatergic inputs from type 2 Off bipolar cell (CBC2) (Figure 3.12) (Duan et al., 2014; Yu et al., 2018). The modulation of CBC7 by On WAC for spatial contextual modulation in the On pathway (Figure 4.1 right portion) may also conform to similar commonality. Moreover, these On WACs also substantially synapse onto amacrine cells (47%) (Figure 2.15), which may further confer the contextual modulation of other retinal circuits.

4.2.3 Stronger contextual modulation in the Off pathway

As we can see from the schematic of the extensive neural network (Figure 4.1), contextual modulation is more powerfully carried out by the Off pathway than the On pathway. Besides possible evolutionary adaptation to match the asymmetric On/Off stimulus distribution in the natural environment (see the section 2.5 in Chapter 2 and section 3.6 in Chapter 3), another possible reason of relying on the Off pathway to execute contextual modulation could be a outcome of cooperation and division of neural circuits. On-Off DSGC shares its On pathway neural circuits with On direction selective ganglion cell (On DSGC) (Oyster and Barlow, 1967), which only exhibits On response and also receives inputs from On SAC (Figure 4.2). However, unlike On-Off DSGC, which is supposed to encode local motion,

On DSGC confers moving direction of global motion (Taylor and Vaney, 2002). Therefore, relying more on the Off pathway to coordinate contextual modulation not only allows for dynamic modulation of On-Off DSGC responses to local motion under variant contexts, but also minimizes the possibility of compromising the encoding of global shifts by the On DSGC.

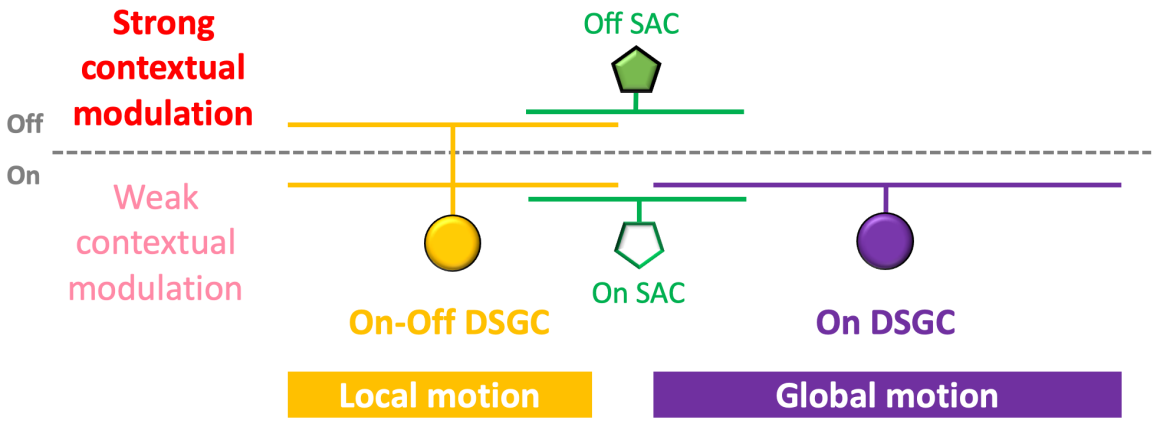

Figure 4.2: **On-Off DSGC and On DSGC partially share the neural circuit in the On pathway.**

4.3 Potential impact on neural encoding in the downstream visual nuclei

Genetic labeling of On-Off DSGCs in the mouse retina reveals that they project to the superficial layers of the superior colliculus and the shell of the dorsal lateral geniculate nucleus (dLGN) (Cruz-Martín et al., 2014; Dhande et al., 2015; Huberman et al., 2009; Kay et al., 2011; Rivlin-Etzion et al., 2011), and they contribute to the direction tuning and orientation tuning in these nuclei (Cruz-Martín et al., 2014; Marshel et al., 2012; Piscopo et al., 2013; Shi et al., 2017; Suresh et al., 2016). Our results of contextual modulation in the retina provide a new starting point for investigating the input-output relationships for the encoding of complex motion patterns in the retinorecipient visual nuclei. A particularly relevant study is

on the spatial contextual modulation in the superficial layers of the superior colliculus using the same set of visual stimuli as ours (Barchini et al., 2018). They found similar pattern of contextual modulation during uniform grating and phase contrast stimuli. But interestingly, they also reported potentiated neural activity during direction contrast, significantly higher than that during the phase contrast stimuli. This indicates local processing on retinal inputs in the SC to boost up the motion saliency. One interesting direction in the future is to identify how impairment of contextual modulation in the retina (for example in the Gabra2 cKO mice) influences the contextual modulation in superior colliculus as well as other retinorecipient visual nuclei, which will be important to understand whether and how the contextual modulation information from the retina is inherited and integrated by the downstream neural circuits.

Furthermore, our study also demonstrates striking asymmetric neural encoding in the retinal circuits, including the unbalanced spatial contextual modulation between the On and Off pathways, as well as the distinct sensitization of visual inputs from the upper versus the lower visual fields. On/Off asymmetry was predicted in visual cortex using a model of early visual pathways to process unbalanced bright/dark stimuli from the natural environment (Cooper and Norcia, 2015). Our finding of differential On/Off contextual modulation in the retina would thus provide more experimental data for modeling asymmetric processing in the visual pathway. Likewise, differential coding of visual inputs from upper and lower visual fields was also reported in mouse visual cortex (Rhim et al., 2017). And the same visual stimulus from the upper and the lower fields can lead to dramatically different behavior outcomes (Ruiz and Theobald, 2020; Salay et al., 2018; Yilmaz and Meister, 2013). Therefore, it will also be very interesting for future studies to explore how the asymmetric retinal codes are conveyed and further processed by the downstream neural circuits in the brain, and whether they can contribute to the distinctive behaviors responding to visual

stimuli from different regions of the visual fields.

4.4 Summary

Visual stimulus in the natural environment is embedded in spatial (surrounding stimulus) and temporal (prior stimulus) contexts, which can remarkably influence the stimulus saliency, modulate neuronal responses and accordingly modulate the visual perception. In this thesis we use the retinal direction-selective circuit as a model system to investigate how sensory coding can be profoundly modulated by spatial or temporal visual contexts. The phenomena as well the mechanisms of contextual modulation identified in the direction selective circuit provide new insights into context-dependent sensory encoding in broader retinal circuits and in downstream visual nuclei of the brain. And it also highlights the importance of taking the naturalistic features of visual stimulus into account when studying the visual processing in the complex natural environment.

4.5 References

Barchini, J., Shi, X., Chen, H., and Cang, J. (2018). Bidirectional encoding of motion contrast in the mouse superior colliculus. ELife 7.

Cooper, E.A., and Norcia, A.M. (2015). Predicting cortical dark/bright asymmetries from natural image statistics and early visual transforms. PLoS Computational Biology 11.

Cruz-Martín, A., El-Danaf, R.N., Osakada, F., Sriram, B., Dhande, O.S., Nguyen, P.L., Callaway, E.M., Ghosh, A., and Huberman, A.D. (2014). A dedicated circuit links direction-selective retinal ganglion cells to the primary visual cortex. Nature 507, 358–361.

Dhande, O.S., Stafford, B.K., Lim, J.-H.A., and Huberman, A.D. (2015). Contributions of Retinal Ganglion Cells to Subcortical Visual Processing and Behaviors. Annual Review of Vision Science 1, 291–328.

Duan, X., Krishnaswamy, A., de la Huerta, I., and Sanes, J.R. (2014). Type II cadherins guide assembly of a direction-selective retinal circuit. Cell 158, 793–807.

Huberman, A.D., Wei, W., Elstrott, J., Stafford, B.K., Feller, M.B., and Barres, B.A. (2009). Genetic identification of an On-Off direction-selective retinal ganglion cell subtype reveals a layer-specific subcortical map of posterior motion. Neuron 62, 327–334.

Kay, J.N., Huerta, I.D. la, Kim, I.-J., Zhang, Y., Yamagata, M., Chu, M.W., Meister, M., and Sanes, J.R. (2011). Retinal Ganglion Cells with Distinct Directional Preferences Differ in Molecular Identity, Structure, and Central Projections. Journal of Neuroscience 31, 7753–7762.

Marshel, J.H., Kaye, A.P., Nauhaus, I., and Callaway, E.M. (2012). Anterior-Posterior Direction Opponency in the Superficial Mouse Lateral Geniculate Nucleus. Neuron 76, 713–720.

Oyster, C.W., and Barlow, H.B. (1967). Direction-selective units in rabbit retina: Distribution of preferred directions. Science.

Piscopo, D.M., El-Danaf, R.N., Huberman, A.D., and Niell, C.M. (2013). Diverse Visual Features Encoded in Mouse Lateral Geniculate Nucleus. Journal of Neuroscience 33, 4642–4656.

Rhim, I., Coello-Reyes, G., Ko, H.-K., and Nauhaus, I. (2017). Maps of cone opsin input to mouse V1 and higher visual areas. Https://Doi.Org/10.1152/Jn.00849.2016 117, 1674–1682.

Rivlin-Etzion, M., Zhou, K., Wei, W., Elstrott, J., Nguyen, P.L., Barres, B.A., Huberman, A.D., and Feller, M.B. (2011). Transgenic Mice Reveal Unexpected Diversity of On-Off Direction-Selective Retinal Ganglion Cell Subtypes and Brain Structures Involved in Motion Processing. Journal of Neuroscience 31, 8760–8769.

Ruiz, C., and Theobald, J.C.T. (2020). Ventral motion parallax enhances fruit fly steering to visual sideslip. Biology Letters 16.

Salay, L.D., Ishiko, N., and Huberman, A.D. (2018). A midline thalamic circuit determines reactions to visual threat. Nature 2018 557:7704 557, 183–189.

Schwartz, O., Hsu, A., and Dayan, P. (2007). Space and time in visual context. Nature Reviews Neuroscience 8, 522–535.

Shi, X., Barchini, J., Ledesma, H.A., Koren, D., Jin, Y., Liu, X., Wei, W., and Cang, J. (2017). Retinal origin of direction selectivity in the superior colliculus. Nature Neuroscience 20.

Suresh, V., Çiftçioğlu, U.M., Wang, X., Lala, B.M., Ding, K.R., Smith, W.A., Sommer, F.T., and Hirsch, J.A. (2016). Synaptic Contributions to Receptive Field Structure and Response Properties in the Rodent Lateral Geniculate Nucleus of the Thalamus. Journal of Neuroscience 36, 10949–10963.

Taylor, W.R., and Vaney, D.I. (2002). Diverse synaptic mechanisms generate direction selectivity in the rabbit retina. The Journal of Neuroscience: The Official Journal of the Society for Neuroscience 22, 7712–7720.

Yilmaz, M., and Meister, M. (2013). Rapid Innate Defensive Responses of Mice to Looming Visual Stimuli. Current Biology 23, 2011–2015.

Yu, W.-Q., El-Danaf, R.N., Okawa, H., Pacholec, J.M., Matti, U., Schwarz, K., Odermatt, B., Dunn, F.A., Lagnado, L., Schmitz, F., et al. (2018). Synaptic Convergence Patterns

onto Retinal Ganglion Cells Are Preserved despite Topographic Variation in Pre- and Post-synaptic Territories. Cell Reports 25, 2017-2026.e3.